

Hydraulic Variable Valve Actuation System: Development & Validation

by

Mitchell Terpstra

A thesis
presented to the University of Waterloo
in fulfillment of the
thesis requirement for the degree of
Master of Applied Science
in
Mechanical and Mechatronics Engineering

Waterloo, Ontario, Canada, 2019

© Mitchell Terpstra 2019

AUTHOR'S DECLARATION

I hereby declare that I am the sole author of this thesis. This is a true copy of the thesis, including any required final revisions, as accepted by my examiners.

I understand that my thesis may be made electronically available to the public.

Abstract

Conventional engines with camshafts with fixed timings force a compromise between performance at high engine loads and fuel economy at low engine loads. Adjusting internal combustion engine valve timing and lift through a variable valve actuation (VVA) system is an established method of improving engine performance [1]. A fully flexible hydraulic variable valve actuation (HVVA) system in development at the University of Waterloo allows the valve timing to be optimized for any engine operating condition.

This project is a further development of this HVVA system. First, the previous prototype was thoroughly tested and evaluated. Major design issues and challenges were addressed, and changes were incorporated into a new prototype design. This prototype was designed to be robust and more compact than the previous system. A completely new concept was developed for the phasing system used to adjust the valve timings. The new HVVA design was manufactured, assembled, and installed on a single cylinder test engine.

Initial experiments of the new HVVA system validated its ability to change engine valve timing and match the profiles of different VVA strategies. The system was able to switch between different profiles in <1s. It also gave insights into the dynamic characteristics of the hydraulic system not discovered during testing of previous prototypes but necessary for further development of the HVVA concept.

Successful combustion tests were run up to 1500 RPM engine speeds using different engine valve timing profiles. The HVVA system reliably operated throughout all testing and proved the feasibility of this more compact system. It will be used as a platform for further demonstrations and validation of the HVVA concept.

Acknowledgements

First, I would like to thank Dr. Amir Khajepour for giving me the opportunity to work in his lab and for his many hours of support and guidance throughout the whole project.

I also want to acknowledge that without the design input and technical abilities of Jeremy Reddekopp, Jason Benninger, and Robert Wagner the project could not be what it is today. Jeff Graansma, thank you for all the hours you spent advising me during the design, testing, and troubleshooting phases of this project; you helped keep me focused on the solution instead of the problem.

Finally, I would like to thank all my family and friends who encouraged me through the challenging days and weeks to get me to the end of this project.

Table of Contents

AUTHOR'S DECLARATION.....	ii
Abstract.....	iii
Acknowledgements.....	iv
Table of Contents.....	v
List of Figures	viii
List of Tables	xii
List of Abbreviations	xiii
List of Symbols	xiv
Chapter 1 Introduction	1
1.1 Motivation.....	1
1.2 Thesis Outline	1
Chapter 2 Background	3
2.1 Literature Review.....	3
2.1.1 Variable Valve Actuation.....	3
2.1.2 VVA Existing Technologies	5
2.1.3 VVA Emerging Technologies.....	9
2.2 HVVA Project Description & Background.....	16
2.2.1 HVVA System Requirements	16
2.2.2 HVVA Description	16
2.2.3 HVVA System Background.....	18
Chapter 3 System Design.....	23
3.1 Previous Prototype Evaluation.....	23
3.1.1 Hydraulic System.....	24
3.1.2 Spool Valves	26
3.1.3 Hydraulic Cylinders	27
3.1.4 Phase Shifters.....	27
3.1.5 Drive System.....	28
3.1.6 Sensors	29
3.2 New System Design.....	30
3.2.1 Hydraulic System.....	31
3.2.2 Spool Valve Assembly.....	40

3.2.3 Hydraulic Cylinders	45
3.2.4 Phase Shifters.....	46
3.2.5 Drive System.....	51
3.2.6 Sensors	52
3.3 Simulation.....	53
Chapter 4 Experimental Setup	57
4.1 Mechanical Setup.....	58
4.1.1 Manufacturing.....	58
4.1.2 Assembly & Install.....	58
4.2 Hydraulic Setup	59
4.3 Electrical Setup	62
4.3.1 Crankshaft Encoder Calibration.....	65
4.3.2 Actuator Encoder Calibration Method.....	65
4.3.3 Linear Displacement Sensor Calibration	66
4.3.4 Electronic Fuel Injection System (EFI).....	67
4.4 Software Setup	68
4.4.1 Simulink Model	68
4.4.2 ControlDesk GUI.....	75
4.4.3 ECU Programming.....	77
Chapter 5 System Validation & Experimental Results	78
5.1 Initial Testing	78
5.1.1 Linear Actuator Testing	78
5.1.2 Hydraulic Cylinder Testing.....	79
5.1.3 Engine Valve Lift.....	80
5.1.4 Valve Lift Height Drop (Pressure fluctuations)	82
5.1.5 Torque Fluctuations	85
5.1.6 System Power Consumption	88
5.2 Valve Profile & Combustion Experiments	88
5.2.1 Original Camshaft Profile (CAM)	90
5.2.2 Optimized Profile (OPT).....	91
5.2.3 IEGR Profile (IEGR)	92
5.2.4 Results.....	93

5.3 Load Cycle Testing	94
5.3.1 Experimental Results	95
5.4 Data Post Processing.....	97
5.4.1 Noise & Sensor Accuracy	98
5.4.2 Filtering.....	98
Chapter 6 Conclusions & Future Work.....	100
6.1 Observations	100
6.2 Conclusions.....	101
6.3 Recommendations/Future Work	101
6.3.1 Mechanical.....	102
6.3.2 Hydraulic.....	103
6.3.3 Software/Control.....	104
References.....	106
Appendix A Parts Lists	109
A.1 Mechanical Parts lists.....	109
A.2 Hydraulic Parts List	109
A.3 Electrical Parts List	110
A.4 Combustion Parts List.....	110
Appendix B Full Combustion Results	111
B.1 Testing at 1300 RPM Engine Speed.....	111
B.2 Testing at 1500 RPM Engine Speed.....	114

List of Figures

Figure 2.1: Typical valve timing of a four-stroke cycle [6]	3
Figure 2.2: Schematic of overhead camshaft setup on an internal combustion engine [7]	4
Figure 2.3: Honda's VTEC system switching process for engine intake valves [11]	6
Figure 2.4: Honda's VTC cam phaser [11]	6
Figure 2.5: Audi's Valvelift system [12]	7
Figure 2.6: BMW's Valvetronic system [13]	7
Figure 2.7: Fiat's Multiair system [14]	8
Figure 2.8: Disassembled Multiair unit	9
Figure 2.9: Multiair hydraulic cylinder	9
Figure 2.10: Hydraulic VVA system [15]	10
Figure 2.11: Diagram of electro-hydraulic VVA system [16]	11
Figure 2.12: MR fluid valve diagram [17]	12
Figure 2.13: Koenigsegg's Freevalve system [18]	13
Figure 2.14: Camcon engine valve actuation mechanism [19]	14
Figure 2.15: Hyundai's CVVD assembly [16]	14
Figure 2.16: Hyundai's mechanism [15]	15
Figure 2.17: Valve lift profiles [15]	15
Figure 2.18: Overall system diagram [3]	17
Figure 2.19: Rotary spool valve cross section [3]	17
Figure 2.21: Pournazeri's prototype [3]	18
Figure 2.22: Pournazeri's spool valve [3]	19
Figure 2.23: Multi cylinder spool shaft design [4]	19
Figure 2.24: Chermesnok's spool valve housing [4]	20
Figure 2.25: Section view of Chermesnok's spool valve [4]	20
Figure 2.26: Chermesnok's planetary gear phase shifter [4]	21
Figure 2.27: Chermesnok's hydraulic cylinder design (with built in hydraulic cushioning)	21
Figure 2.28: Siddiqui's spool valve design [5]	22
Figure 2.29: Siddiqui's hydraulic cylinder design [5]	22
Figure 3.1: General assembly view of Siddiqui's prototype [5]	23
Figure 3.2: Hydraulic schematic [5]	24
Figure 3.3: System fluid flows when operating less than accumulator precharge pressure	25

Figure 3.4: Discrepancy between exhaust and intake valve lifts [5].....	26
Figure 3.5: Spool valves in fully assembled system	27
Figure 3.6: Planetary gear phasing system.....	28
Figure 3.7: Timing belt drive	29
Figure 3.8: Pressure data before and after being filtered	30
Figure 3.9: General assembly view of new prototype.....	31
Figure 3.10: Hydraulic schematic for new HVVA design.....	32
Figure 3.11: Rotary spool valve cross section [3].....	33
Figure 3.12: Spool valve removed from casing	35
Figure 3.13: Flow control valves installed before hydraulic cylinders	36
Figure 3.14: Hydraulic cylinder free body diagram.....	38
Figure 3.15: Hydraulic connections of the spool valve casing block & valve ports section view.....	40
Figure 3.16: Hydraulic connections of the spool valve casing block & supply/return section view	41
Figure 3.17: Cross section of high pressure (red) and low pressure (blue) passages.....	41
Figure 3.18: Cross section of exhaust valve (yellow) and intake valve (green) passages	42
Figure 3.19: HPSV cross section in new prototype	42
Figure 3.20: LPSV cross section in new prototype.....	43
Figure 3.20: Exploded view of spool valve seal assembly	45
Figure 3.21: SMC Pneumatics small bore hydraulic cylinders with end stops installed	46
Figure 3.22: Cross section of phase shifter assembly	47
Figure 3.23: Phase shifter assembly operation.....	47
Figure 3.24: Lead screw assembly	48
Figure 3.25: Lead screw and nut.....	49
Figure 3.26: Linear actuator.....	49
Figure 3.27: Belt drive assembly	52
Figure 3.28: Linear displacement sensor	52
Figure 3.29: Simscape model.....	54
Figure 3.30: HPSV & LPSV open profiles	55
Figure 3.31: Simulink model of flow control valve, hydraulic cylinder, and engine valve.....	55
Figure 4.1: Experimental setup	57
Figure 4.2: Assembly mounted to steel table	58
Figure 4.3: Hydraulic System	59

Figure 4.4: Flow control valves installed in system.....	60
Figure 4.5: Bleed points of hydraulic system	62
Figure 4.6: Electrical panel & dSpace setup	62
Figure 4.7: Crankshaft encoder.....	65
Figure 4.8: Linear actuators with encoders & home position switches	66
Figure 4.9: Linear displacement sensors.....	66
Figure 4.10: EFI ECU (mounted under table).....	67
Figure 4.11: EFI assembled on to the engine.....	67
Figure 4.12: Main view of Simulink model.....	69
Figure 4.13: Actuator homing.....	69
Figure 4.14: TPA timings for engine cycle [2]	70
Figure 4.15: Phase angle controller.....	70
Figure 4.16: Accumulator pressure controller	71
Figure 4.17: Step response results used for lambda tuning method of PI controller	72
Figure 4.18: Crankshaft position output	73
Figure 4.19: Hydraulic system safeties	74
Figure 4.20: Combustion system safeties	75
Figure 4.21: Main ControlDesk interface	76
Figure 4.22: Valve timing settings.....	76
Figure 5.1: Linear actuator velocity test results	78
Figure 5.2: Exhaust and intake valve positions vs. applied pressure	80
Figure 5.3: Intake and exhaust valve lifts before changes to valve springs & accumulator precharge	80
Figure 5.4: Engine valves	82
Figure 5.5: Valve lift height & pressure fluctuations.....	82
Figure 5.6: Simulation results after including fluid inertia	83
Figure 5.7: One-way flow control valve	84
Figure 5.8: Simulation results after adding one-way restriction valves.....	84
Figure 5.9: System results after one-way flow control valves added.....	85
Figure 5.10: Rubber spider for Lovejoy coupler.....	85
Figure 5.11: Hytrel spider & sheared key	86
Figure 5.12: Torque fluctuations.....	86
Figure 5.13: Fast Fourier transform of torque readings	87

Figure 5.14: Torque test after engine flywheel removed	87
Figure 5.15: Valve profiles used in experiments	89
Figure 5.16: CAM simulated (original) profile and experimental results.....	90
Figure 5.17: CAM profile torque results.....	91
Figure 5.18: OPT simulated profile and experimental results	91
Figure 5.19: OPT profile torque results	92
Figure 5.20: IEGR simulated profile and experimental results.....	92
Figure 5.21: IEGR partial load profile torque results	93
Figure 5.22: Simulated load cycle.....	95
Figure 5.23: Spool valve position response	96
Figure 5.24: Single step spool valve position response	96
Figure 5.25: System pressure response	97
Figure 5.26: Average valve lift response	97
Figure 6.1: HPSV cross section for four-cylinder engine with firing order 1-3-4-2.....	102
Figure 6.2: Updated hydraulic schematic	104
Figure A.1: CAM simulated (original) profile and experimental results.....	111
Figure A.2: CAM profile torque results.....	111
Figure A.3: OPT simulated profile and experimental results	112
Figure A.4: OPT profile torque results	112
Figure A.5: IEGR simulated profile and experimental results.....	113
Figure A.6: IEGR partial load profile torque results.....	113
Figure A.7: CAM simulated (original) profile and experimental results	114
Figure A.8: CAM profile torque results.....	114
Figure A.9: OPT simulated profile and experimental results	115
Figure A.10: OPT profile torque results	115
Figure A.11: IEGR simulated profile and experimental results.....	116
Figure A.12: IEGR partial load profile torque results.....	116

List of Tables

Table 3.1: Max Flowrates – Solutions to Equations 3.2, 3.3, & 3.4	34
Table 3.2: Tube & Casing Passage Sizes – Solutions to Equation 3.1	34
Table 3.3: Slot Sizes – Solutions to Equation 3.5.....	35
Table 3.4: Max Flowrates – Solutions to Equations 3.6, 3.7, & 3.8	37
Table 3.5: Valve Pressure Drops – Solutions to Equation 3.9	38
Table 3.6: Accumulator Size Differences – Solutions to Equation 3.10.....	39
Table 3.7: Spool Valve Diameter Tolerances	44
Table 3.8: Linear Actuators Available Torque – Solutions to Equations 3.12, 3.13, & 3.14	51
Table 4.1: Equivalent Bulk Modulus – Solutions to Equations 4.1, 4.2, & 4.3	61
Table 4.2: dSpace Board Descriptions	63
Table 4.3: System Inputs.....	63
Table 4.4: System Outputs.....	64
Table 4.5: EFI Components	68
Table 4.6: Lambda Tuning Results – Solutions to Equation 4.6, 4.7, & 4.8	73
Table 5.1: HVVA System Power Consumption	88
Table 5.1: Testing Details	89
Table 5.2: Results of Combustion Testing	94
Table 5.3: Load Cycle Testing Details.....	95
Table 5.4: Sensor Accuracies & Relative Noise Levels	98
Table A.1: Results of Combustion Testing at 1300 RPM Engine Speed.....	113
Table A.2: Results of Combustion Testing at 1500 RPM Engine Speed.....	116

List of Abbreviations

BDC	Bottom Dead Centre
CA	Crank Angle
CAM	Original Camshaft Valve Profile
ECU	Engine Control Unit
EEVC	Early Exhaust Valve Closing
EFI	Electronic Fuel Injection
EIVC	Early Intake Valve Closure
HPSV	High Pressure Spool Valve
HVVA	Hydraulic Variable Valve Actuation
ICE	Internal Combustion Engine
IEGR	Internal Exhaust Gas Recirculation
LEVC	Late Exhaust Valve Closure
LIVC	Late Intake Valve Closure
LPSV	Low Pressure Spool Valve
NVO	Negative Valve Overlap
OPT	Optimized Valve Profile
PVO	Positive Valve Overlap
TDC	Top Dead Centre
TPA	Tangent Position Angle
VVA	Variable Valve Actuation
VVL	Variable Valve Lift
VVT	Variable Valve Timing

List of Symbols

A_{cyl}	Hydraulic Cylinder Piston Area [mm ²]
a_{valve}	Acceleration of Valve [m/s ²]
b_e	Specific Fuel Consumption [mg/J]
C_v	Valve Coefficient
CO	Controller Output
D	Tube Outer Diameter [mm]
D	Time Delay of the System [s]
d_{tube}	Tube Inner Diameter [m]
dP	Pressure Drop [Pa]
E	Young's Modulus of 316 SS [Pa]
e	Error Between PV and SP
F_k	Spring Force [N]
F_P	Pressure Force [N]
I	Spool Valve, Shaft, & Lead Screw Mass Moment of Inertia [kgmm ²]
k	Spring Stiffness [N/m]
K_C	Controller Gain
K_P	Process Gain
k_{tor}	Torsional Stiffness [N/rad]
l_{max}	Max. Valve Lift Height [mm]
L_r	Lead of Linear Actuator Captive Lead Screw [mm]
L_{slot}	Length of Port Slots [mm]
L_{sv}	Lead Screw Lead [mm]
\dot{m}	Fuel Mass Flowrate [mg/s]
N_e	Engine Speed [RPM]
P_0	Accumulator Precharge Pressure [Pa]
P_1	Accumulator Initial Pressure [Pa]
P_2	Accumulator Final Pressure [Pa]
P_A	Accumulator Pressure [Pa]
P_{atm}	Atmospheric Pressure [Pa]

P_e	Specific Power Output [W]
P_{max}	Linear Actuator Max. Thrust [N]
P_{min}	Min Cylinder Pressure [Pa]
P_{min}	Linear Actuator Min. Thrust [N]
P_{oper}	System Operating Pressure [Pa]
PV	Present Value of Controlled Variable
Pwr_{HVVA}	HVVA System Power Consumption [W]
Pwr_{LA}	Linear Actuator Holding Power Consumption [W]
Q	Fluid Flowrate [m^3/s]
Q_{max}	Max. Oil Flowrate [m^3/s]
Q_P	Pump Flow [m^3/s]
S	Relative Amount of Trapped Air [%]
SG	Specific Gravity of Hydraulic Oil
SP	Setpoint Value of Controlled Variable
t	Hydraulic Tube Thickness [mm]
T_{hold}	Linear Actuator Holding Torque [Nmm]
T_i	Integral Time for Controller
T_{iner}	Linear Actuator Inertial Torque [Nmm]
T_m	Mean Torque Output over Cycle [Nm]
t_{open}	Spool Valve Open Duration [s]
T_P	Process Time Constant [s]
T_{phase}	Linear Actuator Phasing Torque [Nmm]
V_0	Accumulator Total Volume [m^3]
v_{max}	Max. Oil Velocity [m/s]
V_{max}	Max. Cylinder Volume [m^3]
x_i	Spring Preload Displacement [m]
α	Angular Acceleration [rad/s^2]
β_a	Air Bulk Modulus [Pa]
β_c	Equivalent Steel Tube Bulk Modulus [Pa]
β_e	Equivalent Bulk Modulus [Pa]

β_l	Hydraulic Oil Bulk Modulus [Pa]
ΔV	Change in Accumulator Volume [m^3]
$\Delta\theta$	Open Duration of Spool Valve [deg]
η_b	Lead Screw Backdrive Efficiency [%]
θ_c	Casing Position Angle [deg]
θ_r	Angular Displacement of Linear Actuator Rotor [deg]
θ_s	Spool Angular Position [deg]
θ_{s1}	Spool Start to Open Angle [deg]
θ_{s2}	Spool Fully Closed Angle [deg]
θ_{sv}	Angular Displacement of Spool Valve [deg]
λ	Controller Tuning Parameter
ϕ_c	Casing Port Angle [deg]
ϕ_s	Spool Port Angle [deg]
ω	Engine Speed [rad/s]
ω_n	Natural Frequency [Hz]

Chapter 1

Introduction

1.1 Motivation

Despite recent advancements in hybrid & electric vehicles, the internal combustion engine (ICE) remains a dominate technology in the transportation system. Therefore, any design improvements related to the ICE have the potential for widespread application and impact. Furthermore, any technology that improves engine fuel efficiency and reduces exhaust emissions also reduces the overall environmental impact of the engine. Variable valve actuation technology has the potential to greatly improve engine power output and fuel economy and reduce total exhaust emissions.

A typical engine uses camshafts to open and close engine valves with fixed timing. This timing is a compromise of performance at high engine speeds and fuel economy at low engine speeds. Variable valve actuation technology changes engine valve lift profiles to maximize produced power and fuel efficiency at different engine operating points.

Variable valve actuation systems are widely used by most engine manufacturers for significant improvement of engine power and efficiency. The main systems in production still use camshafts for valve actuation and have limited adjustment of valve timings (typically switching between just two different timings). The Mechatronics Vehicle Systems Lab (MVSL) at the University of Waterloo has designed and prototyped a fully flexible hydraulic variable valve actuation (HVVA) system giving full control over engine valve timing at any engine operating point. This system has the potential for a 10% average increase in engine power at full load, and 13% reduction in fuel consumption at partial loads [2].

This HVVA system was initially modelled and prototyped by Mohammad Pournazeri [3], further developed by Matthew Chermesnok [4], and first installed on a test engine by Mohammad Sharif Siddiqui [5]. Yangtao Li developed an engine model simulation in GT Power and created optimal VVA strategies to validate the performance of the HVVA system [2].

This project aimed to develop this system to the next phase to be able to demonstrate the technology and bring further innovation of the internal combustion engine.

1.2 Thesis Outline

The main objective of this project was to improve the HVVA system and build a reliable and more compact assembly to better demonstrate the HVVA technology. This thesis gives the background of VVA

technology, describes the design process of the new system, details the assembly and testing of this system, and presents the results from testing.

The thesis is divided into six chapters. The first chapter gives the motivation for this research and the outline of the thesis.

In Chapter 2, the strategies and benefits of VVA are explained in further detail and existing/emerging technologies are presented. Additionally, the operating principles of the HVVA system are given and the work of previous grad students on this project is detailed.

Chapter 3 discusses the evaluation of the previous HVVA prototype and the design of the new prototype.

The experimental setup is detailed in Chapter 4. This includes the assembly of the new system, incorporation of electrical components and sensors, installation of an electronic fuel injection system, and the development of software for data acquisition and control.

Results of system testing are found in Chapter 5. This chapter describes the initial testing performed to do basic system validation and final testing of the system under combustion used to confirm the ability of the system to run typical VVA profiles.

Chapter 6 presents the observations and conclusions about the system after testing was completed. It also gives future recommendations for the project based on the experience gained throughout the project.

Chapter 2

Background

2.1 Literature Review

2.1.1 Variable Valve Actuation

The internal combustion engine uses intake valves to introduce fresh air and fuel into the combustion chamber and exhaust valves to allow products of combustion to be removed from the chamber. The four-stroke engine cycle consists of four main events: intake, compression, combustion, exhaust. During the intake stroke, the intake valves open and fresh air and fuel are pulled into the combustion chamber by the downward motion of the piston. This fresh charge is compressed by the upward motion of the piston during the compression stroke. Just before the piston reaches its highest point in the combustion cylinder (top dead centre, TDC), the spark plug ignites the compressed charge of air and gas and the force of combustion pushes the piston down to the bottom of the cylinder (power stroke). Just before bottom dead centre (BDC), the exhaust valves open and the upward motion of the piston pushes out all the products of combustion (exhaust stroke). Figure 2.1 shows the exhaust and intake strokes of the four-stroke cycle and the corresponding engine valve lift profiles.

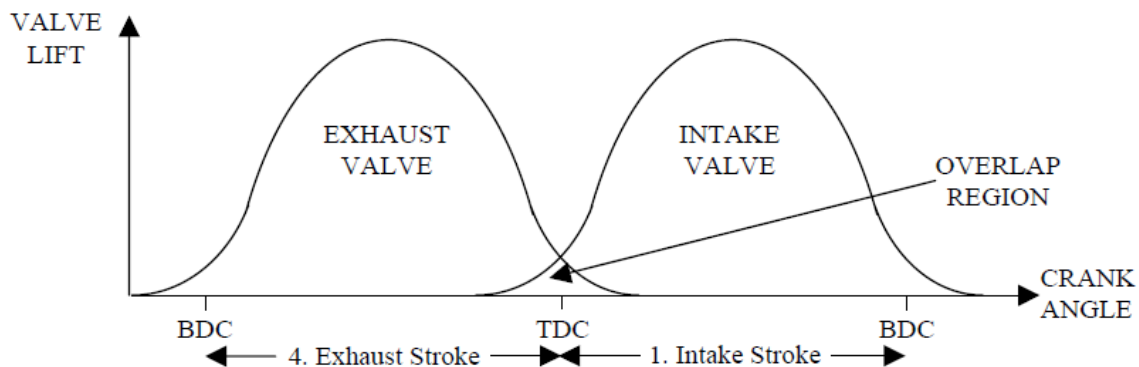


Figure 2.1: Typical valve timing of a four-stroke cycle [6]

Typical engines use mechanical camshafts synchronized to rotate with the engine crankshaft. The camshaft rotates at half of the engine speed as each engine valve only opens once every two engine rotations. The shape of the cams determines the engine valve lift heights and when they open and close. An example of how this method is implemented on an engine is shown in Figure 2.2.

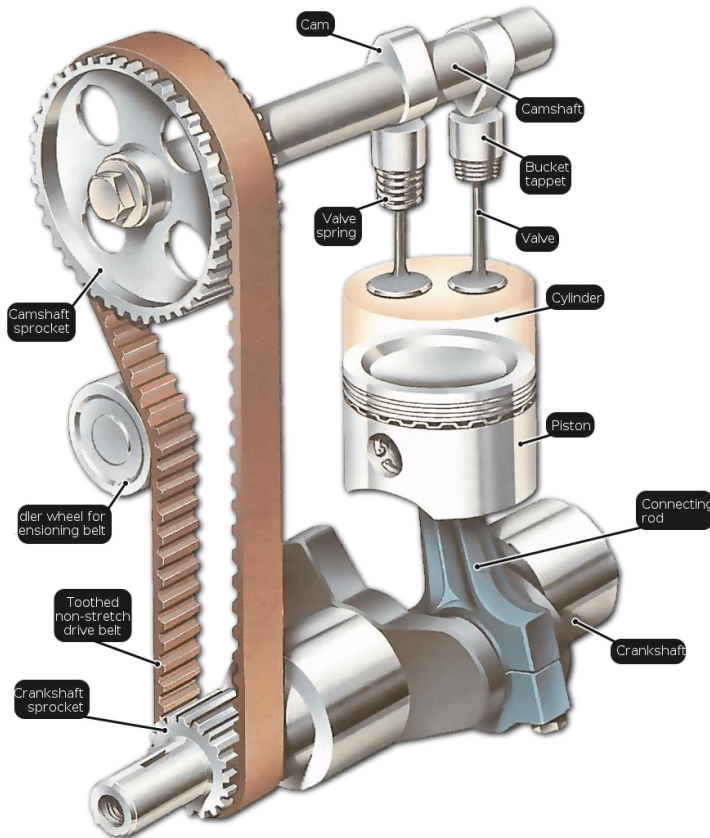


Figure 2.2: Schematic of overhead camshaft setup on an internal combustion engine [7]

Valve opening and closing times and valve lift heights cannot be adjusted when using conventional camshafts. Variable valve actuation (VVA) technology includes technology used to change valve timing, variable valve timing (VVT), and change valve lift, variable valve lift (VVL). VVA allows valve lifts and timing to be adjusted and optimized based on the engine's current state. With VVA, an engine can be tuned to maximize fuel economy at partial load operation with no compromise of power at full load. Common VVA strategies include shifting the valve timings to achieve internal exhaust gas recirculation (IEGR) [8], [9] and using the Atkinson cycle by employing late intake valve closing (LIVC) [10].

IEGR uses positive valve overlap (PVO) or negative valve overlap (NVO) to control engine output without the use of a throttle (throttleless or unthrottled operation). PVO is achieved with a late exhaust valve closing (LEVC) time. This causes exhaust gas to be drawn back into the cylinder during the intake stroke. NVO is a combination of early exhaust valve closing (EEVC) and late intake valve opening (LIVO). Residual exhaust gas is trapped in the cylinder due to EEVC. Both PVO and NVO result in residual exhaust

gas in the engine cylinder. This residual gas reduces the fresh air charge that is drawn into the cylinder and consequently lowers the engine pumping losses. Lower combustion temperatures reduce NOx formation, and reburning the exhaust gas reduces unburnt hydrocarbons.

The Atkinson cycle uses LIVC to reduce engine output without the use of a throttle valve. The intake valve is left open past top dead centre (TDC) and part of the fresh charge of air is pushed back into the intake manifold. The total fresh charge is thereby reduced without using a throttle plate and pumping losses are reduced. Additionally, the charge of air pushed back into the intake manifold will increase the pressure in the manifold. The higher pressure will further reduce pumping losses in the subsequent engine cycle.

Another benefit of VVA is the ability to change the lift height of intake and exhaust valves. The intake valve lift height can be adjusted to throttle the fresh air charge into the engine. Using the intake valves to throttle the air flow instead of a typical throttle body will increase the pressure in the intake manifold and result in lower pumping losses overall. Additionally, reducing the intake valve lift height at low engine loads can increase mixing of the air and gas, allowing more homogeneous combustion [6].

2.1.2 VVA Existing Technologies

Variable valve actuation has been applied to many different engines currently in production. Some of the most notable applications are Honda's Variable Valve Timing and Lift Electronic Control (VTEC) [11], Audi's Valvelift [12], BMW's Valvetronic [13], and Fiat/Chrysler's Multiair systems [14].

Honda VTEC

Honda's basic VTEC system uses two different cam profiles to change the lift height and timing of the engine input valves. A low lift profile cam is used at low engine speeds. At higher engine speeds a hydraulically actuated pin is inserted to engage a second cam rocker and switch to a higher valve lift (Figure 2.3). As there are only two different cam profiles, this type of VVA can optimize the engine efficiency at just two points.

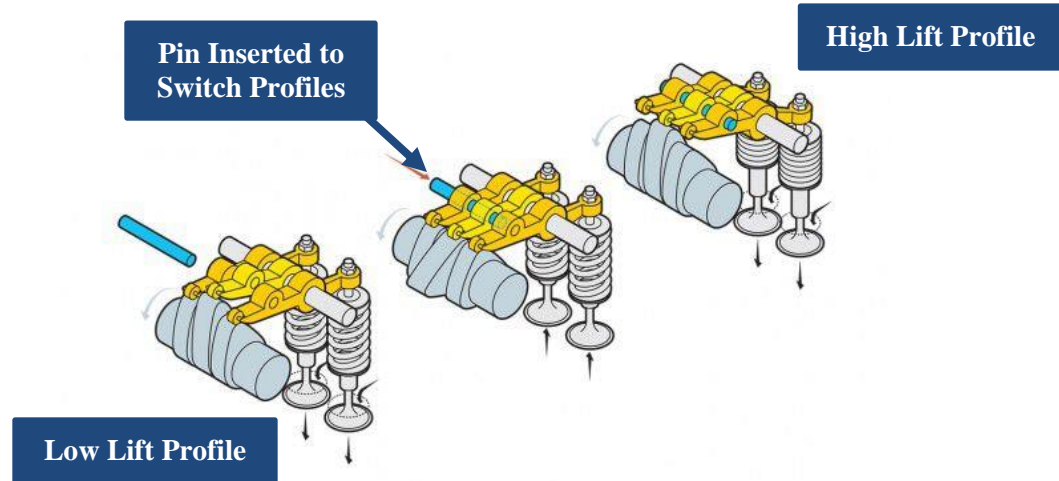


Figure 2.3: Honda's VTEC system switching process for engine intake valves [11]

Honda also incorporates variable timing control (VTC) using cam phasers. These cam phasers (Figure 2.4) are located in between the timing chain sprocket (grey) and the camshaft (yellow). Pressurized hydraulic oil (red) is used to advance or retard the camshaft timing relative to the crankshaft. This is a binary system that is limited to two different valve timing positions and it cannot change valve opening and closing times independently.

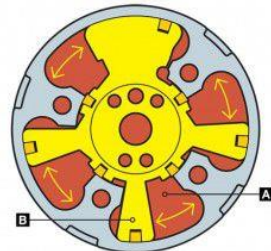


Figure 2.4: Honda's VTC cam phaser [11]

Audi Valvelift

Like VTEC, Audi's Valvelift switches between two different cam profiles (Figure 2.5). It uses electromagnetic valves to engage a pin in a groove on the camshaft to move the cams axially along the camshaft and engage different sets of cam profiles. The switchover point is based on engine speed and load. It is also limited to just two valve profiles.

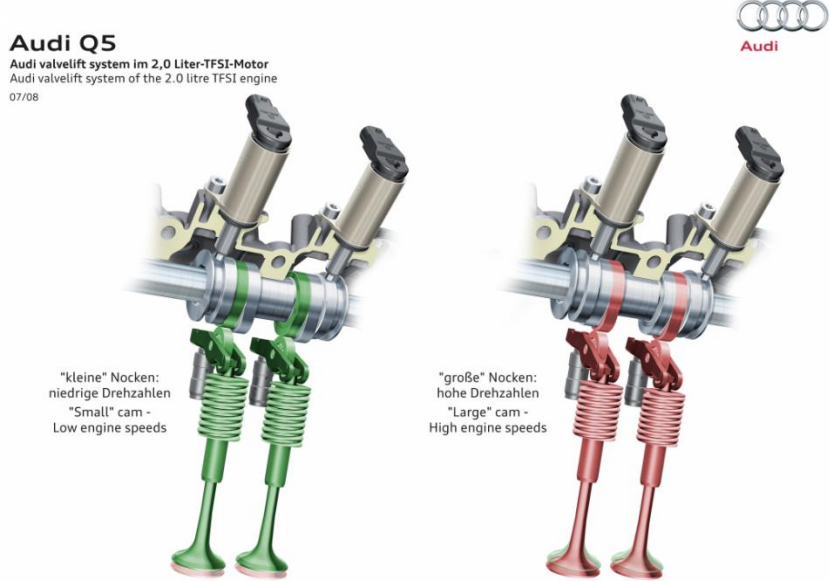


Figure 2.5: Audi's Valvelift system [12]

BMW Valvetronic

BMW's Valvetronic system provides continuously variable valve lift. This system can be used to throttle the engine by reducing the intake valve lift height. It varies the valve lift by changing the position of an intermediate lever between the cam and the valve rocker (Figure 2.6). This system can be used to throttle the air intake by reducing the intake valve lift height instead of using a throttle valve to reduce pumping losses and improve engine response. However, it cannot be used to implement different VVA timing strategies and requires a more complex cam follower mechanism than a typical engine.

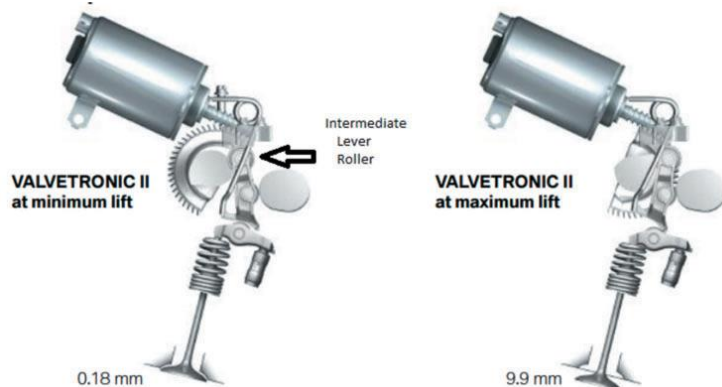


Figure 2.6: BMW's Valvetronic system [13]

Valvetronic is often combined with BMW's VANOS system to phase valve timing. The VANOS system has two positions for each camshaft, giving two timing options. It does not allow for independent valve opening and closing times.

Fiat Multiair

Fiat employs a hydraulic variable valve system in its Multiair engine (Figure 2.7). This engine has been in production since 2009. Multiair engines use a standard camshaft to actuate hydraulic pistons. The pistons pressurize hydraulic fluid to actuate the hydraulic cylinders and open the engine valves. A solenoid on each valve can be used to dump the hydraulic pressure to open the valve late, close it early, or not open it at all (cylinder shut off).

This system offers the variable valve lift benefits of BMW's Valvetronic system without the complex mechanical system. It demonstrates the real-world feasibility of a system using hydraulically actuated engine valves.

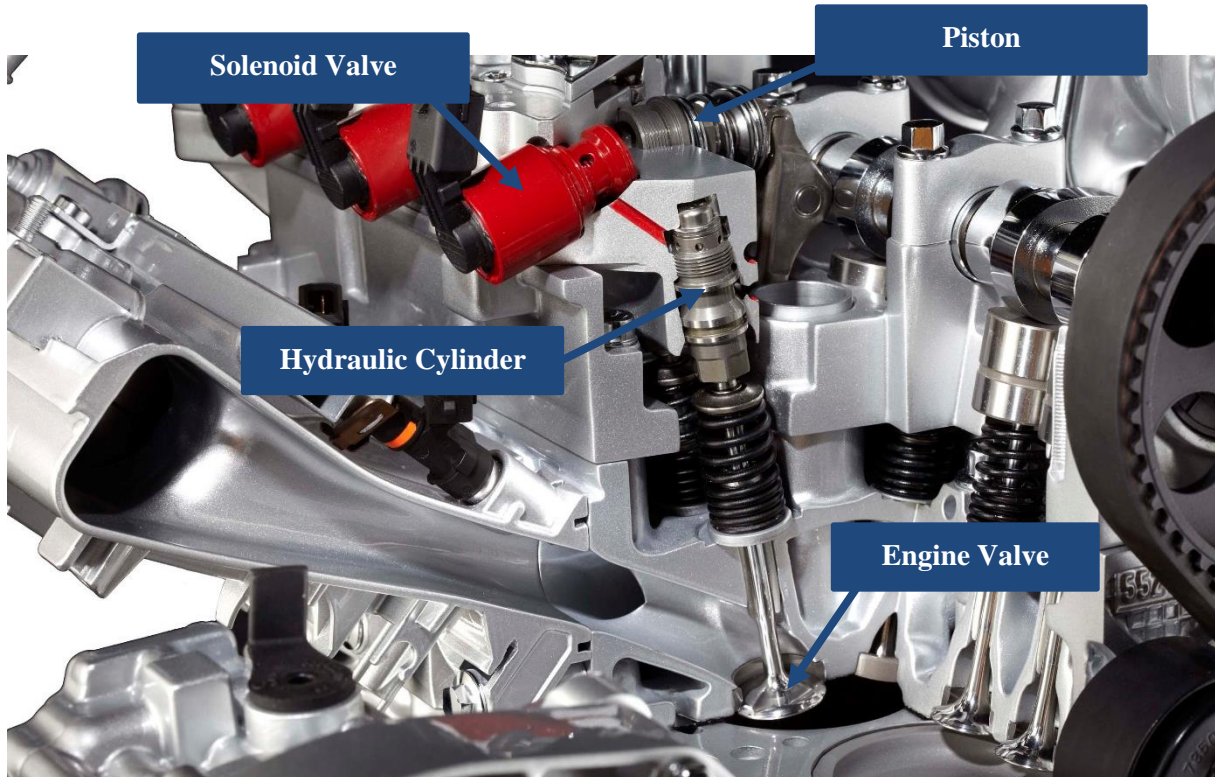


Figure 2.7: Fiat's Multiair system [14]

Multiair Disassembly

The MVSL purchased a Multiair unit to disassemble and see a practical application of hydraulically operated engine valves (Figure 2.8). The most significant components in relation to this research project were the hydraulic cylinders used to actuate the engine valves.



Figure 2.8: Disassembled Multiair unit

The hydraulic cylinders (Figure 2.9) of the Multiair system are compact and modular. They screw directly into the Multiair unit and have built in hydraulic cushioning to reduce engine valve closing speeds (improving engine valve and valve seat life).



Figure 2.9: Multiair hydraulic cylinder

2.1.3 VVA Emerging Technologies

There are multiple VVA technologies currently being developed but not yet available in production vehicles. A hydraulic VVA system [15], an electro-hydraulic VVA system [16], a variable valve lift (VVL)

system using magneto-rheological (MR) fluid [17], Koenigsegg's Freevalve [18], Camcon's intelligent Valve Technology (iVT) [19], and Hyundai's Continuously Variable Valve Duration (CVVD) technology [20], [21] are all detailed below.

Hydraulic VVA System

A hydraulic VVA system (Figure 2.10a) is in development at Shandong University in China. This system uses a similar concept to the Fiat Multiair system (detailed above). A camshaft is used to actuate a hydraulic tappet. The tappet pressurizes hydraulic oil and pushes on the hydraulic piston to open the engine valve. There is an oil relieving valve in between the piston and the tappet that can be used to bleed the hydraulic pressure and close the engine valve.

The oil relieving valve is a rotary spool valve (Figure 2.10b) The spool rotates with the camshaft and the valve sleeve can be rotated independently. Both the spool and the sleeve have an outlet port (A & B). If these ports line up during a valve open event, the hydraulic pressure will be bled to the low pressure oil reservoir and the valve will close. The position of valve sleeve will determine when this valve closure will occur.

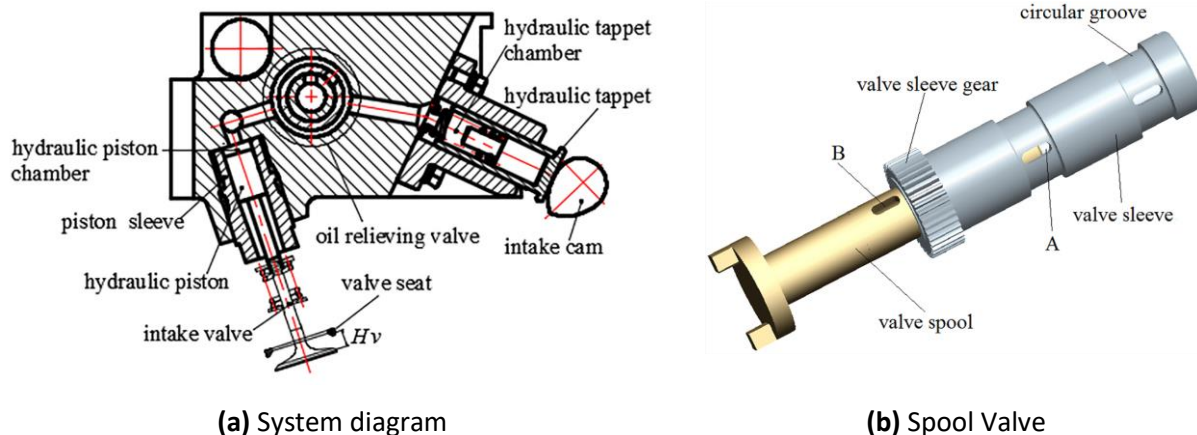


Figure 2.10: Hydraulic VVA system [15]

Experimental results from this system showed pressure and valve lift height fluctuations at high engine speeds [15]. The initial impulse causing these vibrations was from the profile of the intake cam, so a less aggressive profile was recommended.

This system is limited to the range of the cam profile and can only change the closing point of the valve.

Electro-Hydraulic VVA System

An electro-hydraulic VVA system (Figure 2.11) is being developed by Jiangsu Gongda Power Technologies Ltd. and Michigan State University. This system uses solenoid actuated control valves to direct high pressure oil to open the engine valves.

This setup can be used to produce two discrete valve lift heights. For high valve lift, the lift control sleeve is held in the lower position (as shown in Figure 2.11) by low pressure oil. For low valve lift, the lift valve is opened, and the sleeve is held in the upper position (red outline in Figure 2.11) by high pressure oil.

The control for this system is complex as it must account for the transportation delay of the fluid and the delay in energizing the solenoid electro-magnetic coil [22].

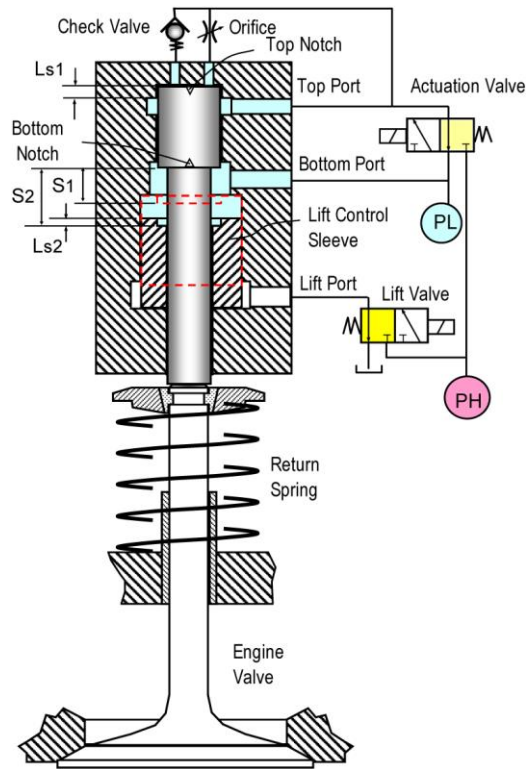


Figure 2.11: Diagram of electro-hydraulic VVA system [16]

Magneto-Rheological Fluid VVL System

A VVL system using MR fluid is in development at the Taipei University of Technology. MR fluid changes its resistance to flow in the presence of a magnetic field. The stronger the magnetic field, the stronger the

resistance will be. This system uses a typical camshaft to actuate a rocker arm. This arm pushes on a magnetic plate block suspended in MR fluid surrounded by an electromagnetic coil (Figure 2.12).

If no current is applied to the coil, the MR fluid will have minimal resistance and the engine valve lift will match the cam profile. When current is applied, the fluid will offer resistance and reduce the total lift height of the valve. If enough current is applied, the valve will remain fully closed.

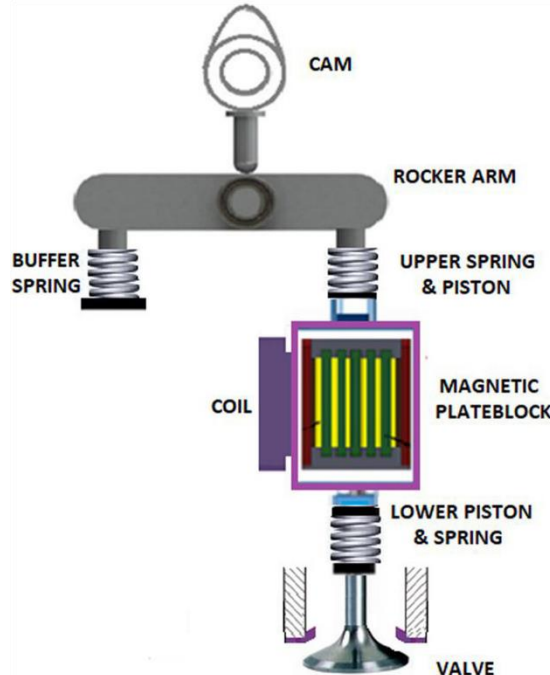


Figure 2.12: MR fluid valve diagram [17]

The MR fluid valve can be used for throttleless engine control by restricting the total valve lift height. It can also be used for VVA strategies that require a late valve opening. However, it is unable to change the closing point of the engine valve and cannot move outside of the standard cam profile without an additional VVT system.

Koenigsegg Freevalve

Koenigsegg has developed a camless fully variable valve actuation system (Figure 2.13) [18]. It uses electro-hydraulic-pneumatic actuators to open and close the engine valves. Solenoids are used to control the valve timing and lift, high pressure air is used to open the valves, hydraulic oil is used to hold the valves open, pneumatic springs are used to close the valves, and hydraulic oil provides cushioning for valve closure.

This system shows the desirability of a fully variable system but requires complex control of precision solenoid valves and is not mechanically coupled to the engine crankshaft. It is not currently installed on any production cars.



Figure 2.13: Koenigsegg's Freevalve system [18]

Camcon iVT

Camcon's intelligent Valve Technology (Figure 2.14) [19] uses precision electric rotary actuators driving individual camshafts for each engine valve. The camshafts can be operated at any point of the engine cycle (giving fully flexible valve timing). The actuators can rotate the camshaft through a full rotation for full valve lift (a standard valve profile) or rotate the camshaft partially then reverse direction and close the valve for partial valve lift. This system is fully flexible in terms of valve timings and lifts. It is a desmodromic system: the same mechanism that opens the valves also closes them and no valve springs are required.

Like Koenigsegg's Freevalve, Camcon's system is mechanically decoupled from the engine crankshaft. It is completely digitally controlled, requiring high frequency controls and precision high speed actuators. It also requires a complex cam follower mechanism.

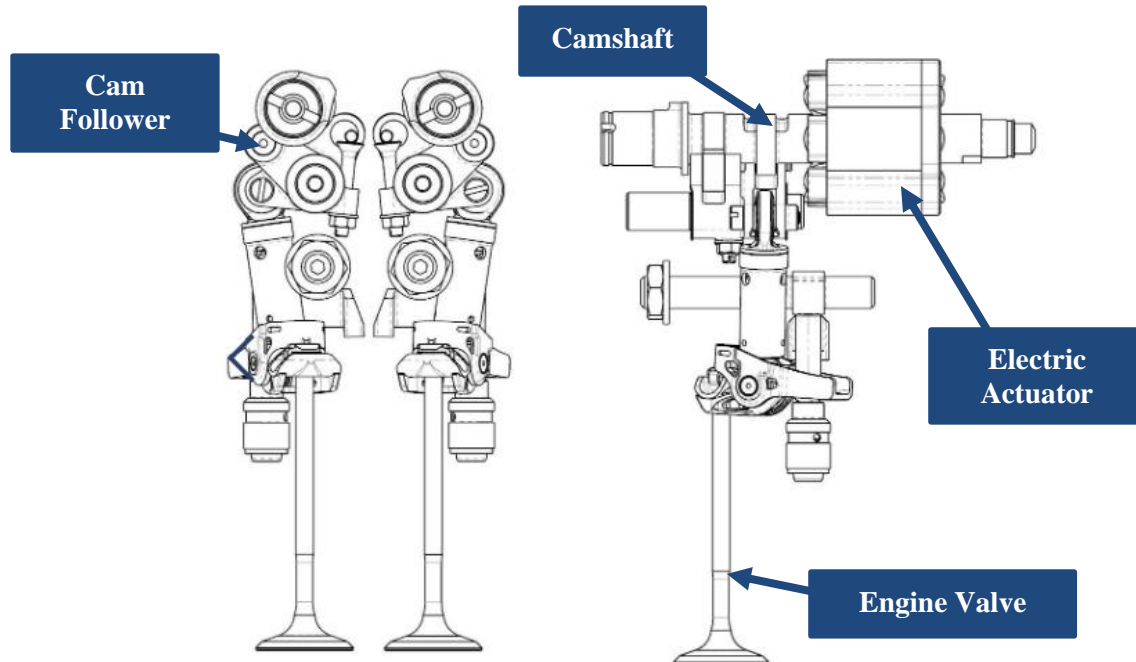


Figure 2.14: Camcon engine valve actuation mechanism [19]

Hyundai's CVVD System

Hyundai has recently unveiled a continuously variable valve duration system (Figure 2.15) to be used on upcoming Hyundai and Kia vehicles.



Figure 2.15: Hyundai's CVVD assembly [16]

This system uses a linkage mechanism to connect the cams and camshaft and adjust valve timing. The cams and camshaft share the same axis of rotation but can rotate separately. The cam rotates with the blue arm in Figure 2.16, and the camshaft rotates with the red arm. The location of the pivot point of the

interconnecting grey linkage determines the relationship between the cam and camshaft rotation and the resulting engine valve lift profile.

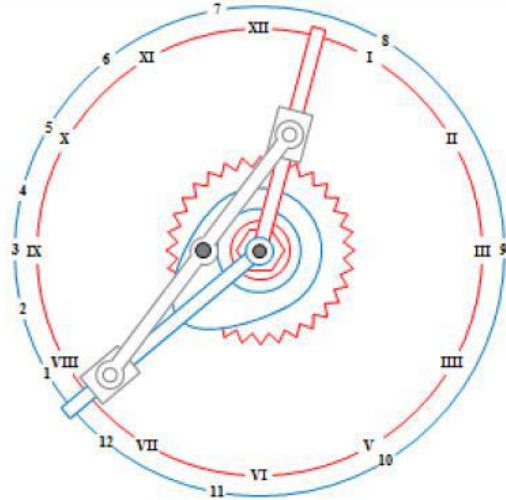
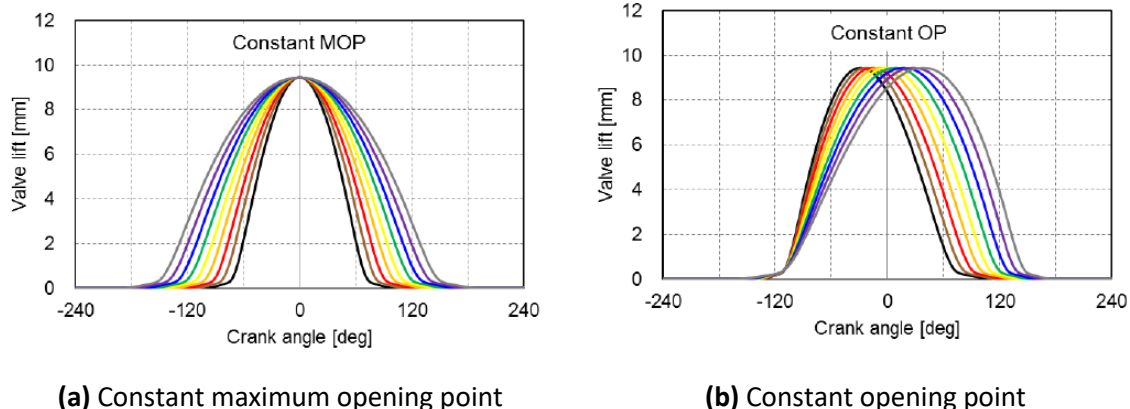


Figure 2.16: Hyundai's mechanism [15]

The pivot point can be adjusted to keep a constant maximum opening point (Figure 2.17a), a constant opening point (Figure 2.17b), or a constant closing point for the engine valve.



(a) Constant maximum opening point

(b) Constant opening point

Figure 2.17: Valve lift profiles [15]

Hyundai's system gives the benefit of maintaining the maximum valve lift height while changing the valve timing, but it still requires an additional VVT system to give fully independent control of each valve open/close event.

2.2 HVVA Project Description & Background

2.2.1 HVVA System Requirements

In order to be a viable and meaningful alternative to the new and existing VVA technologies described above, a successful HVVA system must have:

- Fully flexible valve timing
 - The open and close point of either engine valve must be adjustable between 0 and 720°CA
- Fully flexible valve lift height
 - Adjustable from 0 to 5.5mm for Honda GX200 test engine
- Reliable operation in typical engine operating speeds and conditions
- Power consumption similar to a cam based system valvetrain (125 W for two engine valves at 1500 RPM [23])
- Compact physical size to mount on existing engine blocks

The HVVA system by the Mechatronics vehicle systems lab at UW is being developed to meet or exceed these requirements.

2.2.2 HVVA Description

The basic HVVA system is shown in Figure 2.18. A hydraulic system supplies pressure to hydraulic cylinders to open and close the engine intake and exhaust valves. High pressure spool valves (HPSV) and low pressure spool valves (LPSV) rotate with the crankshaft and control the timing of valve opening and closing events. A hydraulic accumulator is used to provide constant pressure through the cyclic opening and closing of engine valves.

A phasing system between the crankshaft and each spool valve is used to change the angular position of the spool valve relative to the crankshaft. The valves can then be phased to any position, and the intake and exhaust valves can be open or closed at any desired crank angle.

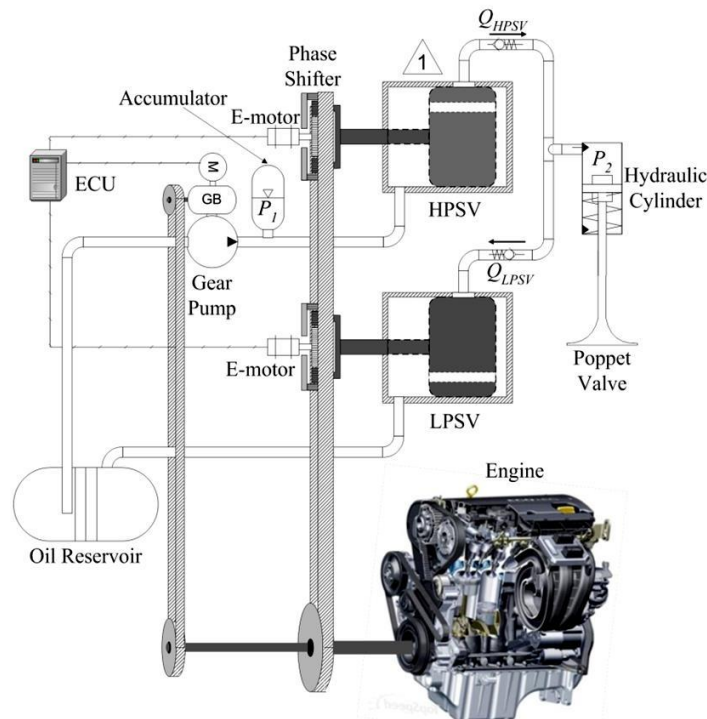


Figure 2.18: Overall system diagram [3]

The rotary valves have ports on the spool and ports on the valve casing (Figure 2.19). When these ports line up, the high pressure spool valve (HPSV) supplies high pressure fluid to the hydraulic cylinders or the low pressure spool valve (LPSV) opens a fluid path to the system reservoir. When the HPSV ports line up, the engine valve will open. When the LPSV ports line up, the engine valve will be forced closed by the engine valve spring.

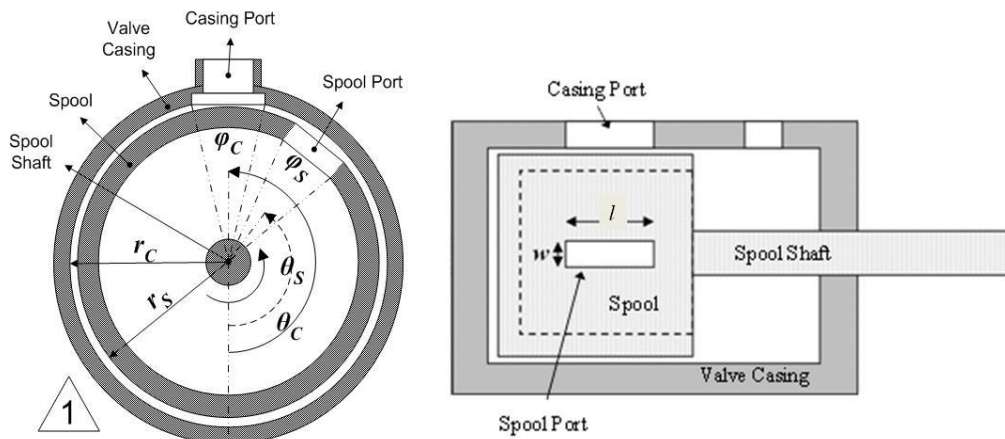


Figure 2.19: Rotary spool valve cross section [3]

2.2.3 HVVA System Background

This project is an iteration of work completed by previous graduate students. Contributions by Pournazeri [3], Chermesnok [4], and Siddiqui [5] are detailed below.

Pournazeri's Work

An initial system concept for the HVVA system was patented by Pournazeri and Amir Khajepour [24]. Pournazeri took this concept and developed a mathematical system model and single valve prototype. The concept was designed to eliminate the camshaft from an internal combustion engine and replace it with a fully flexible hydraulic system.

Pournazeri's math model gave initial sizes for his prototype, and his spool valve leakage calculations were used to size the clearance between the spool valve and the spool valve casing for Siddiqui's project and the current project iteration.

His prototype (Figure 2.20) actuated a single valve and was not connected to an engine. The spool valves were made by pressing a larger diameter spool onto a spool shaft and fitting this inside of the valve casing (Figure 2.21). Servo motors were used to rotate each spool valve separately and valve timing was completed at the software level. This prototype did not have a phasing system.

This first prototype proved the feasibility of the HVVA system and laid the foundation for future work.

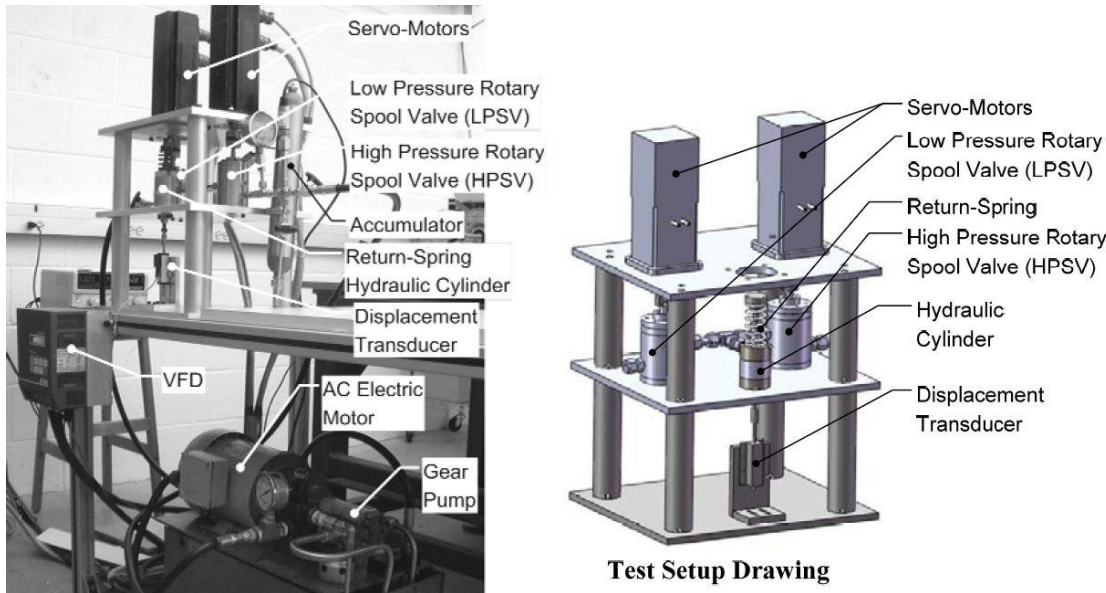


Figure 2.20: Pournazeri's prototype [3]

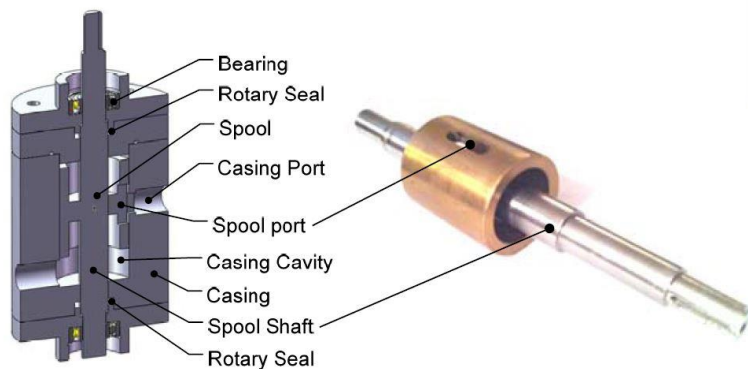


Figure 2.21: Pournazeri's spool valve [3]

Chermesnok's Work

Chermesnok extended Pournazeri's prototype to work with multiple cylinders. He added ports to a hollow spool shaft to feed multiple engine cylinders (Figure 2.22).

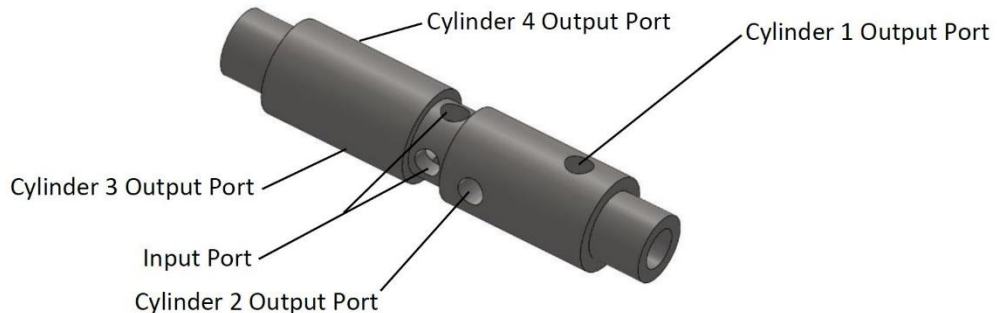


Figure 2.22: Multi cylinder spool shaft design [4]

For the HPSV, the input port is connected to the high pressure supply line. For the LPSV, the input port is connected to the reservoir. The remaining ports are connected to the engine valves of the corresponding cylinders (Figure 2.23 & Figure 2.24)

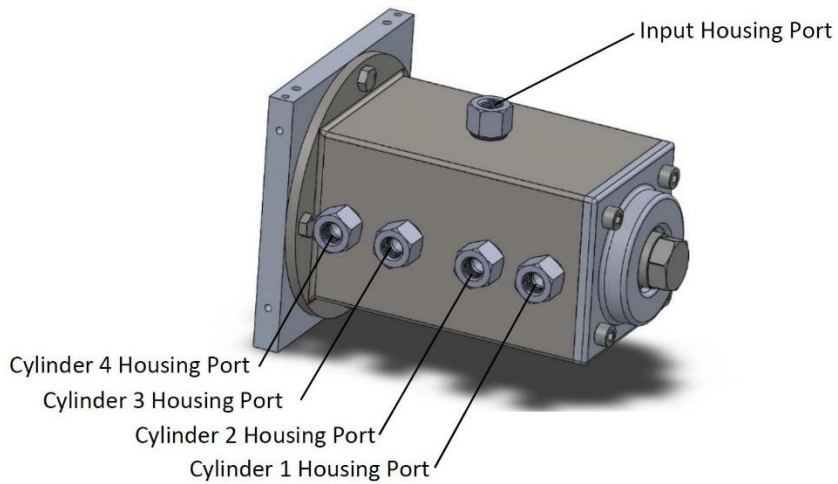


Figure 2.23: Chermesnok's spool valve housing [4]

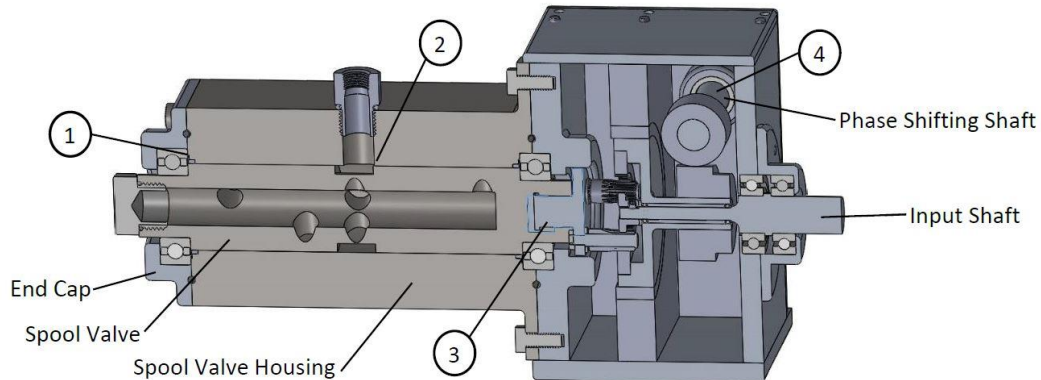


Figure 2.24: Section view of Chermesnok's spool valve [4]

Ultimately, this larger diameter shaft proved difficult to seal, and fell out of straightness tolerance after heat treatment, creating problems due to friction.

Chermesnok added phase shifting to his prototype. He used a planetary gear setup (Figure 2.25) where the sun gear is connected to the input (from the crankshaft) and the output (to the spool valve) is connected to the planet gears. The ring gear can be rotated using a worm gear actuated with a servo valve. Rotating the ring gear will change the position of the spool valve relative to the crankshaft.

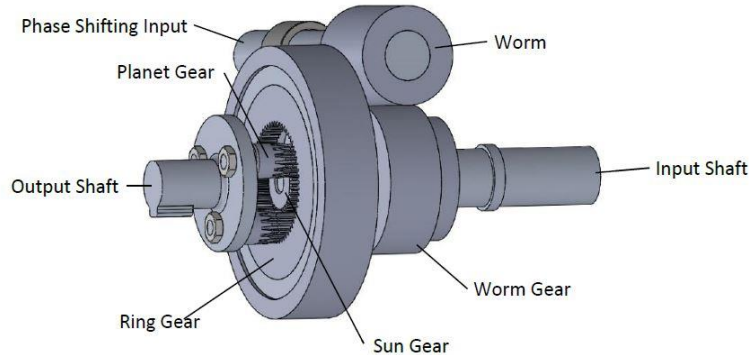


Figure 2.25: Chermesnok's planetary gear phase shifter [4]

Chermesnok also designed and prototyped custom hydraulic cylinders with built in hydraulic cushioning to reduce the valve seating velocity (Figure 2.26).

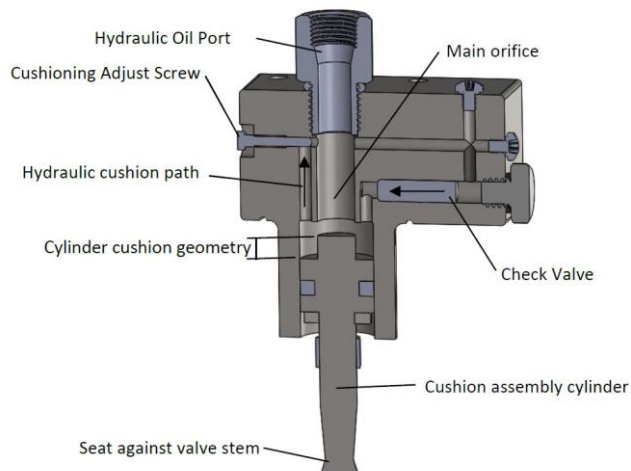


Figure 2.26: Chermesnok's hydraulic cylinder design (with built in hydraulic cushioning)

Chermesnok ran single valve experiments using his updated spool valve and hydraulic cylinder designs. Data collected from running his setup was used to develop the next prototype by Siddiqui.

Siddiqui's Work

Siddiqui's prototype was the first to be installed on a Honda GX200 test engine and used to perform combustion testing.

He returned to the spool valve design used by Pournazeri and added the planetary gear phasing design used by Chermesnok. This was all combined into two pairs of spool valves to actuate the intake and exhaust valves of a single cylinder engine.

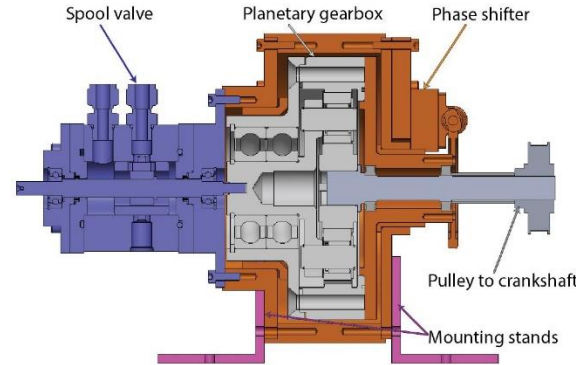


Figure 2.27: Siddiqui's spool valve design [5]

He modified the hydraulic cylinder designed created by Chermesnok by extending the top of the valve shaft to establish two points of contact for the sliding valve and prevent twisting of the valve.

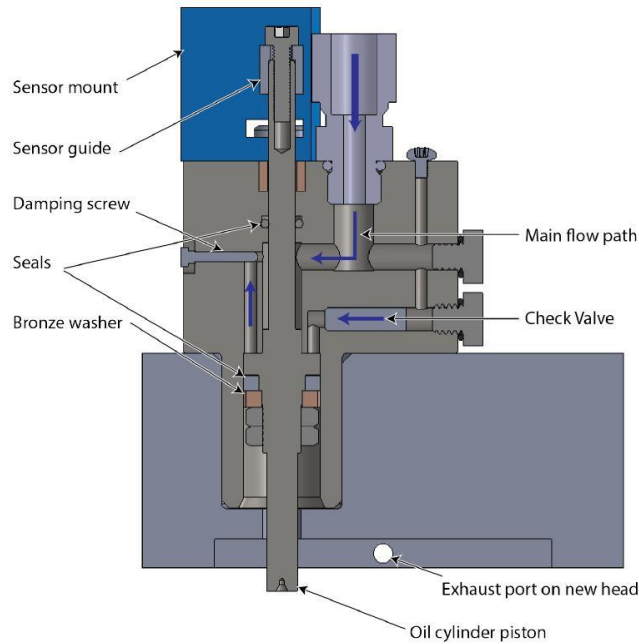


Figure 2.28: Siddiqui's hydraulic cylinder design [5]

Combustion experiments were run using the original Honda GX200 engine carburetor setup. Siddiqui's design is discussed in detail in Section 3.1.

Chapter 3

System Design

A new VVA system was designed and built using experience and knowledge gained from the previous prototypes with the same working principle (see Section 2.2.1). The main focus of the new design was to minimize the complexity and the size of the system while maintaining the reliability and functionality of the most recent prototype by Siddiqui [5]. His prototype worked consistently through many hours of testing but is much larger than required. Additionally, the experimental setup was subject to large amplitude vibrations at certain (common) operating points.

3.1 Previous Prototype Evaluation

Siddiqui's prototype was tested both to test Yangtao Li's optimized engine valve timings [2] and evaluate the performance of this HVVA system iteration. The results of this evaluation are detailed below.

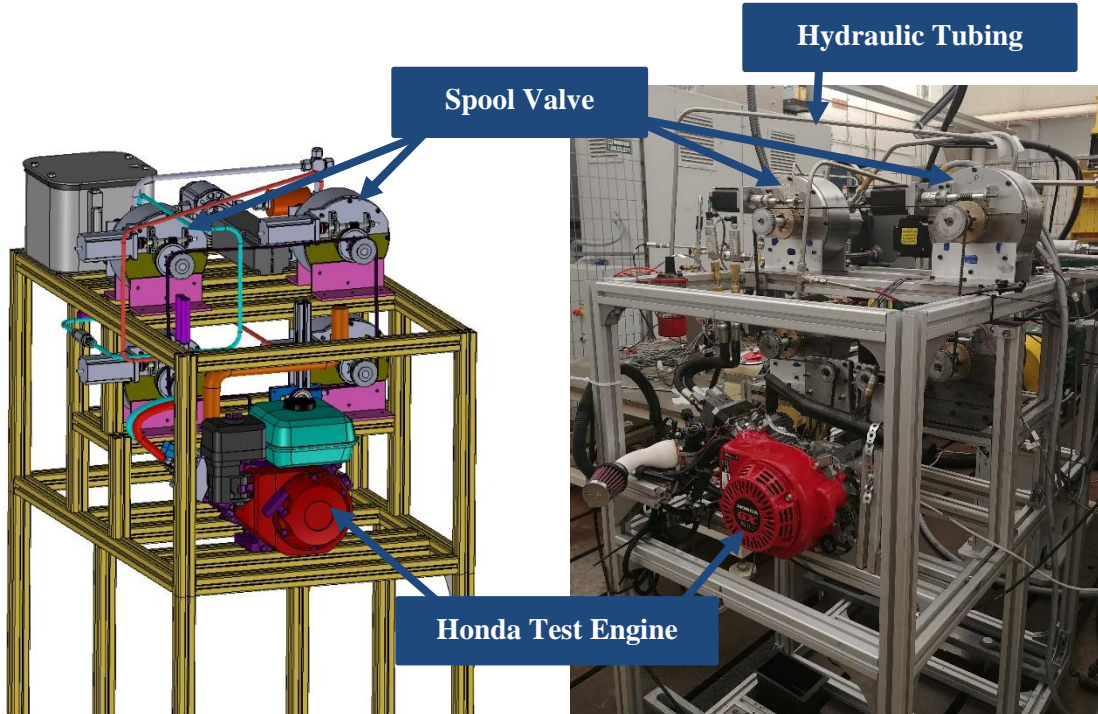


Figure 3.1: General assembly view of Siddiqui's prototype [5]

3.1.1 Hydraulic System

Siddiqui's prototype was developed to prove that the hydraulic VVA system would perform as expected. The size and layout (Figure 3.2) of the hydraulic system was therefore not optimized when it was installed. This resulted in long tubing runs between spool valves and engine valves (Figure 3.1). Additionally, uneven lengths of tubing were run from the high pressure spool valves to the intake and exhaust valves on the engines.

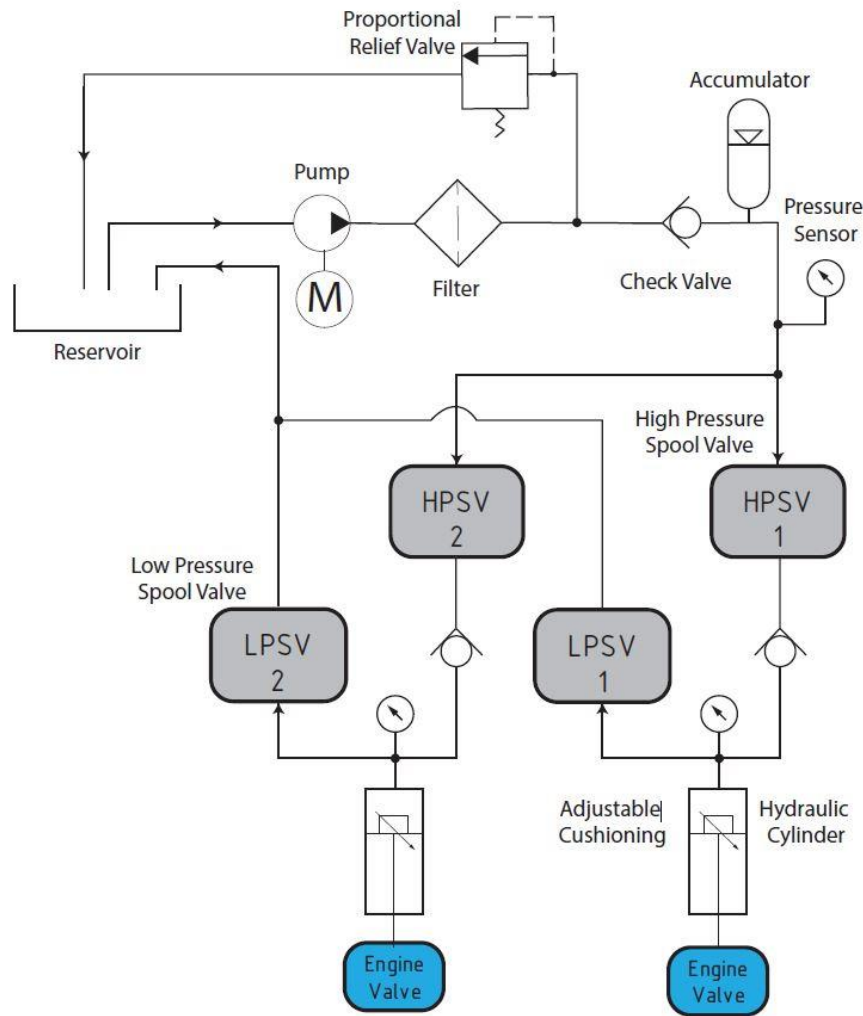


Figure 3.2: Hydraulic schematic [5]

The added length of tubing created unnecessary pressure drop and the uneven lengths of tube for the different engine valves contributed to low intake valve lift heights.

The large amount of tubing also required many tubing connections. Under excessive system vibration, some of these tubing connections and the seal of the hydraulic pump failed. Both failures caused leakage in the hydraulic system.

The accumulator installed in the hydraulic system was designed to have a precharge pressure of 250psi. The actual precharge pressure of the accumulator was measured to be >350psi. Therefore, with typical operating pressures of 250-300psi, no fluid was being stored in the accumulator. The only flow available to each engine valve was flow directly from the pump and the small amount of compressibility in the system (from trapped air and system stiffness).

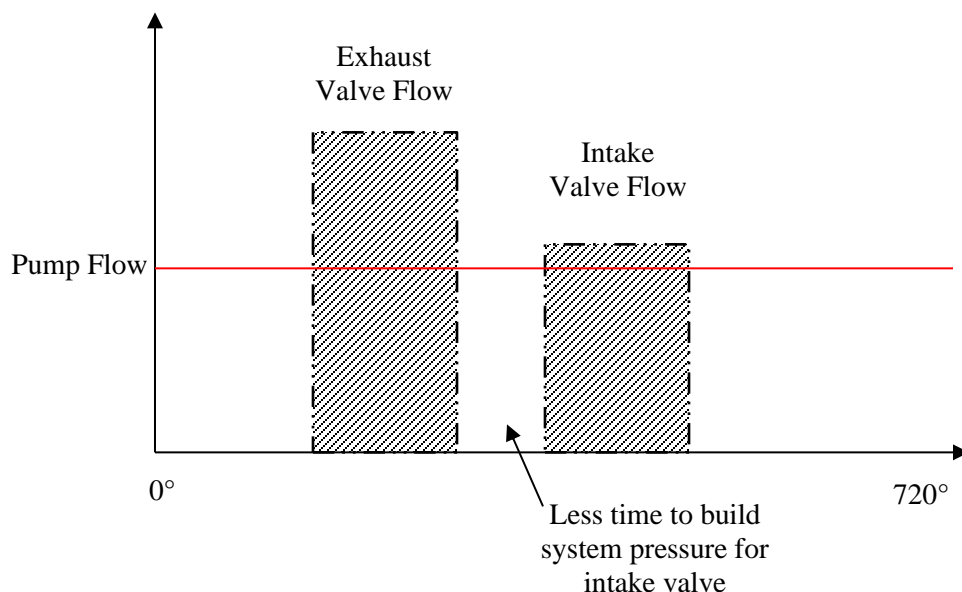


Figure 3.3: System fluid flows when operating less than accumulator precharge pressure

With no fluid stored in the accumulator, the small amount of fluid stored due to system compressibility would be available to lift the exhaust valve (as the exhaust valve opens before the intake valve in a four-stroke engine cycle, see Figure 2.1) but not available to lift the intake valve (Figure 3.3). This would be equivalent to having a very small accumulator in the system with insufficient volume to lift both valves. Therefore, this contributed to a system showed a consistently higher exhaust valve lift than intake valve lift (Figure 3.4). For this system, equal exhaust and intake valve lift heights were required.

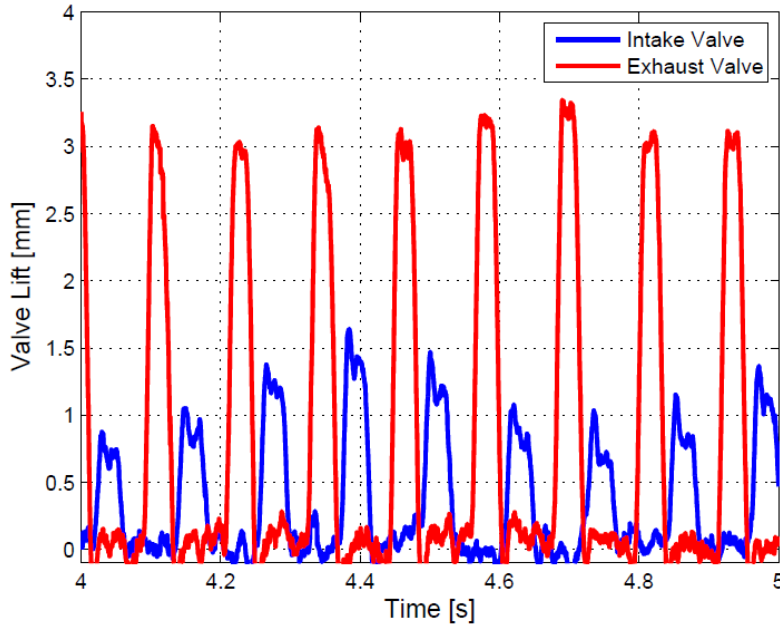


Figure 3.4: Discrepancy between exhaust and intake valve lifts [5]

Siddiqui's hydraulic system was mounted on top of one large aluminum frame. The frame supported the hydraulic pump, reservoir, all four spool valves, tubing, and the test engine. When running tests, vibration from both the pump and the engine would resonate through the frame. This vibration contributed to many issues in the system.

3.1.2 Spool Valves

As Siddiqui reverted to the spool valve design of Pournazeri, they ran without the large amounts of heat observed in Chermesnok's prototype. Siddiqui used the leakage calculations developed by Pournazeri to determine the maximum gap between the spool and the spool casing. Testing of the system did not show early opening or closing of engine valves that would indicate excessive spool valve leakage. The overall design and tolerances of Siddiqui's design were therefore carried over to the new design.

However, the spool valves of Siddiqui's design take up a very large amount of space (Figure 3.5). Each spool has its own casing and planetary gear for phase shifting. They were all mounted separately, and a long timing belt was used to couple them to the crankshaft.

Additionally, the shaft diameter used at the point of sealing was larger than required and necessitated the purchase of expensive flanged rotary seals. These seals were rated for the shaft speed and system operating pressure but leaked when there was no pressure applied to the system.

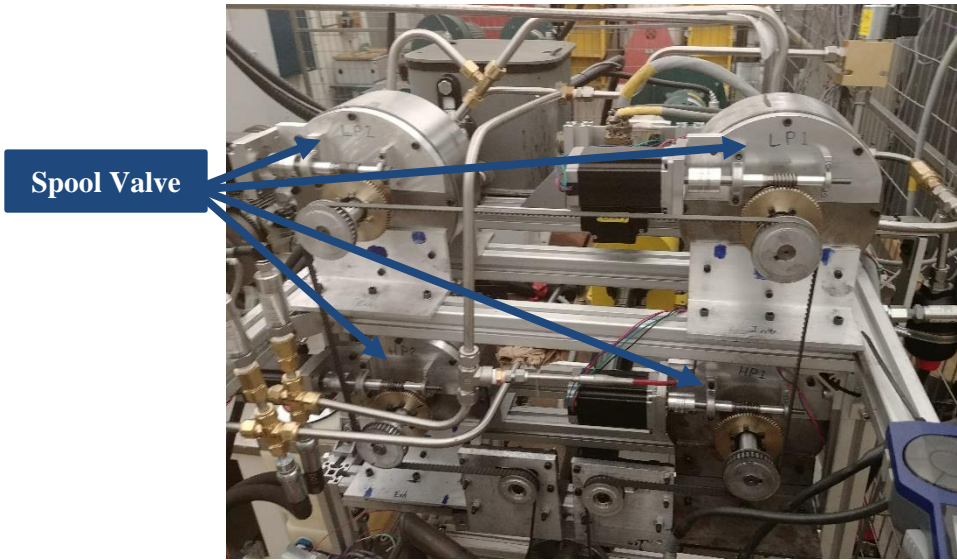


Figure 3.5: Spool valves in fully assembled system

Through simulations and testing by Siddiqui, the size of the outlet ports on the low pressure spool valves were found to be too small. At high engine speeds, there was valve float: the engine valves did not fully close between cycles. To avoid this, stiffer springs were added to the engine valves. However, this solution also increases the pressure and energy required to operate the system.

3.1.3 Hydraulic Cylinders

The hydraulic cylinders developed by Siddiqui functioned well at engine speeds up to 2000 RPM but did not prove to be reliable over repeated testing cycles. After continued use of the system, the nuts used to hold the valve seals in place vibrated loose and each valve leaked significant amounts of hydraulic fluid into the engine crank case and combustion chamber.

3.1.4 Phase Shifters

Siddiqui's prototype used planetary gears to adjust the phase angle of each of the spool valves (Figure 3.6). The worm gear acts as the phasing input and is connected to the ring gear. During normal operation, the phasing input (ring gear) is fixed and the engine input (sun gear) is directly transmitted to the spool valve input (planet carrier output). If different valve timing is required, a stepper motor rotates a worm that drives the worm gear and the worm gear rotates the ring gear. As the ring gear rotates it changes the position of the carrier relative to the sun gear.

This system greatly increased the size of each spool valve assembly and added the complexity of many precision parts to the system.

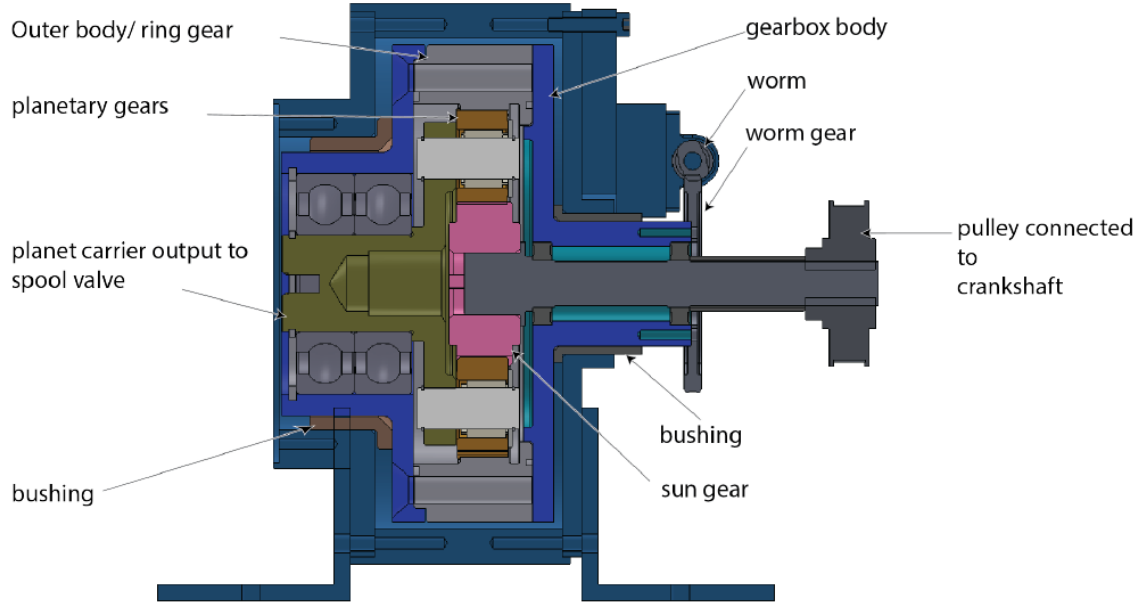


Figure 3.6: Planetary gear phasing system

3.1.5 Drive System

All the spool valves were driven by a timing belt coupled to the engine crankshaft (Figure 3.7). A very long (83") belt was required to connect all the spool valves of this large prototype. Each spool valve timing belt pulley had less than one quarter of its teeth engaged with the belt. This low engagement was the potential cause for the HPSV shifting out of phase under excessive system vibration.

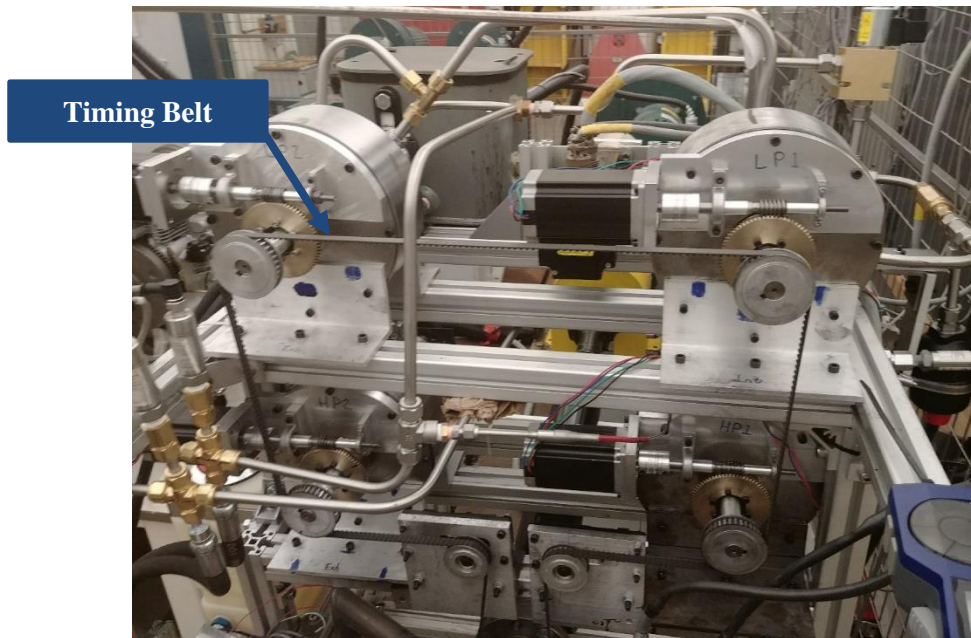


Figure 3.7: Timing belt drive

3.1.6 Sensors

Over the course of many tests (both with and without combustion), multiple pressure sensors and encoders on this system failed due to excessive vibration and inadequate support.

The linear displacement sensors used to measure valve lift provided very noisy data. They only outputted correct measurements in a very limited range and proved difficult to implement.

Valve pressure transducers were not mounted directly at the valves and pressure reading fluctuations did not always correlate with the valve position sensors. More significantly, pressure data was improperly filtered before being recorded and the data collected was not reflecting actual changes in the system. The filter had a delay of 100 ms with valve opening event durations less than 13 ms. Figure 3.8 shows the significant loss of available pressure data after being filtered.

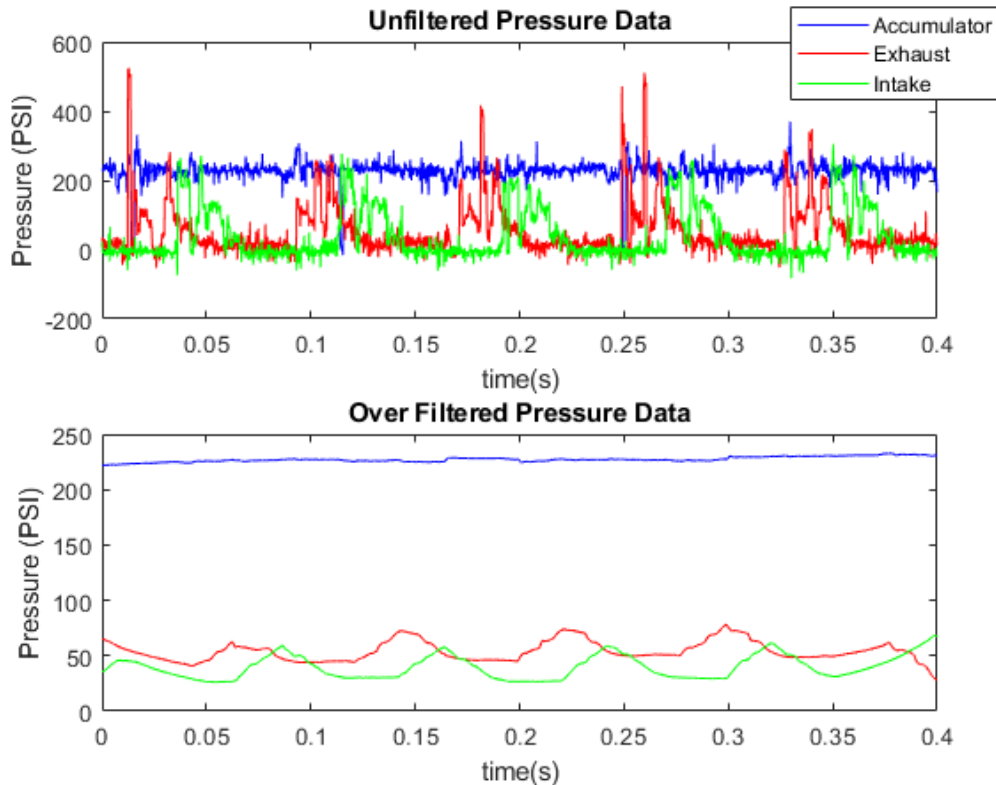


Figure 3.8: Pressure data before and after being filtered

3.2 New System Design

Experience gathered from running experiments on Siddiqui's prototype led to the design of a new prototype. This new design combines the four spool valves into one unit (the spool valve assembly). This reduces the overall size of the system and reduces the length and complexity of hydraulic tubing. Additionally, the phase shifting system has been completely redesigned into a smaller, simpler package. Overall the new design retains the best parts of Siddiqui's design while being more compact and more resistant to system vibration. The full CAD model of the design is shown in Figure 3.9. The new setup will be installed on a Honda GX200 single cylinder engine with two engine valves (one intake & one exhaust). The engine is rotated using a dynamometer (dyno) that sets a constant speed and measures input and output torque (for combustion tests).

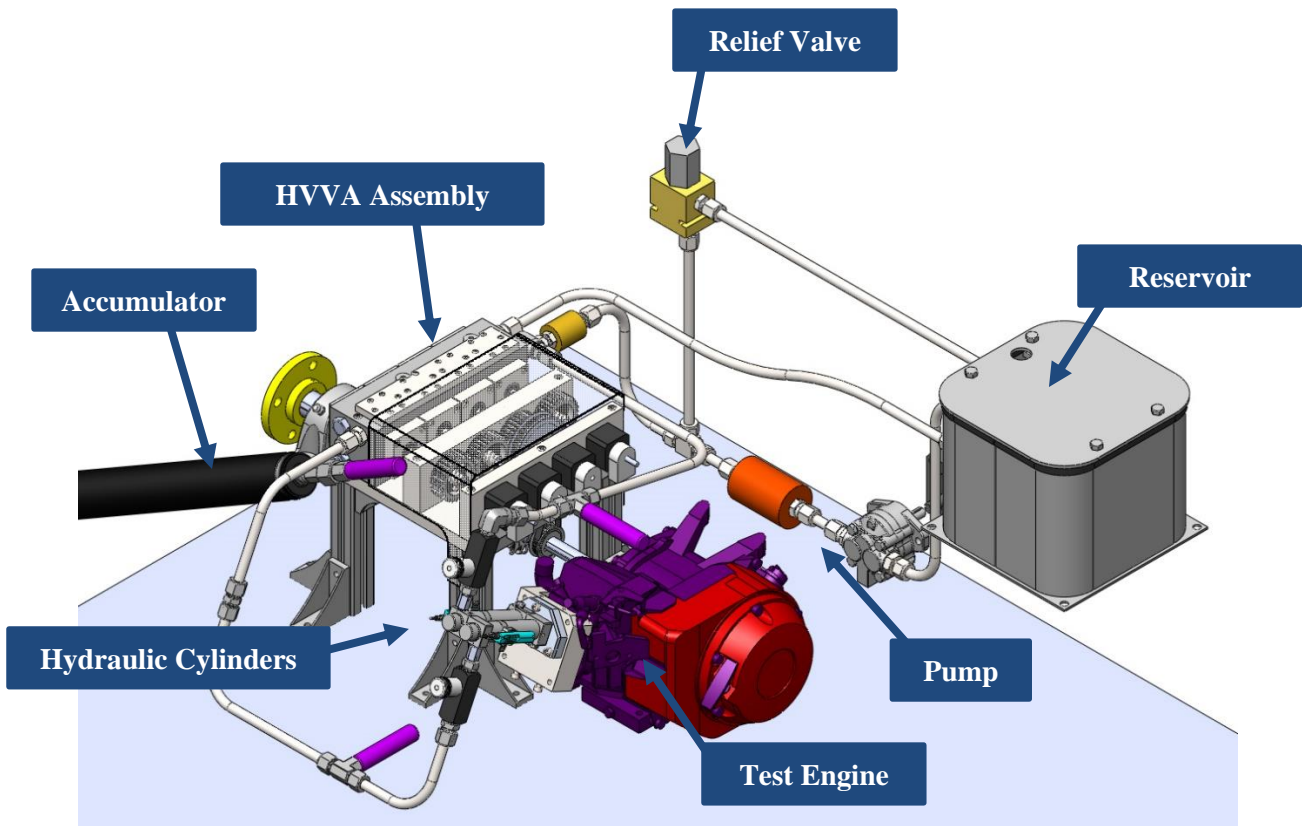


Figure 3.9: General assembly view of new prototype

3.2.1 Hydraulic System

The hydraulic system has been simplified and optimized for the new HVVA design (Figure 3.10). Hydraulic tubing has been minimized combining all four spool valves together in one block (eliminating any external tubing interconnecting the spool valves). Tube sizes & port sizes have been designed to reduce pressure drop, flow control valves have been added to dampen pressure fluctuations, and the whole system has been rigidly mounted to a steel table to reduce vibration amplitudes and resulting failures.

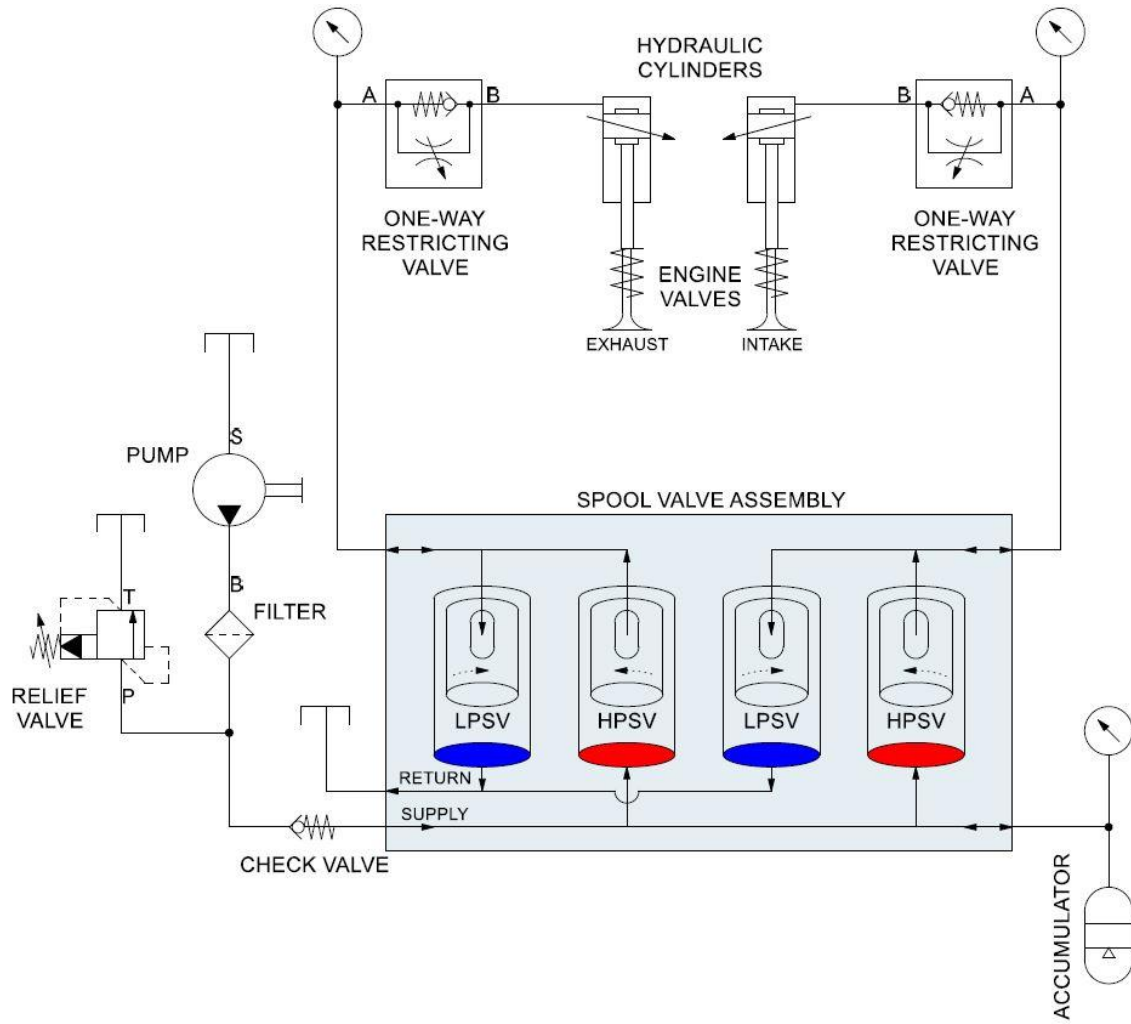


Figure 3.10: Hydraulic schematic for new HVVA design

Tube Sizing

The hydraulic tubing and passages in the spool valve block were sized to minimize pressure drop (resulting in lower system losses and greater overall efficiency). To this end, passages and tubing were generally oversized in order to ensure maximum velocities, v_{max} , would be less than 3.05 m/s (10 ft/s) for return lines and 7.62 m/s (25 ft/s) for pressure lines [25]. The maximum flow in the tube (Q_{max}) is used to calculate the required tube diameter (d_{tube}) as [25]:

$$d_{tube} = 4.61 \left(\frac{Q_{max}}{v_{max}} \right)^{0.5} \quad (3.1)$$

The maximum flow for each tube section will be the maximum volume of oil in the hydraulic cylinder (V_{max}) divided by the total time (t_{open}) to fill or empty the cylinder. The maximum instantaneous flow is calculated as:

$$Q_{max} = \frac{V_{max}}{t_{open}} \quad (3.2)$$

The maximum volume in the cylinder is the maximum valve lift height (l_{max}) multiplied by the cylinder cross sectional area (A_{cyl}). The time to lift the valve is the length of time that either the HPSV or LPSV is open and allowing passage of oil.

The open duration, $\Delta\theta$, of a spool valve starts when the leading edge of the spool port touches the leading edge of the casing port (when $\theta_S = \theta_{S1}$) and ends when the trailing edge of the spool port touches the trailing edge of the casing port (when $\theta_S = \theta_{S2}$). The angles are shown in Figure 3.11 and calculated by:

$$\begin{aligned} \theta_{S1} &= \theta_C - \left(\frac{\varphi_C}{2} + \frac{\varphi_S}{2} \right) \\ \theta_{S2} &= \theta_C + \left(\frac{\varphi_C}{2} + \frac{\varphi_S}{2} \right) \\ \Delta\theta &= \theta_{S2} - \theta_{S1} = \varphi_C + \varphi_S \end{aligned} \quad (3.3)$$

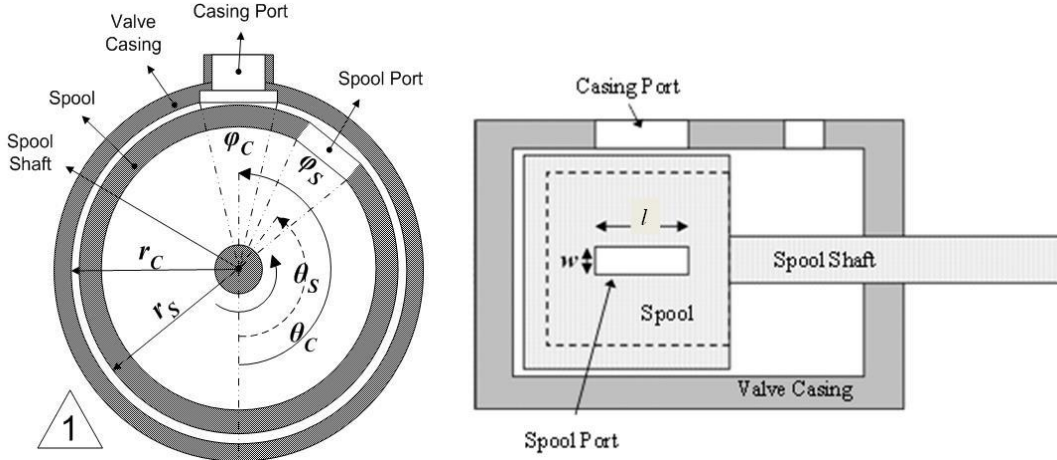


Figure 3.11: Rotary spool valve cross section [3]

The total open time of the spool valve is the opening duration in degrees divided by the angular velocity of the spool valve as calculated by:

$$t_{open} = \frac{\varphi_c + \varphi_s}{\frac{N_e}{2} \left(\frac{360}{60} \right)} \quad (3.4)$$

The spool valves rotate at half of the engine speed (N_e).

Table 3.1: Max Flowrates – Solutions to Equations 3.2, 3.3, & 3.4

Description	Variable	Value
Max Engine Speed	N_e	3600 RPM
Max Valve Lift Height	l_{max}	7 mm
Hydraulic Cylinder Area	A_{cyl}	315 mm ²
Max Cylinder Volume	V_{max}	2205 mm ³
Spool Valve Port Angle	φ_s	20°
HPSV Casing Port Angle	φ_c	20°
HPSV Open Duration	t_{open}	3.7 ms
LPSV Casing Port Angle	φ_c	62°
LPSV Open Duration	t_{open}	7.6 ms
Max Opening Flow	Q_{max}	35.7 lpm
Max Closing Flow	Q_{max}	17.4 lpm

The minimum tube diameter for each tube section and spool valve casing passages can then be calculated using Equation 3.1 with maximum velocities of 3.05 m/s for return lines and 7.62 m/s for pressure lines and maximum flows shown in Table 3.1. Minimum diameters are shown in Table 3.2.

Table 3.2: Tube & Casing Passage Sizes – Solutions to Equation 3.1

Pressure/Return Flow	Flow (Q_{max})	Min. Diameter (d_{tube})
Pressure	35.7 lpm	10.0 mm
Return	17.4 lpm	11.0 mm

The oil passages that run to each hydraulic cylinder are used for both pressure and return flow. To avoid excessive back pressure for return flow, these lines were all sized for max 3.05 m/s oil velocity. Therefore, all lines were sized or manufactured to be minimum Ø11mm. In order to use standard sizes, Ø1/2" steel tubing was used for all external tubing. For cross drilled holes in the spool valve casing (to allow for flow between spool valves), Ø12mm diameter passages were used. Tube and block minimum thicknesses were designed for 1000 PSI system pressure. Actual operating pressures were limited to 500 PSI.

Port Sizing

The port size on the spool valves (Figure 3.12) affects how much pressure drop there will be across the valves. Therefore, the port size was designed to have low velocities to minimize the pressure drop.

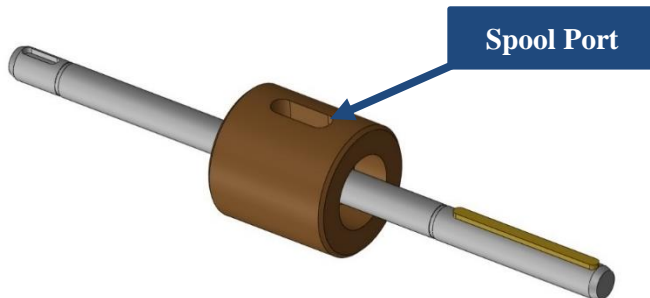


Figure 3.12: Spool valve removed from casing

The ports are slot shaped and the width is fixed at 6.1mm for a 20° port angle (φ_S) and a 35mm spool diameter (Figure 3.11). The minimum open area is calculated using the maximum return flow and the maximum return line velocity. The opening area is adjusted by changing the length of the slot. Slot length is calculated as:

$$L_{slot} = \frac{\left(\left(\frac{Q_{max}}{v_{max}} \right) - \frac{\pi (6.1mm)^2}{4} \right)}{6.1mm} \quad (3.5)$$

Table 3.3: Slot Sizes – Solutions to Equation 3.5

Pressure/Return Flow	Flow (Q _{max})	Min. Slot Length (L _{slot})
Pressure	35.7 lpm	8.0 mm
Return	17.4 lpm	10.8 mm

As the casing block passage sizes were sized at 12mm, a 12mm slot length was chosen for the spool valve ports and the casing block ports, greater than the minimum required slot lengths for both high pressure and low pressure spool valves.

Flow Control Valves

To reduce pressure fluctuations in the hydraulic system (see Section 6.1.4 for details), one way flow control valves were installed before each hydraulic cylinder (Figure 3.13). These valves have an adjustable restriction for the high pressure oil flowing into the cylinders but have unrestricted flow (through a check valve) in the return direction.

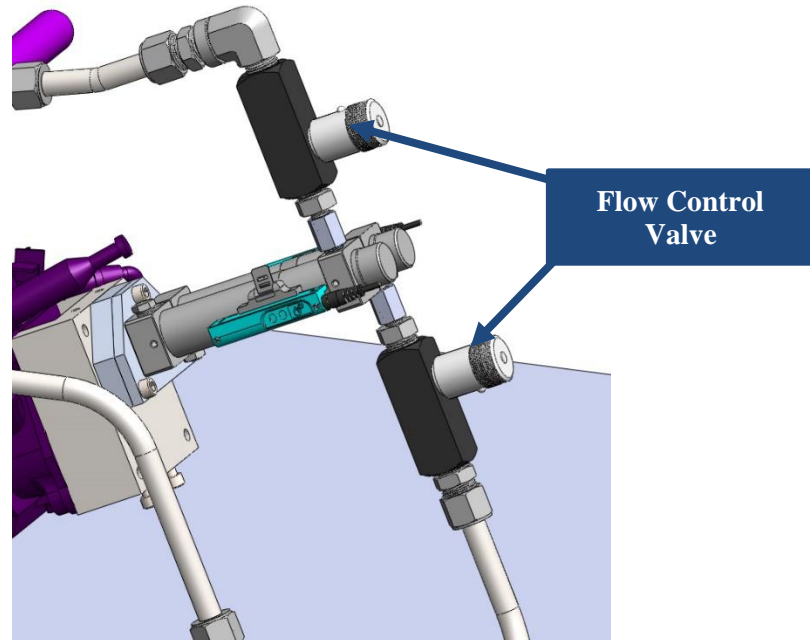


Figure 3.13: Flow control valves installed before hydraulic cylinders

The flow control valves were sized to minimize the pressure drop for return flow out of the cylinders. To close an engine valve, the valve spring pushes on the hydraulic cylinder and pushes the stored hydraulic fluid through the return line and flow control valve. The minimum available spring force, (F_k), will be the spring stiffness (k) multiplied by the preload displacement of the spring (x_i). Neglecting friction for this general sizing calculation, the return pressure (P) generated at the point of spring preload is calculated by equating the spring force to the pressure force in the hydraulic cylinder (F_P , Figure 3.14). The force balance is given by:

$$ma_{valve} = F_k - F_p \quad (3.6)$$

Where:

$$\begin{aligned} F_{k,min} &= kx_i \\ F_p &= PA_{cyl} \end{aligned} \quad (3.7)$$

The valve acceleration (a_{valve}) must be greater than 0 before the valve starts to move. Therefore, the pressure force must be greater than the minimum spring force. The required pressure is calculated as:

$$P > \frac{kx_i}{A_{cyl}} \quad (3.8)$$

Table 3.4: Max Flowrates – Solutions to Equations 3.6, 3.7, & 3.8

Description	Variable	Value
Spring Stiffness	k	24,430 N/m
Initial Displacement	x_i	9 mm
Hydraulic Cylinder Area	A_{cyl}	315 mm ²
Minimum Available Pressure	P_{min}	695 kPa

A maximum instantaneous valve closing speed of 1.2 m/s was measured during testing of the system (at 1500 RPM engine speed). This is equal to an instantaneous flowrate (Q) of 22.7 lpm. This flowrate and published valve coefficients (C_v) are used to calculate the maximum pressure drop through the flow control valves as [26]:

$$dP = SG \left(\frac{0.696Q}{C_v} \right)^2 \quad (3.9)$$

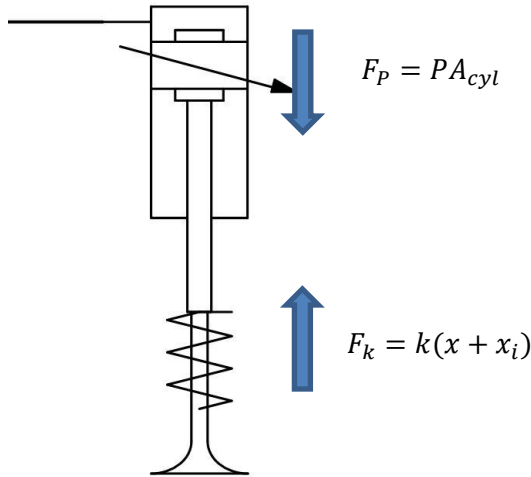


Figure 3.14: Hydraulic cylinder free body diagram

Table 3.5: Valve Pressure Drops – Solutions to Equation 3.9

Description	Variable	Value
Specific Gravity of Hydraulic Oil	SG	0.83
Fluid Flow	Q	22.7 lpm
1/4" Flow control Valve Coefficient	C_v	0.43
1/4" Flow control Valve Pressure Drop	dP	1075 kPa
3/8" Flow control Valve Coefficient	C_v	0.79
3/8" Flow control Valve Pressure Drop	dP	329 kPa

Two different flow control valve sizes were considered: 1/4" and 3/8" sizes from McMaster-Carr. The calculated pressure drop for the 1/4" valve (Table 3.5) was 1075 kPa. This is higher than the minimum pressure supplied by the valve springs and therefore too small to be used. The 3/8" valves were selected and installed on the system.

Accumulator

The bladder type accumulator used by Siddiqui was replaced with a much larger piston type accumulator. It is mounted directly to the spool valve assembly to further reduce the amount of external piping in the hydraulic system.

Increasing the volume of the accumulator will reduce the difference in valve lift between the intake and exhaust valves. A greater overall volume will reduce the relative volume change after opening the exhaust valve and there will be a smaller difference in the accumulator pressure between the exhaust and intake valve lift events. The accumulator total volume (V_0) is calculated using the change in volume (ΔV), precharge pressure (P_0), and initial & final pressure (P_1 & P_2) as [27]:

$$V_0 = \frac{\Delta V}{\frac{P_0}{P_1} - \frac{P_0}{P_2}} \quad (3.10)$$

Table 3.6: Accumulator Size Differences – Solutions to Equation 3.10

Description	Variable	Value
Max Hydraulic Cylinder Volume	ΔV	2205 mm ³
Precharge Pressure	P_0	85 PSI
Initial Pressure	P_1	200 PSI
Small Accumulator Total Volume	V_0	0.25 L
Small Accumulator Final Pressure	P_2	195.9 PSI
Large Accumulator Total Volume	V_0	1.00 L
Large Accumulator Final Pressure	P_2	199.0 PSI

Table 3.6 shows how a larger accumulator volume results in a lower drop in pressure after a valve open event. In this example, the larger accumulator (1L) drops from 200 psi to 199 psi. The smaller accumulator (0.25L) drops to 196 psi. This is not a complete representation of what is happening in the system, but this calculation demonstrates the benefit of using a larger accumulator in the system for more consistent valve lift between cycles and when comparing the intake and exhaust valves.

The precharge pressure (P_0) was reduced from Siddiqui's 250 psi setting. After running tests of the new system, the minimum operating pressure (P_{oper}) of the system was approximately 120 psi. As the system is subject to shock loading (due to rapidly opening and closing valves) the accumulator was set at 85psi. This setpoint is based on the range given by HYDAC for using an accumulator under shock loading conditions [27] and is calculated as:

$$P_0 = (0.6 \text{ to } 0.9) \times P_{oper} \quad (3.11)$$

3.2.2 Spool Valve Assembly

The hydraulic system has been simplified by adding cross-drilled holes to the block containing all four spool valves (the spool valve assembly). These holes connect the high and low pressure spool valves together without any external piping (schematically shown in Figure 3.10). They also connect the outlets of both exhaust spool valves and both intake spool valves respectively. Therefore, the spool valve casing block has only four hydraulic connections: high pressure supply, low pressure return, engine exhaust valve, and engine intake valve (Figure 3.15 & Figure 3.16). The previous prototype required eight hydraulic connections for all the spool valves, and more complex runs of tubing between each spool valve.

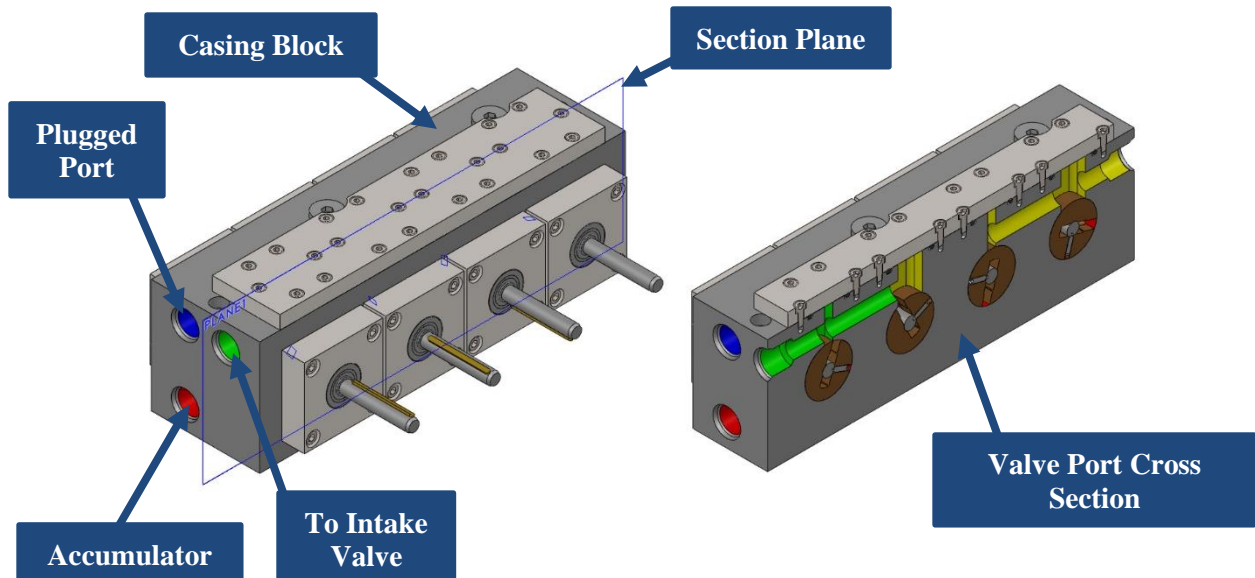


Figure 3.15: Hydraulic connections of the spool valve casing block & valve ports section view

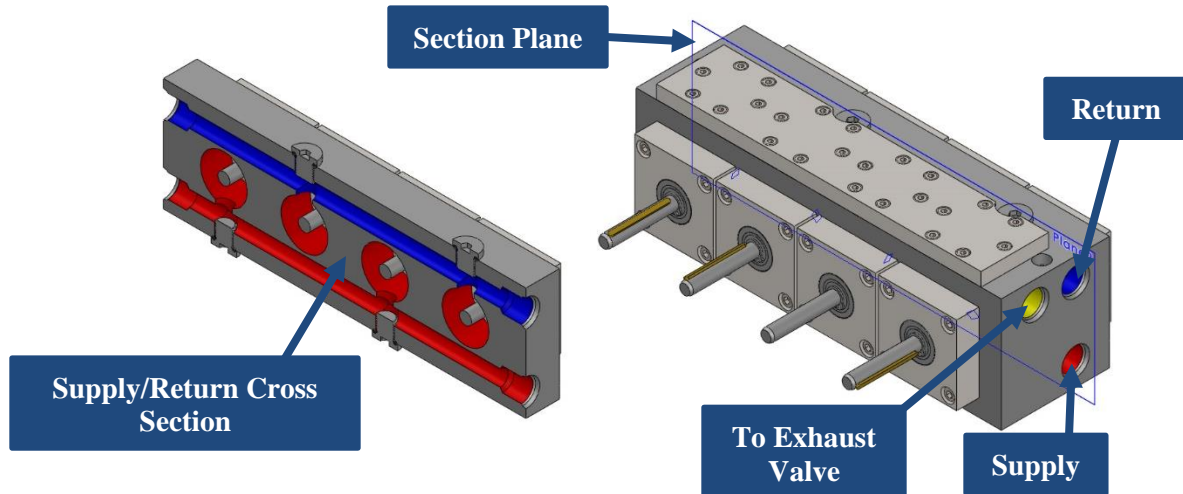


Figure 3.16: Hydraulic connections of the spool valve casing block & supply/return section view

Spool Valve Block Passages

By adding all four spools to one block, the casings could be combined and condensed to a smaller size. Additionally, each spool casing could be connected internally with cross drilled holes in the block.

The main cavity of each casing connected to the high pressure supply (for HPSVs) or the low pressure return (for LPSVs). A passage is drilled through the length of the block for both the low pressure return line and the high pressure supply line (Figure 3.17). Holes drilled from the top and bottom of the block connect the spool valve cavities to the passages (Figure 3.19 & Figure 3.21).

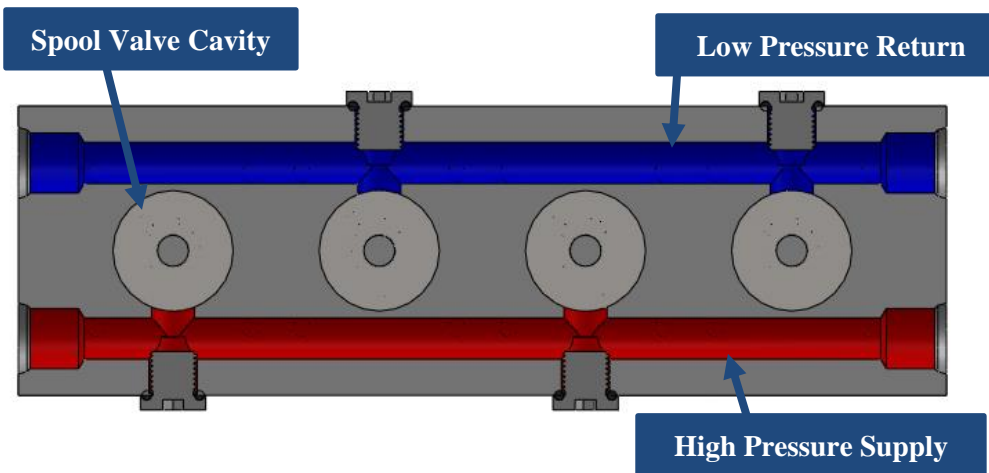


Figure 3.17: Cross section of high pressure (red) and low pressure (blue) passages

Similarly, internal passages connect each pair of spool valves to their respective hydraulic cylinder and engine valve (Figure 3.18). Ports are machined from the top of the block to the spool valve cavities (Figure 3.19 & Figure 3.21) and connected with holes drilled from the ends of the block.

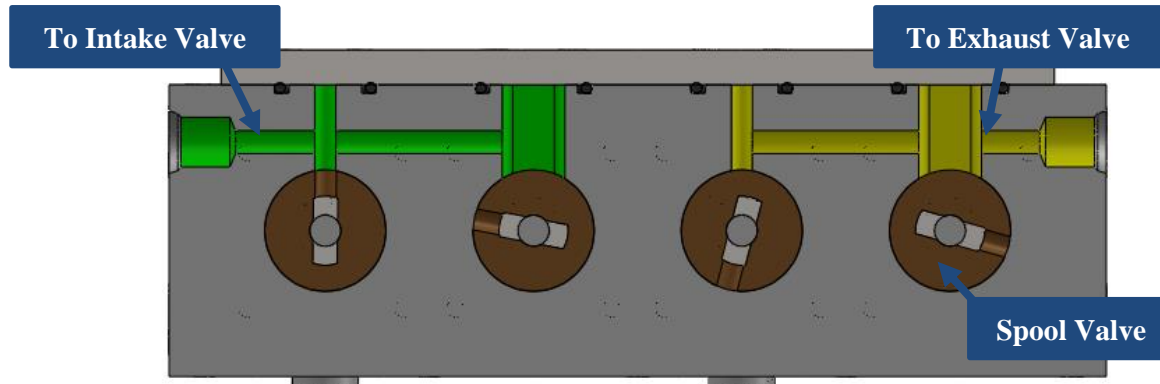


Figure 3.18: Cross section of exhaust valve (yellow) and intake valve (green) passages

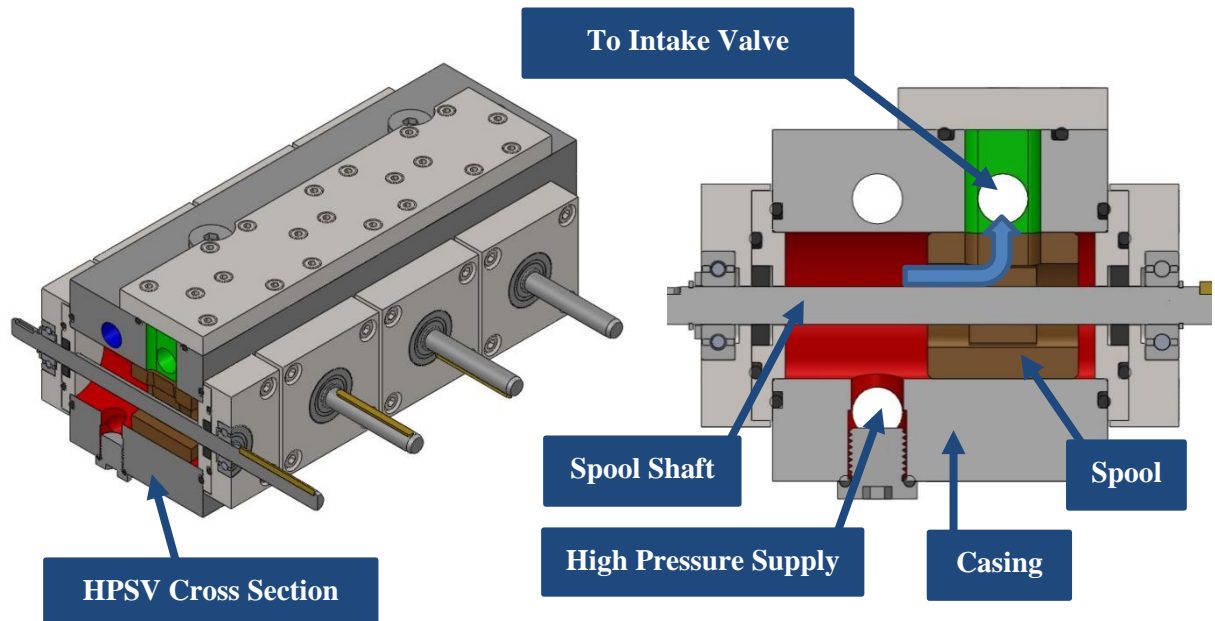


Figure 3.19: HPSV cross section in new prototype

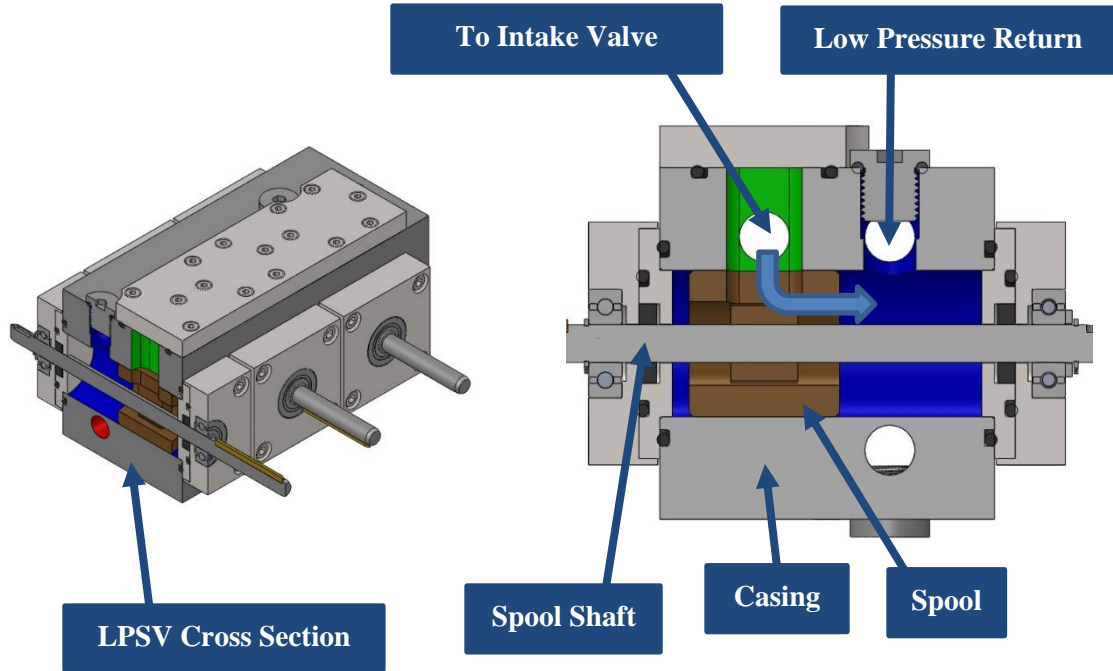


Figure 3.20: LPSV cross section in new prototype

Casing Port Angle

The larger the sum of the spool angle and casing angle (Equation 3.3, Figure 3.11), the longer the spool valve will be open. This sum should be minimized for the HPSVs as the open duration will limit the minimum amount of time that the engine valve can be open for (the HPSV must be closed before the valve can close). The casing angle of the high pressure ports on the spool valve block were set at 20°.

The open duration limit is not applicable to the LPSVs. These valves can be open for a longer duration to allow more time for the valve close event.

Experimental and simulation results by Siddiqui showed valve float (failure to fully close valves) at high engine speeds (>3000 RPM). This can be addressed by either increasing the valve spring stiffness or increasing the open duration of the LPSVs.

Increasing spring stiffness is the common solution for fixing valve float in a standard cam based engine. However, stiffer springs require more force to open. In the HVVA system, stiffer springs require a higher pressure to open the valves and higher overall energy usage. Increasing the casing angle of the low pressure ports on the spool valve block requires no additional system energy and will not affect system performance.

The low pressure spool valve casing angle was set at 60°. This gives a total open duration of 80° (160° CA, Equation 3.3) to provide more time for the valves to close.

Spool Valve & Casing Sizing

Both the spool and the spool valve casings are nominally Ø35mm. The spool was designed to be undersized and the casing was oversized. The small difference in diameters is a trade-off between friction and valve leakage. A larger gap will have more leakage (causing the engine valves to start to open or close prematurely) and a smaller gap is more likely to cause interference and binding between the spool and casing. The tolerances used by Siddiqui for the spool valve and casing diameter were carried over to the new design.

A nominal difference of 0.003" between spool and casing diameters was used in the previous prototype. Testing this system showed minimal levels of leakage and friction. Therefore, the same tolerances were used for the new prototype (Table 3.7).

Table 3.7: Spool Valve Diameter Tolerances

Dimension	Tolerance
Spool Outer Diameter	35.00mm +0.00/-0.03
Casing Inner Diameter	35.00mm +0.07/+0.05
Casing Diameter – Spool Diameter	0.00mm +0.05/+0.10 [0.000" +0.002/+0.004]

Sealing

The shaft of each spool valve shaft was reduced from the Ø12mm used by Siddiqui to Ø9mm. This smaller diameter results in smaller diameter rotary seals and a lower seal speed rating requirement. Simpler rotary seals could be used instead of the very expensive seals used in the last design.

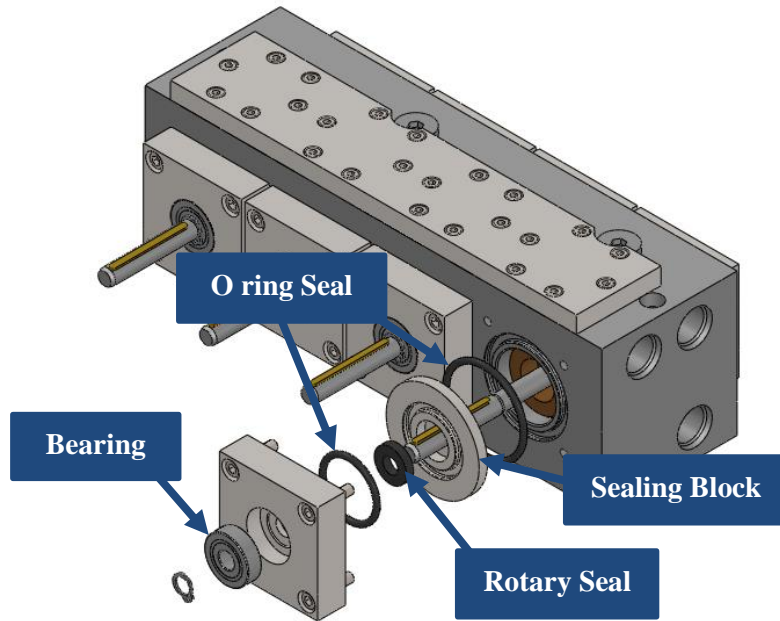


Figure 3.21: Exploded view of spool valve seal assembly

3.2.3 Hydraulic Cylinders

The cushion devices of Siddiqui's system have been replaced with purchased hydraulic cylinders from SMC (Figure 3.22). Purchasing a pre-engineered product from an outside company should result in a product with less friction and no hydraulic fluid leakage. The cylinders also offer consistent performance for both the intake and exhaust valves.

These cylinders have built in cushioning to slow the piston down when approaching the end of their stroke. However, the cushion length is longer than the maximum engine valve lift height. Therefore, if the cylinders were operated near their fully retracted positions, the whole closing stroke of the engine valves would be restricted by the cushioning. This restriction could cause valve float, especially at high engine speeds.

To avoid this problem, hard stops were added to the end of the cylinder rods to shift the operating range outside of the cushioning region. These stops are positioned to give some cushioning to the valves and ensure constant contact between the cylinder rods and engine valves.

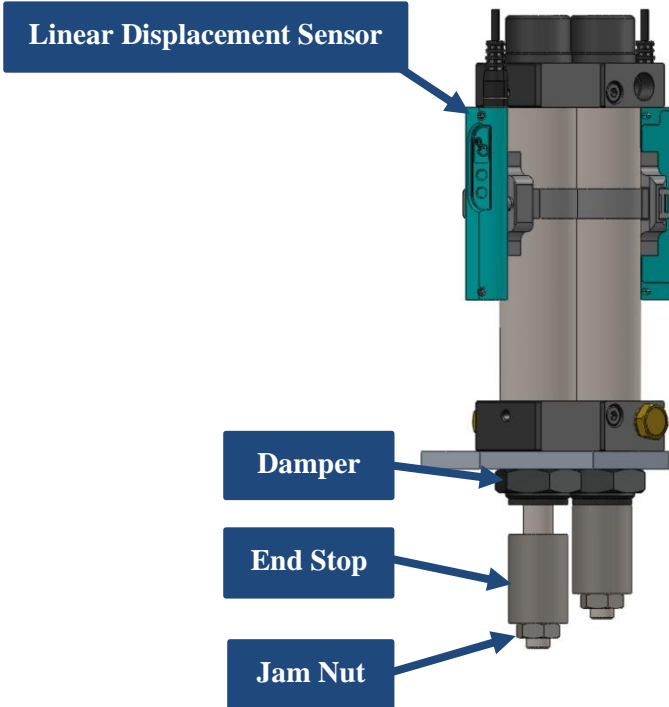


Figure 3.22: SMC Pneumatics small bore hydraulic cylinders with end stops installed

3.2.4 Phase Shifters

The completely new phase shifter was designed to be more compact than the previous design. Instead of planetary gears, the new design uses lead screws, nuts, and linear actuators to change the position of each spool valve relative to the crankshaft.

A timing belt connects a pulley on the crankshaft to a pulley driving each spool valves through spur gears. Each spool valve has a lead screw nut attached to a spur gear. Inserted into this nut is a lead screw connected to a linear actuator (Figure 3.23).

When the linear actuator is locked in place, the lead screw will rotate with the same angular displacement as the gear. As the actuator changes the linear displacement of the lead screw, it will rotate in the nut relative to the gear (and the crankshaft) based on the lead of the lead screw. Figure 3.24a shows the actuator in a fully retracted position. When the actuator is extended (Figure 3.24b) with the gear fixed in place, the spool shaft can be seen to rotate ($\sim 180^\circ$ in Figure 3.24).

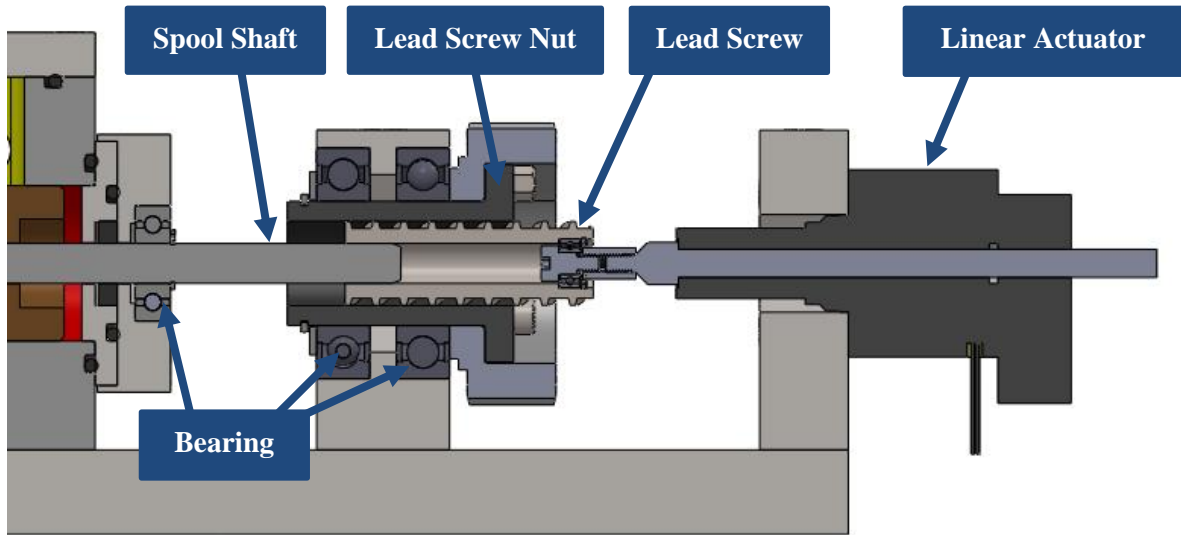


Figure 3.23: Cross section of phase shifter assembly

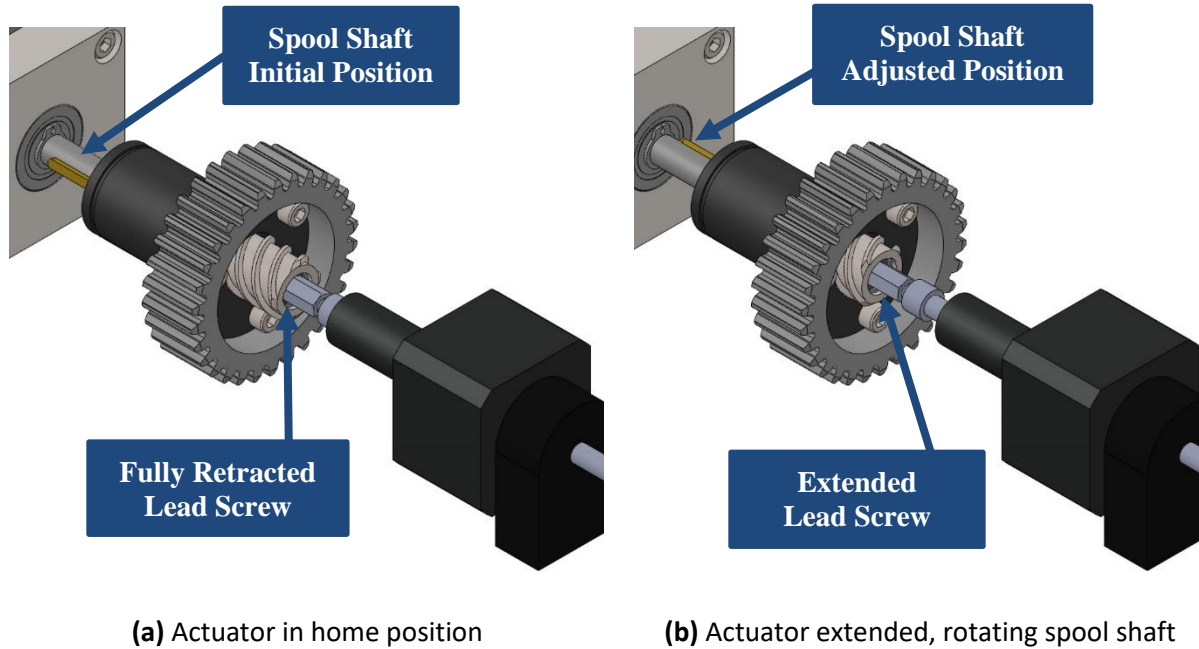


Figure 3.24: Phase shifter assembly operation

Each lead screw is drilled and keyed to fit onto a spool valve shaft so that the spool valve rotates with the lead screw. The linear actuators have enough linear travel to rotate the lead screws 360°. They can therefore set each spool valve to any position relative to the crankshaft (each valve can open or close at any position between 0 and 720°CA), making the valve timings fully flexible.

For a specific set of timings, the actuators move to the required location and hold the lead screw in that location. As the actuator is holding it in place, the spool valve will rotate with the crankshaft at the correct timing.

Lead Screws

Typically lead screws are used to turn rotation into linear motion. This system uses linear motion of the linear actuators to rotate the lead screws (backdriving the screws). This requires lead screws with high efficiency: low friction and high lead angles.

Lead screws will be back drivable if they have efficiencies greater than 50% [28]. Haydon Kerk, the lead screw supplier for this project, recommends a lead of less than $\frac{1}{4}$ of the screw diameter to guarantee no back driving [29]. This system uses a Ø19mm screw with a 25.4mm lead ($\gg 1.4 \times \emptyset$). The screws are coated in Haydon Kerk's Kerkote Teflon for a low coefficient of friction and have a published efficiency of 81%.

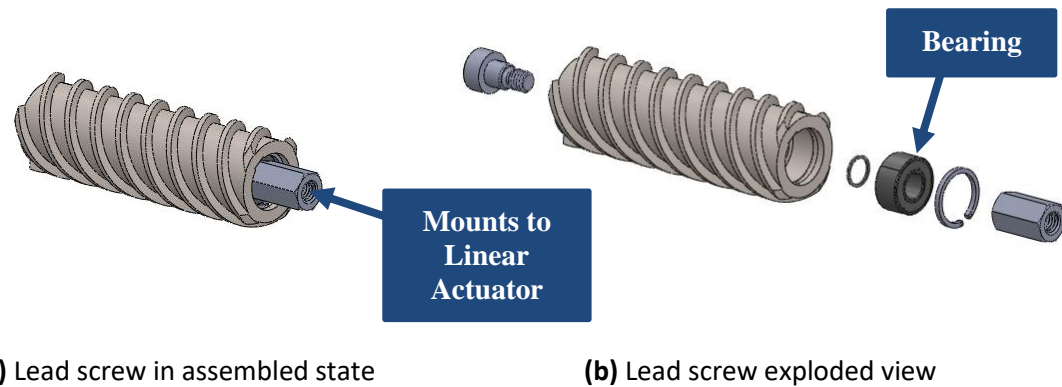


Figure 3.25: Lead screw assembly

A single lead screw and nut were purchased to confirm that the selected components could be back driven (Figure 3.26). The nuts were shown to operate with no noticeable restriction when operating within the Teflon coated portion of the screw.



Figure 3.26: Lead screw and nut

Linear Actuators

Linear actuators drive the lead screws to their required positions and hold them there during operation of the engine. They are required to physically fit in the assembly, move the lead screws one rotation in 1 second (requires a linear speed of 25.4 mm/s based on the lead of the lead screw), have enough torque to push the lead screws, and have enough holding torque to maintain spool valve positions during engine operation.

The selected actuators are Nema 17 stepper motors, size 43mm (Figure 3.27). These actuators fit the 60mm spool valve spacing. The recommended maximum axial load for these actuators is 50 lbs. They have a max rated speed of 20 mm/s (with 20 lbs of thrust). The linear speed is lower than the desired speed of 25.4 mm/s but was deemed acceptable due to lack of alternative actuators. This compromise will result in lower phasing speeds in this prototype.

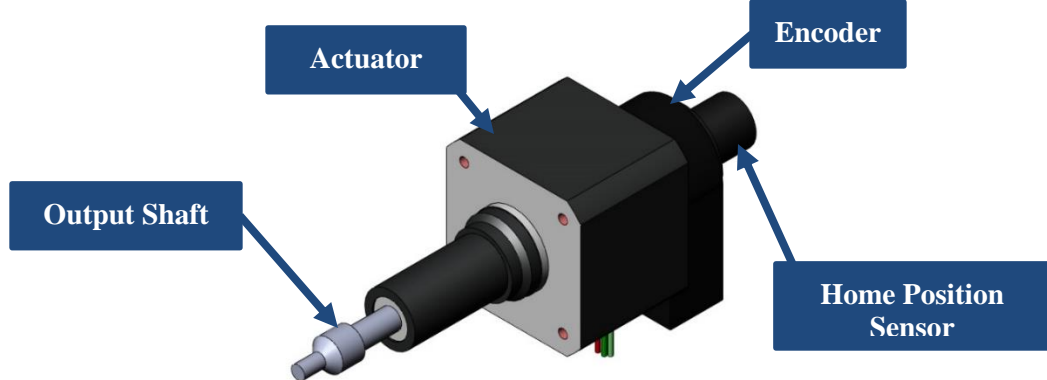


Figure 3.27: Linear actuator

The linear actuators create linear motion by rotating an internal lead screw nut (the rotor). A lead screw inserted into the rotor moves axially forward and back when the rotor is rotated. The output shaft of the actuator is fixed to move with this lead screw. This output shaft pushes on the phasing system lead screw to change the phase of the attached spool valve. The current phase of each spool valve can be determined using a calibrated offset and the current linear displacement of the phasing system lead screw. The displacement of the lead screw can be calculated using the lead of the rotor and the total rotation of the rotor (see section 4.3.2).

The available holding torque is calculated using the stall load from the actuator (P_{max}), the lead of the lead screw (L_{SV}), and the backdrive efficiency of the lead screw (η_b) as [29]:

$$T_{hold} = \frac{P_{max}L_{SV}\eta_b}{2\pi} \quad (3.12)$$

The available holding torque must be greater than the drag torque developed from friction between the spool valve and valve casing, bearing friction, and (most significantly) friction from the rotary seals on the spool shaft.

To phase the valves, the linear actuators need to provide enough torque to accelerate the spool valve and spool valve shaft while still overcoming drag torque in the system. The maximum available torque to overcome the drag is a function of the inertial torque (T_{iner}) and the developed torque of the actuators operating at maximum linear velocity using the minimum actuator load (P_{min}). This phasing torque is calculated as:

$$T_{phase} = \frac{P_{min}L_{SV}\eta_b}{2\pi} - T_{iner} \quad (3.13)$$

Where the inertial torque is calculated as:

$$T_{iner} = \alpha I \quad (3.14)$$

The maximum angular acceleration (α) is calculated assuming the actuator reaches its maximum speed in 0.1s. The actual time will vary based on available torque in the final setup. The total mass moment of inertia (I) is a sum of the individual mass properties of the spool valve, spool shaft, and lead screw. Individual terms are found using the mass properties of the modelled components in Solidworks. Solutions to the above equations can be found in Table 3.8.

For the experimental setup, the crankshaft is rotated with a dynamometer. The spool valves can be phased while the crankshaft is rotating and the linear actuators only need to overcome dynamic friction, not static friction.

The timeline of this project required that the linear actuators be purchased before the rest of the system was assembled. It was not possible, therefore, to obtain values for friction with any confidence. If the actuators have difficulty overcoming the friction in the system, phasing speeds will be reduced to what can be achieved. The data gained from this setup can then be used to better estimate the linear actuation required on the next design iteration.

Table 3.8: Linear Actuators Available Torque – Solutions to Equations 3.12, 3.13, & 3.14

Description	Variable	Value
Actuator Max. Thrust	P_{max}	222.4 N
Actuator Min. Thrust	P_{min}	89.0 N
Backdrive Efficiency	η_b	81%
Leadscrew lead	L_{SV}	25.4 mm
Max. Angular Acceleration	α	98.9 rad/s ²
Spool Valve, Shaft, & Lead Screw Mass Moment of Inertia	I	43 kgmm ²
Inertial Torque	T_{iner}	4.3 Nmm
Holding Torque	T_{hold}	1711.5 Nmm
Phasing Torque	T_{phase}	680.3 Nmm

3.2.5 Drive System

The spool valves are all mounted in the same block and can therefore be connected by spur gears instead of with one long belt. A much shorter belt (compared to Siddiqui's prototype) is used to drive the spool valve assembly from the crankshaft (Figure 3.28). The spool valves spin at half the speed of the crankshaft (as the engine valves open every two engine cycles), so the spool valve timing pulley is twice the diameter of the crankshaft pulley.

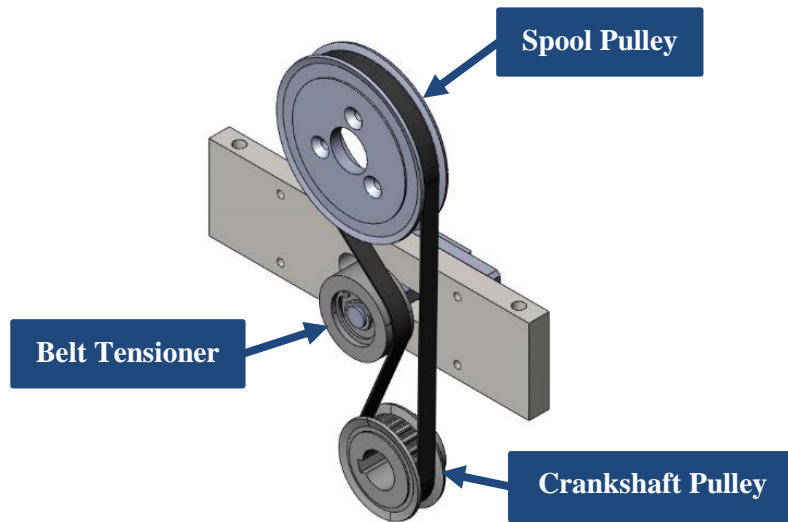


Figure 3.28: Belt drive assembly

3.2.6 Sensors

New lift sensors (Figure 3.29) have been purchased to reduce measurement noise compared to the lift sensors used by Siddiqui. The new sensors are production units instead of the prototype units used in the previous design. They use a row of hall effect sensors to measure the linear position of a magnet in the hydraulic cylinder piston. The total range of each sensor is 0-50 mm. The range is set to match the total stroke of the purchased hydraulic cylinders.

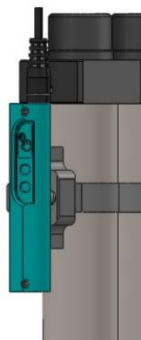


Figure 3.29: Linear displacement sensor

The pressure sensors are mounted directly at the engine valves instead of after a length of flexible hose. This gives a better simultaneous relationship between valve lift and pressure. Excessive filtering has been removed and the sensors now output raw measurement data for post processing.

Through-bore encoders (Figure 3.27) are mounted to the linear actuator rotors. These are incremental encoders: they output the total angular displacement of each actuator rotor as measured from the fully retracted position. The linear displacement of the actuator can be calculated using the total angular displacement, and the current phase of the spool valve can be calculated from the actuator linear displacement (see section 4.3.2).

A home position proximity sensor (Figure 3.27) is used to home the position sensors each time the system is started up. The linear actuators are driven in reverse until they are fully retracted and the home position sensors are tripped. At this home position, the encoders are reset to a calibrated offset.

3.3 Simulation

A mathematical model of the full HVVA system was developed in Simulink. This model was used to simulate the system and troubleshoot problems in the hydraulic setup before making physical changes to the experiment.

Siddiqui's project used a system average model of a single engine valve that calculated instantaneous pressure drop, flow, and leakage through the spool valves. It used a force balance at the hydraulic cylinder to calculate valve lift. This model did not include the effects of adding the second engine valve, the hydraulic accumulator, pipeline pressure losses, or hydraulic fluid inertia.

A new mathematical model was developed using Simulink's Simscape hydraulic package (Figure 3.30). This package includes function blocks for accumulators, tubing, and fluid inertia. These functions greatly simplified the building of a complete system model with all four spool valves and both engine valves. The model was further simplified by ignoring spool valve leakage (<0.1% of total valve flow according to Siddiqui's model and not seen as a problem in testing).

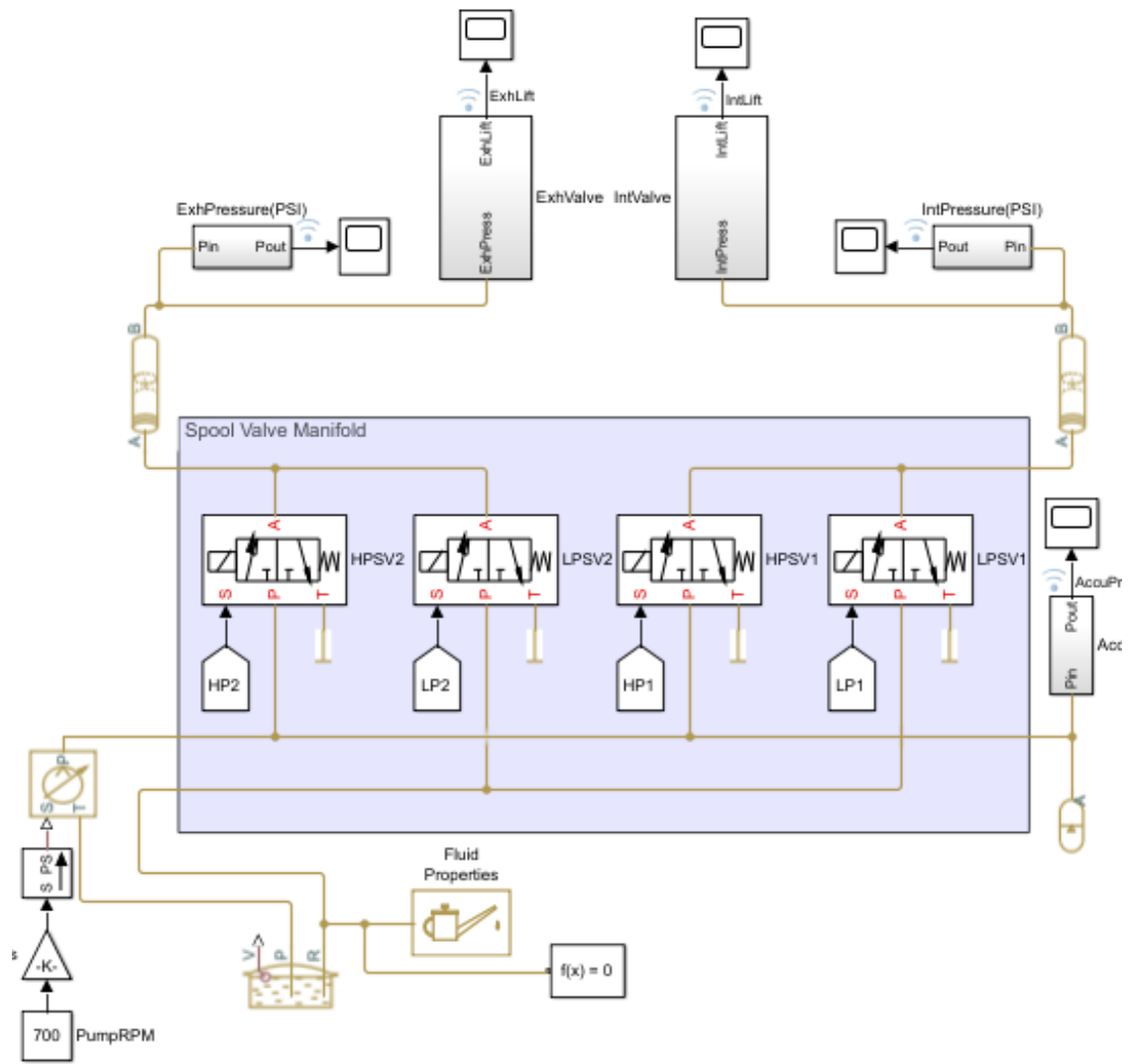


Figure 3.30: Simscape model

The model uses a constant flowrate source to represent the pump supplying hydraulic oil to the HPSVs and the accumulator. The accumulator is a piston type accumulator with the same volume and precharge as the physical system. The spool valves are modeled as 3-way valves with one port plugged. The valves start to open based on valve timing and the open area varies linearly with the spool valve angle (up to max. opening area and back down to zero, see Figure 3.31). Note that the opening duration is longer for the LPSV as it has a larger casing port.

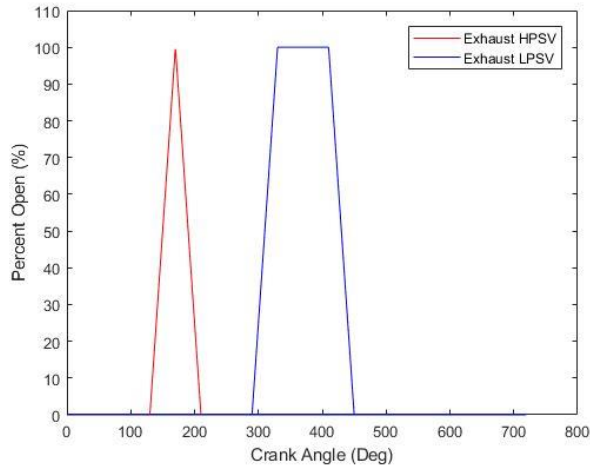


Figure 3.31: HPSV & LPSV open profiles

The hydraulic cylinders and engine valves were modeled with Simscape hydraulic cylinder, mass, and spring blocks (Figure 3.32). The restriction valves are modelled using an adjustable needle valve and check valve.

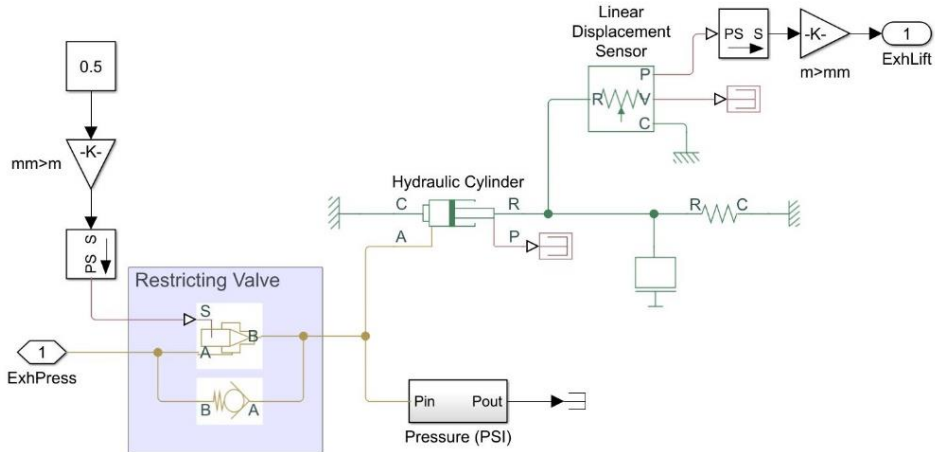


Figure 3.32: Simulink model of flow control valve, hydraulic cylinder, and engine valve

A segmented pipe with fluid inertia was included between the spool valves and hydraulic cylinders to model the length of tubing present on the physical setup. Multiple segments in the pipe better represent the interaction of fluid pressure waves within the pipe, instead of treating it as one lumped mass [30]. Including fluid inertia in the model gave insight into problems experienced in the experimental setup and helped test potential solutions before committing to installing them.

The model was used as a tool to help direct the design and is not expected to be an exact representation of the system. It was primarily useful to visualize flow variations and compare pressure fluctuations rather than estimating exact pressure and flow requirements.

Chapter 4

Experimental Setup

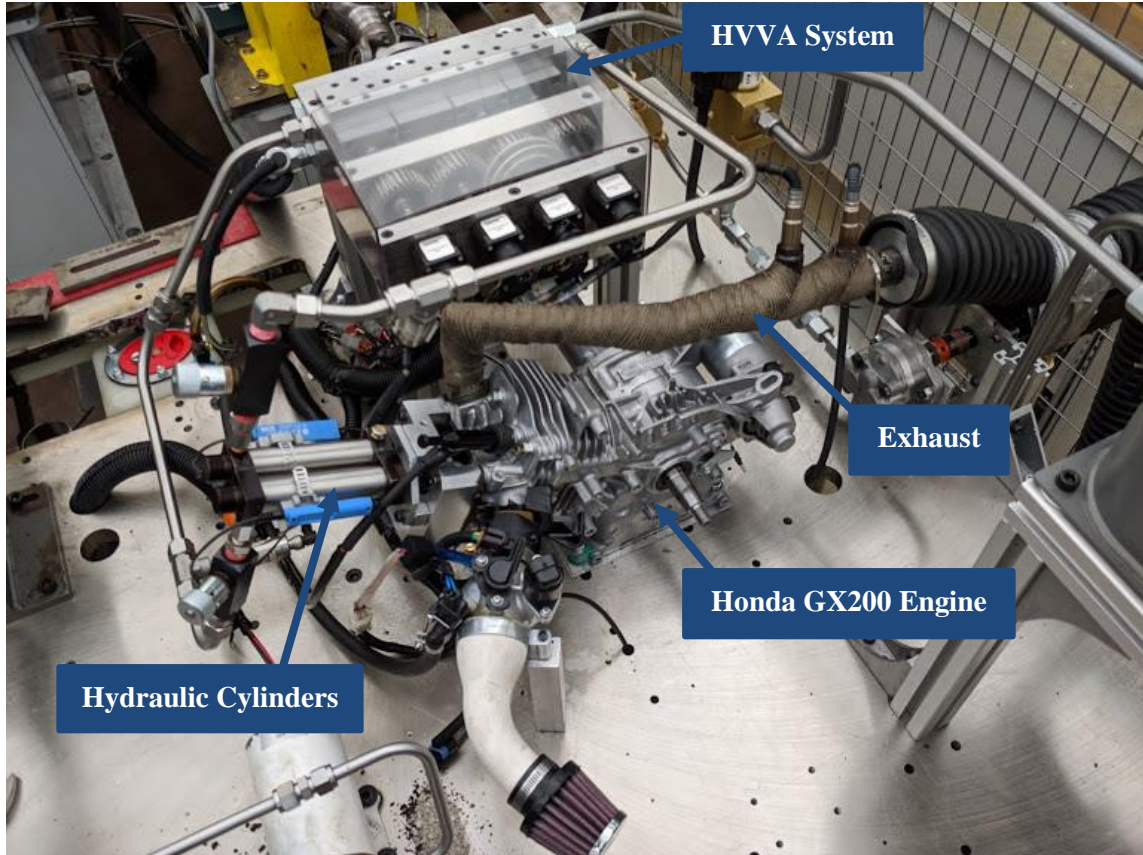


Figure 4.1: Experimental setup

The final experimental setup is shown in Figure 4.1. The HVVA system was installed and connected to the Honda GX200 test engine with a timing belt. The engine crankshaft is coupled to a dynamometer used to spin the engine for testing. An external exhaust removes products of combustion during combustion testing.

4.1 Mechanical Setup

4.1.1 Manufacturing

The new design detailed in Chapter 3 was fully modelled in SolidWorks, material and components were purchased, and full fabrication drawings were issued to machinists in the UW mechanical engineering department. Full parts lists can be found in Appendix A.

4.1.2 Assembly & Install

Once the HVVA system was assembled, it was mounted to a rigid steel table (Figure 4.2). The high system stiffness reduced problems with vibration seen in the previous prototype.

The engine crankshaft is connected to the dyno with a solid coupler. The dyno is used to rotate the engine for all tests. For combustion tests, the engine is run at a constant speed by the dyno and a torque sensor measures the output torque delivered by the engine.

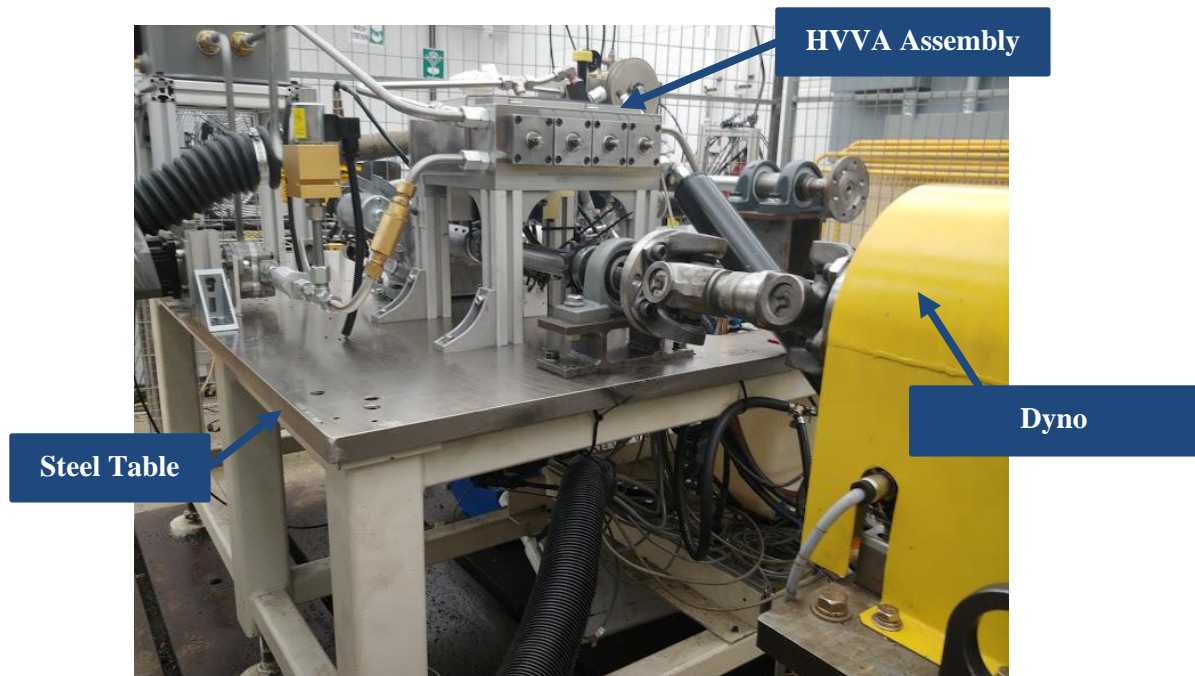


Figure 4.2: Assembly mounted to steel table

4.2 Hydraulic Setup

Hydraulic components were assembled as per the hydraulic schematic shown in Figure 3.10. The final assembly can be seen in Figure 4.3.

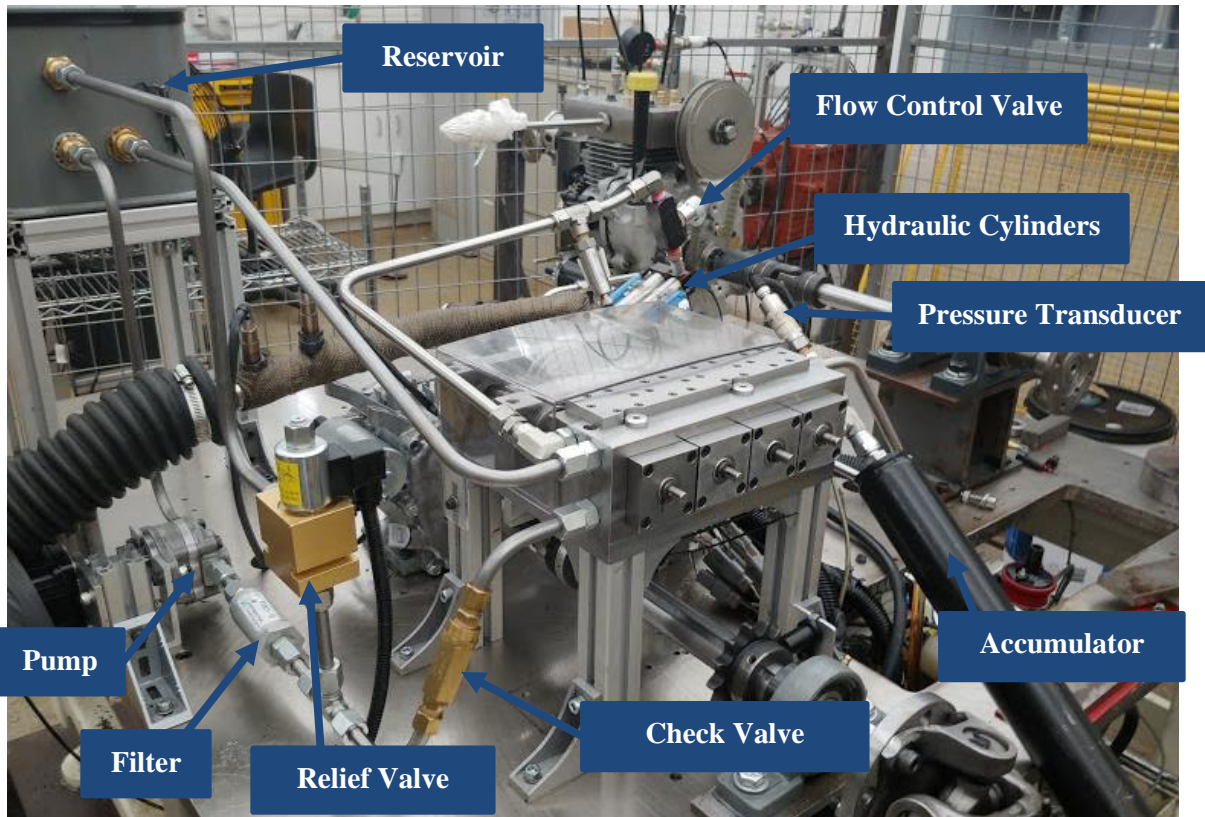


Figure 4.3: Hydraulic System

Flow Control Valves

The flow control valves were installed as close as possible to the hydraulic cylinders (Figure 4.4). They were adjusted to their current flow control positions using experimental results. Set screws are used to lock the valves in position.

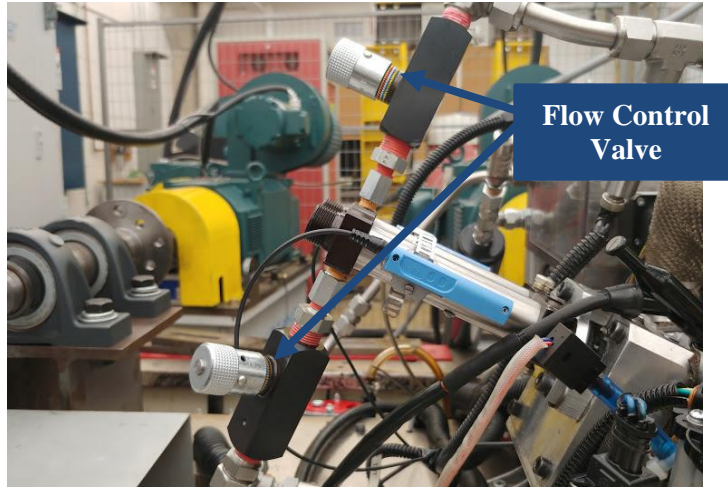


Figure 4.4: Flow control valves installed in system

Air Removal

The equivalent stiffness of a hydraulic system is the bulk modulus of the hydraulic oil. Typically, the bulk modulus is large enough that the natural frequencies of the system will be much higher than the resonance of the system input [31]. However, if there is significant compliance in the hydraulic tubing and trapped air in the system, the effective bulk modulus will be reduced and potentially create resonance problems in the system. The effective bulk modulus (β_e) is calculated using the bulk modulus of the oil (β_l), the relative amount of trapped air in the oil (S), the bulk modulus of air (β_a), and the equivalent bulk modulus of the steel tubing (β_c) as [30]:

$$\frac{1}{\beta_e} = \frac{1}{\beta_l} + S \frac{1}{\beta_a} + \frac{1}{\beta_c} \quad (4.1)$$

Where the bulk modulus of air is:

$$\beta_a = (P + P_{atm}) \quad (4.2)$$

And the equivalent bulk modulus of steel is calculated using the pipe thickness (t), elastic modulus (E), and diameter (D) as:

$$\beta_c = \frac{tE}{D} \quad (4.3)$$

The solutions to the above equations (Table 4.1) show that a small amount of trapped air (2%, typical for a hydraulic system [30]) has a very large impact on the effective bulk modulus of the system. The trapped

air is particularly significant as the system is running at relatively low pressures for a hydraulic system and the bulk modulus of air is proportional to the absolute system pressure.

Table 4.1: Equivalent Bulk Modulus – Solutions to Equations 4.1, 4.2, & 4.3

Description	Variable	Value
Bulk Modulus of Hydraulic Oil	β_l	1.459 GPa
System Operating Pressure	P	830 kPa
Atmospheric Pressure	P_{atm}	101 kPa
Bulk Modulus of Air	β_a	931 kPa
Relative Amount of Trapped Air	S	2%
Hydraulic Tube Thickness	t	0.89 mm
316 SS Tube Young's Modulus	E	190 GPa
Tube Outer Diameter	D	12.7mm
Equivalent Steel Tube Bulk Modulus	β_c	13.3 GPa
Equivalent Bulk Modulus	β_e	0.365 GPa

To maximize the effective bulk modulus, the rubber hoses connecting the spool valves to the hydraulic cylinders were replaced with hard steel tubing and efforts were made to remove as much air from the system as possible.

To remove any trapped air in the system, the system was bled at the high points of the hydraulic tubing. The spool valve block design allows for air to be trapped at the top of the block where the ports of the spool casing were machined out. To remove this air, the top sealing plate from the spool valve block was removed while running the pump to push out the air (Figure 4.5).



Figure 4.5: Bleed points of hydraulic system

4.3 Electrical Setup

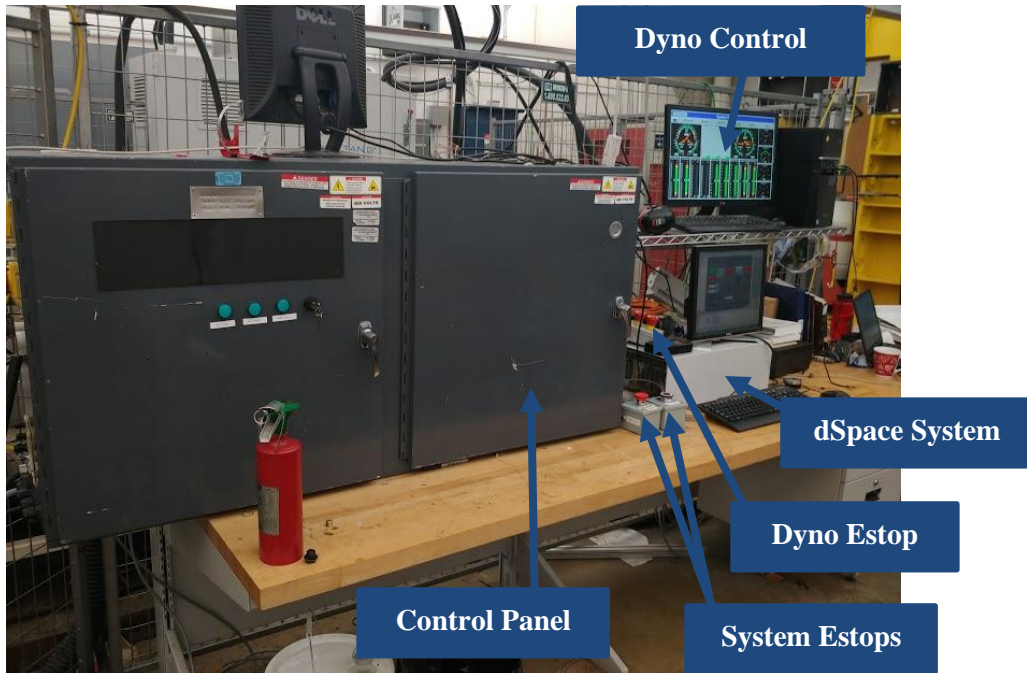


Figure 4.6: Electrical panel & dSpace setup

The electrical inputs and outputs are all processed through a modular dSpace data acquisition and control system. Raw input data from sensors is processed through analog, digital, or encoder input boards and control signals are sent from analog or digital output boards (Table 4.2).

Table 4.2: dSpace Board Descriptions

dSpace Board	Description
DS2002	Multi-Channel Analog-to-Digital Board
DS2103	Multi-Channel Digital-to-Analog Board
DS3001	Incremental Encoder Interface Board
DS4004	HIL Digital I/O Board

The system sensors, actuators, and control wiring are routed through the electrical control panel. The control panel contains the pump servo drive, stepper motor drivers, power supplies, relays, and terminal connections. Terminal blocks for each dSpace board are used to communicate to the dSpace system.

Figure 4.6 shows the physical layout of the electrical system. Table 4.3 and Table 4.4 list and describe all the inputs and outputs. A detailed parts lists can be found in Appendix A.

Table 4.3: System Inputs

Input	Sensor Type	Description	dSpace Board
Linear Actuator Angle	Incremental Encoder	Current angle of linear actuator rotor (used to calculate spool valve phasing position)	DS3001
Actuator Home Position	Hall Effect Proximity Sensor	Indicates when linear actuator is in its fully retracted position	DS4004
Crankshaft Angle	Incremental Encoder	Angle of crankshaft (resets once per revolution)	DS3001
Pump Speed	Servo Drive Tachometer	Speed of hydraulic pump	DS2002
Accumulator Pressure	Pressure Transducer	Pressure at hydraulic accumulator	DS2002
Intake Pressure	Pressure Transducer	Pressure at intake valve hydraulic cylinder	DS2002

Exhaust Pressure	Pressure Transducer	Pressure at engine exhaust valve hydraulic cylinder	DS2002
Intake Valve Lift	Linear Displacement Sensor	Lift height of intake valve	DS2002
Exhaust Valve Lift	Linear Displacement Sensor	Lift height of exhaust valve	DS2002
Engine Torque	Torque Transducer	Torque outputted by the engine (can be positive or negative)	DS2002
Pump Drive Status	Servo Drive Contact	Status of pump drive, contact closes when drive is ready	DS4004
Estop	Estop Button	Cuts power to 24VDC power supply and pump drive	DS4004

Table 4.4: System Outputs

Output	Actuator Type	Description	dSpace Board
Pump Current	Servo Motor	Commanded operating current for the servo motor driving the hydraulic pump (signal sent to Servo Drive)	DS2103
Dyno Speed	Dynamometer	Commanded engine speed (signal sent to Dyno controller)	DS2103
System Enable	Relay	Enables power to the pump drive	DS4004
Relief Valve Position	Solenoid Valve	Sets position of relief valve (PWM signal)	DS4004
Linear Actuator Frequency	Stepper Motor	Sets frequency of linear actuator stepper motor (signal sent to stepper motor driver) Typical for all four linear actuators	DS4004
Linear Actuator Direction	Stepper Motor	Sets direction of linear actuator stepper motor (signal sent to stepper motor driver)	DS4004
Crank Angle Pulse	-	Pulse to ECU to indicate crankshaft position for injection and ignition timing	DS4004
EFI Enable	Relay	Enables power to the electronic fuel injection (EFI) systems engine control unit (ECU)	DS4004

4.3.1 Crankshaft Encoder Calibration

There is an incremental encoder installed on the driveshaft of the engine measuring the current angle of the crankshaft (Figure 4.7). It resets once per revolution, so it will always output a signal corresponding to an angle between 0 and 360°.

To calibrate the encoder, the engine crankshaft was rotated until the piston reached top dead centre (TDC). TDC was measured by physically observing the top of the piston through its stroke. The offset of the encoder was set so that it outputs 0° at TDC.

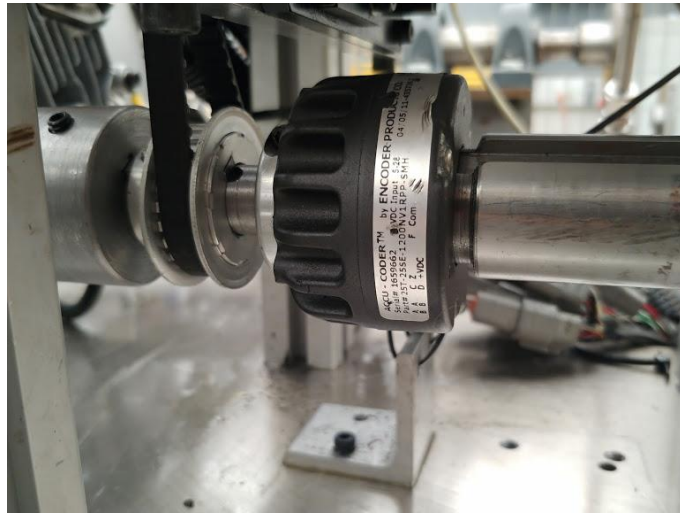


Figure 4.7: Crankshaft encoder

4.3.2 Actuator Encoder Calibration Method

The rotary spool valve phasing positions are measured with incremental encoders mounted to the rotor (internal rotating nut) of the linear actuator stepper motors. The rotor rotation (θ_r) is converted to linear motion through a captive lead screw (with lead L_r) in the linear actuator. The linear motion is converted back into rotary motion of the spool valve (θ_{SV}) by pushing or pulling the lead screw (with lead L_{SV}) mounted to each spool valve shaft. The relationship between the rotor and spool valve angular displacement is:

$$\theta_{SV} = \frac{\theta_r L_r}{L_{SV}} \quad (4.4)$$

Before being moved to the phasing position, each encoder must be reset by being fully retracted. In this position, the end of the shaft will trigger a proximity sensor used to reset the encoder to a pre-set offset. When the actuator moves from this position, the encoder will keep track of the positive and negative rotation

of the rotor and output the current angle difference between the rotor and the home position. There is no additional reset for these encoders, they will read $>360^\circ$ from the home position when the rotor has moved more than one full rotation.

The offset used for these encoders is the angle the spool valve must rotate before the port on the spool valve is pointing straight up when the crankshaft is at TDC.

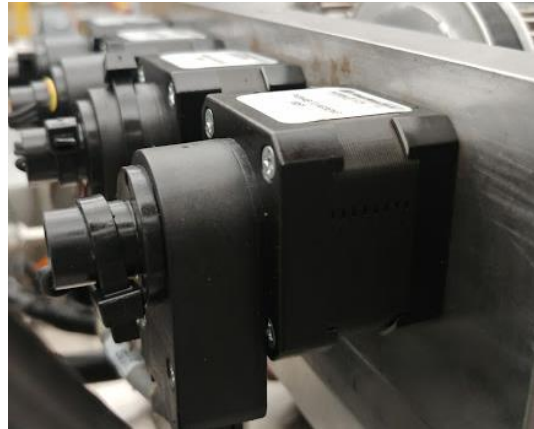


Figure 4.8: Linear actuators with encoders & home position switches

4.3.3 Linear Displacement Sensor Calibration

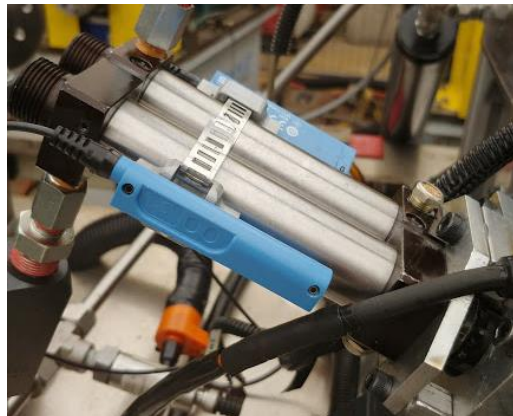


Figure 4.9: Linear displacement sensors

The linear displacement sensors output a 0-5VDC signal for the range of the sensor (0-50mm). The offset is calibrated every time the engine is started (it is the average value read over multiple cycles when the valve is in the closed position).

4.3.4 Electronic Fuel Injection System (EFI)



Figure 4.10: EFI ECU (mounted under table)

The Honda GX200 engine used for testing originally used a carburetor for mixing fuel and air for combustion. This did not give any flexibility to change the air fuel ratio (AFR) or the spark timing. These were necessary to fully validate the VVA strategies developed by Yangtao Li [2].

An electronic fuel injection (EFI) system was installed on the system to give this flexibility. It can control the AFR, spark timing, and many other variables through programming the engine control unit (ECU, Figure 4.10). The full list of components in the EFI system is shown in Table 4.5 and the assembly can be seen in Figure 4.11. Manufacturer details of EFI components can be found in Appendix A.

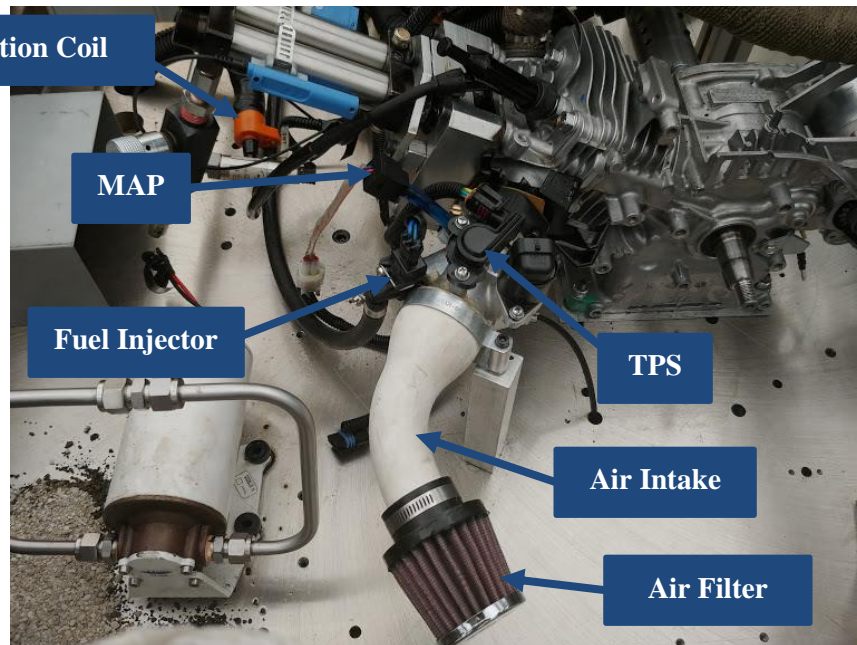


Figure 4.11: EFI assembled on to the engine

Table 4.5: EFI Components

Component	Description
ECU	Main controller for the EFI system, can be programmed to change key operating parameters
Fuel Pump	Keeps fuel lines pressurized
Fuel Injector	Injects fuel into the throttle body
Capacitive Discharge Ignition (CDI)	Sends power to ignition coil when commanded by the ECU
Ignition Coil	Sends power to the spark plug
Air Filter	Filters air
Air Intake Manifold	Directs air into engine
Air Throttle Body	Throttles the amount of air into the engine
Manifold Air Pressure (MAP) Sensor	Measures the air pressure after the throttle plate
Throttle Position Sensor (TPS)	Measures the current position of the throttle plate
Intake Air Temperature Sensor (IAT)	Measures the air temperature at the intake
Engine Coolant Temperature (ECT) Sensor	Measures the temperature of the engine

For combustion testing, the engine is run at a constant speed by the dyno before the EFI system is powered on. Once the EFI system is powered, it allows fuel and a spark to be delivered to the engine.

4.4 Software Setup

The entire system is controlled and data is collected through a Simulink program embedded on the dSpace hardware. During testing, a ControlDesk (program by dSpace) GUI is used to view live data, change variables, and record data.

4.4.1 Simulink Model

Chapter 5A discrete Simulink model is separated between system Inputs and Outputs. The Inputs block applies calibrations to sensor data and sends it to the Outputs block. The Outputs block uses the sensor data and user input to control the system.

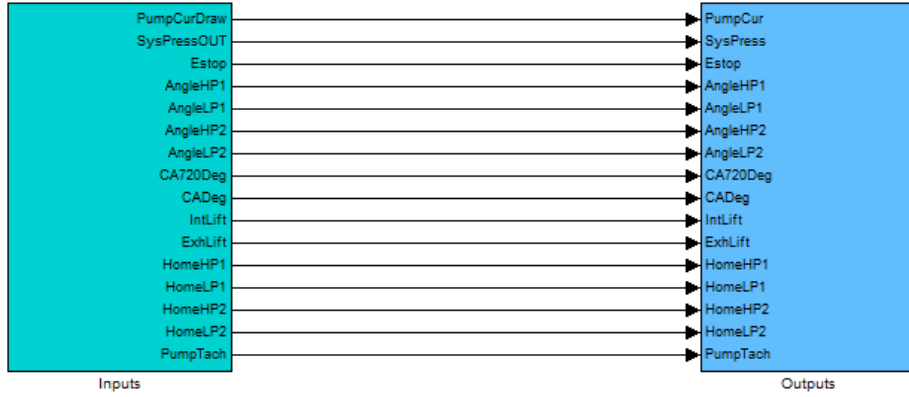


Figure 4.12: Main view of Simulink model

Actuator Homing

Every time that the system is started, the encoders must be reset. The crankshaft encoder is reset when it is rotated through a full revolution. The linear actuator encoders are reset by homing the actuators (Figure 4.13). When the homing is initiated, the actuators are driven in reverse until the home position proximity switches are tripped. As each actuator reaches its home position, its encoder is reset to the calibrated offset.

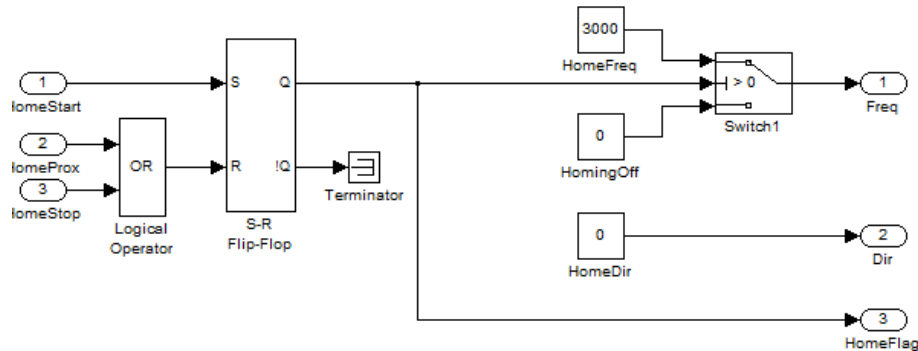


Figure 4.13: Actuator homing

Phasing Control

User input for the phasing position of each spool valve is used to control the spool valves to those positions. The user inputs the tangent position angle (TPA) required for each spool valve. The TPA is the angle at which the spool valve port just starts to line up with the spool valve casing port. At this point the engine valve will just start to open (for the HPSVs) or just start to close (for the LPSVs). This can be seen in Figure 4.14.

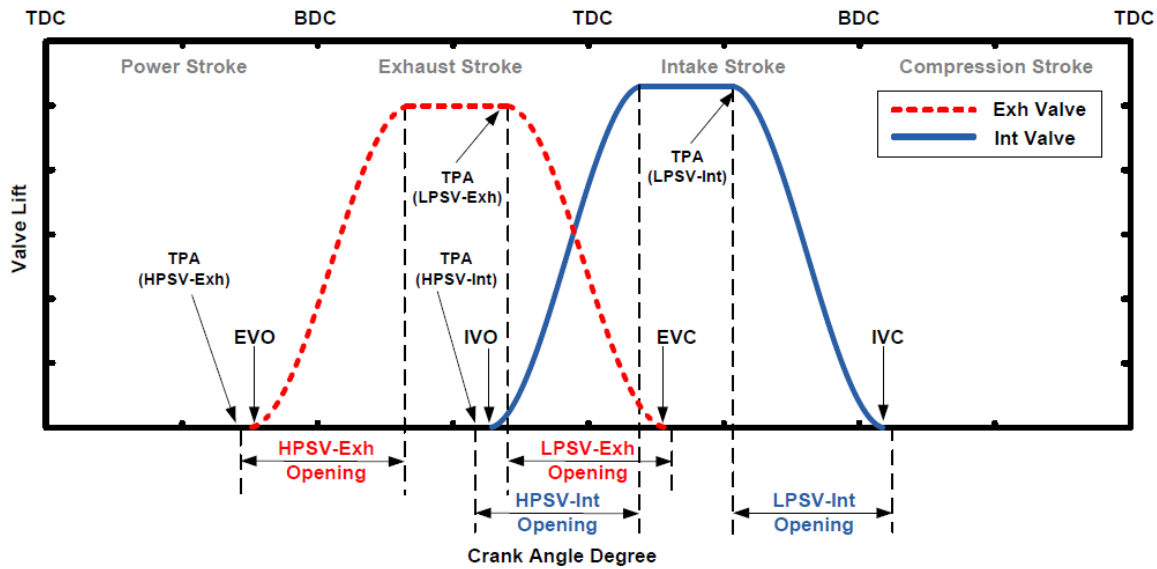


Figure 4.14: TPA timings for engine cycle [2]

The Simulink program converts the TPA into a setpoint position for the linear actuator encoder. The error between the setpoint and the current angle of the spool valve is fed into a simple discrete proportional controller (Figure 4.15) to move the linear actuators to the correct positions. If any of the spool valves move $>0.5^\circ$ out of position during operation, the controller will automatically move the linear actuator back into position.

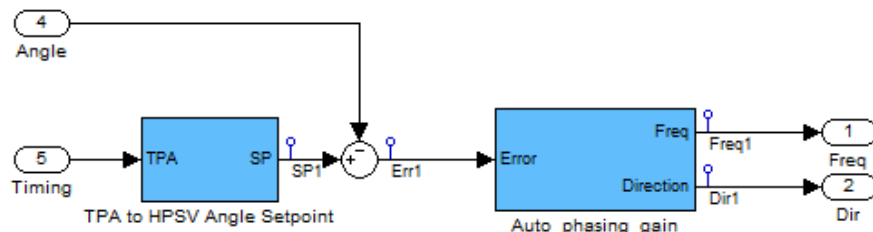


Figure 4.15: Phase angle controller

Pressure Control

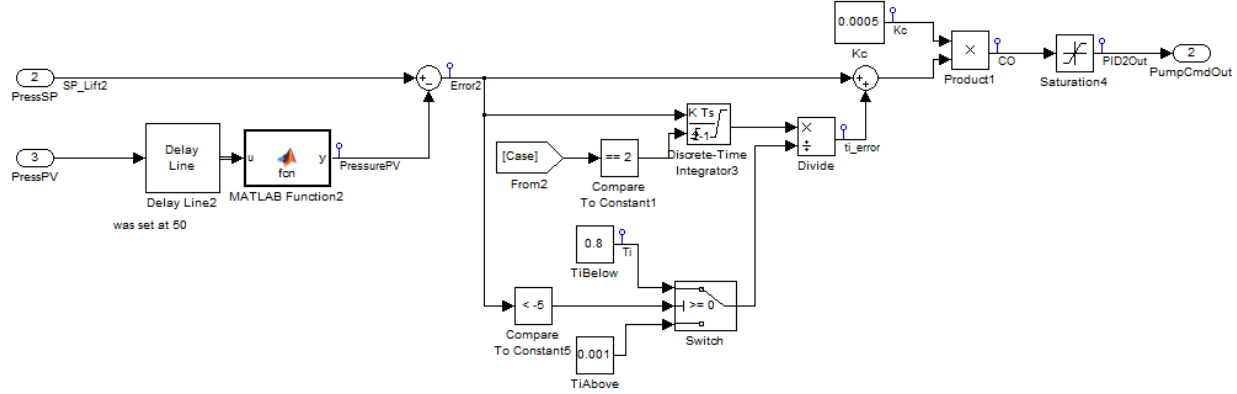


Figure 4.16: Accumulator pressure controller

The engine valve lift is a function of the system pressure and engine speed (higher engine speeds require a higher pressure for the same valve lift). A discrete Proportional Integral (PI) controller (Figure 4.16) was developed to control the accumulator pressure (setpoint) by changing the current supplied to the pump servo drive (controller output).

The controller output (CO) is calculated using the controller gain (K_C), integral time (T_i), and the error (e) between the setpoint and present value of the accumulator pressure. The controller output is:

$$CO(t) = K_C \left[e(t) + \frac{1}{T_i} \int e(t) dt \right] \quad (4.5)$$

The lambda tuning method [32] was used for initial setting of controller parameters. This method gives a slow, stable response for the system. It was used to avoid any pressure overshoots (causing excessive valve lift height) and because the large accumulator volume prevents any quick changes in system pressure.

The lambda tuning method calculates the controller parameters using the open loop system response to a manual step change in the controller output (Figure 4.17). The controller gain is calculated using the process gain (K_P), the time delay (D) of the system after the step input, the process time constant (T_P), and the user selected λ value as:

$$K_C = \frac{T_P}{K_P(\lambda + D)} \quad (4.6)$$

Where the process gain is calculated using the change in process variable (ΔPV) and the change in controller output (ΔCO) as:

$$K_P = \frac{\Delta PV[\%]}{\Delta CO[\%]} \quad (4.7)$$

The integral time is calculated as:

$$T_i = T_P \quad (4.8)$$

A larger λ will lead to a slower system response. It is normally set between T_P and $3T_P$. The integral time is set equal to the process time constant.

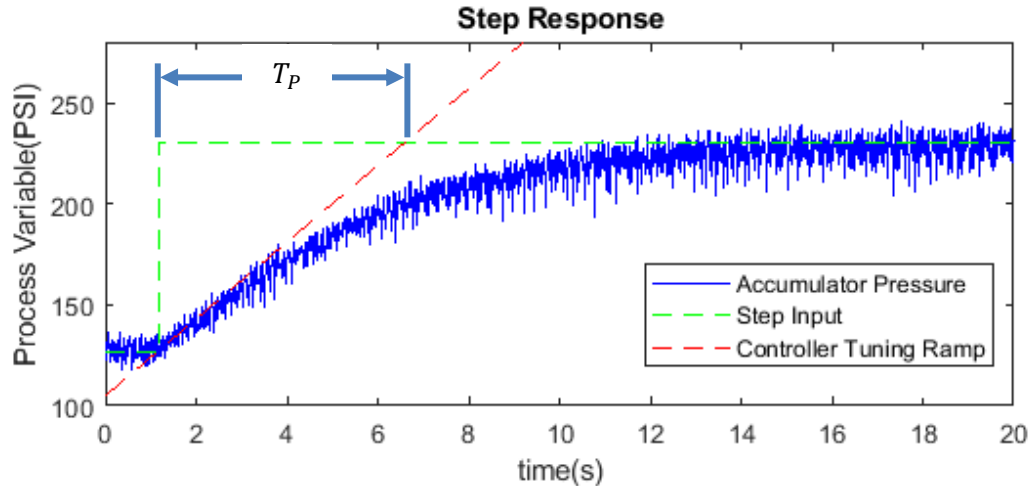


Figure 4.17: Step response results used for lambda tuning method of PI controller

The results of the lambda tuning gave a starting point for controller tuning. These parameters gave a stable response if the controller was started when the system operating pressure was above the precharge pressure of the accumulator.

If the controller was turned on with the accumulator pressure close to the precharge pressure, the delay to start to fill the accumulator produced a large wind up effect in the PI controller and caused system overshoot above the setpoint. To compensate for this, a larger integral term ($1/T_i$) was used above the setpoint versus below to quickly drop the controller output after overshooting the setpoint.

Table 4.6: Lambda Tuning Results – Solutions to Equation 4.6, 4.7, & 4.8

Description	Variable	Value
Process Variable Range	PV	120-300 PSI
Controller Output Range	CO	0.4-4 amps
Step Input	ΔCO	8.3%
Pressure Change	ΔPV	57.2%
Process Time Constant	T_p	5.4 s
Time Delay	D	0 s
Lambda ($3T_p$)	λ	16.2 s
Process Gain	K_p	6.9
Controller Gain	K_c	0.049 (%CO/%PV) 0.00097 (Amps/PSI)
Integral Time	T_i	5.4 s

Crankshaft Position Output

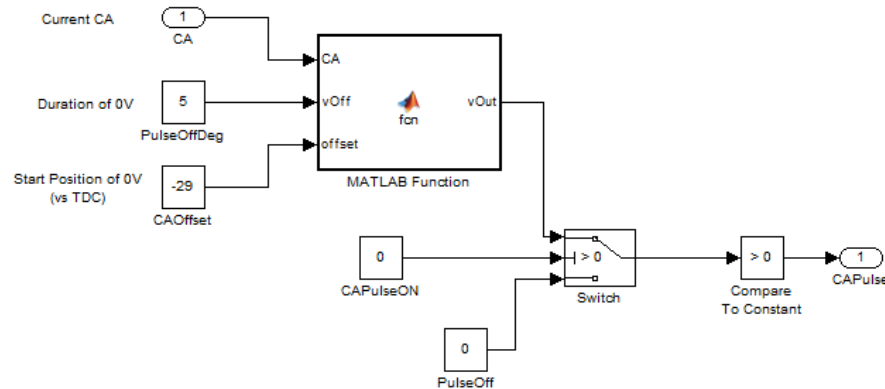


Figure 4.18: Crankshaft position output

To properly time fuel injection and spark ignition, the ECU needs a crank angle position (CKP) pulse signal from dSpace. The Simulink program outputted this signal based on the reading of the crank angle

encoder and the parameters seen in Figure 4.18. This block simulates a hall effect sensor outputting 5VDC normally and 0VDC when triggered. The 0VDC signal starts as specified by *CAOffset* with a duration of *PulseOffDeg*. The ECU will not send fuel to the engine unless it receives this signal from dSpace. The *CAPulseON* parameter can effectively be used to start and stop combustion by controlling if the CKP signal is being sent to the ECU.

Safety Measures

There are many physical and software safeties present in the system to prevent damage to the system or harm to the operator. In order to run the hydraulic system, none of the conditions connected to the OR block in Figure 4.19 can be true. If ever the pump current, pump speed, engine valve lift, or system pressure are too high or the Estop button is pressed, the hydraulic pump will turn off.

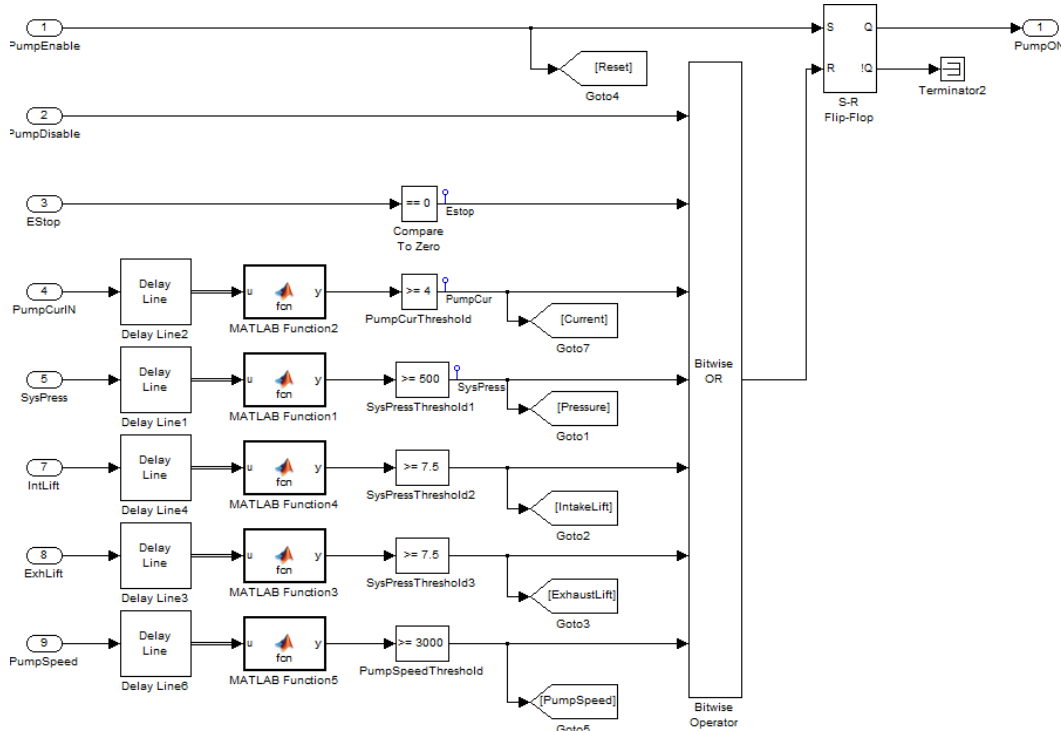


Figure 4.19: Hydraulic system safeties

Similarly, the combustion system can only be turned on if the hydraulic pump is on and the engine speed is greater than 200 RPM (Figure 4.20).

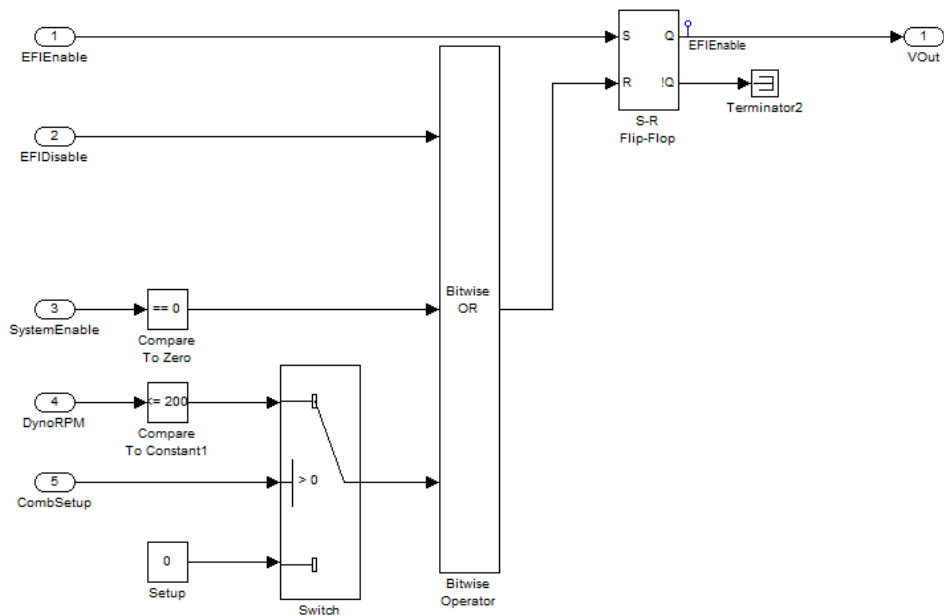
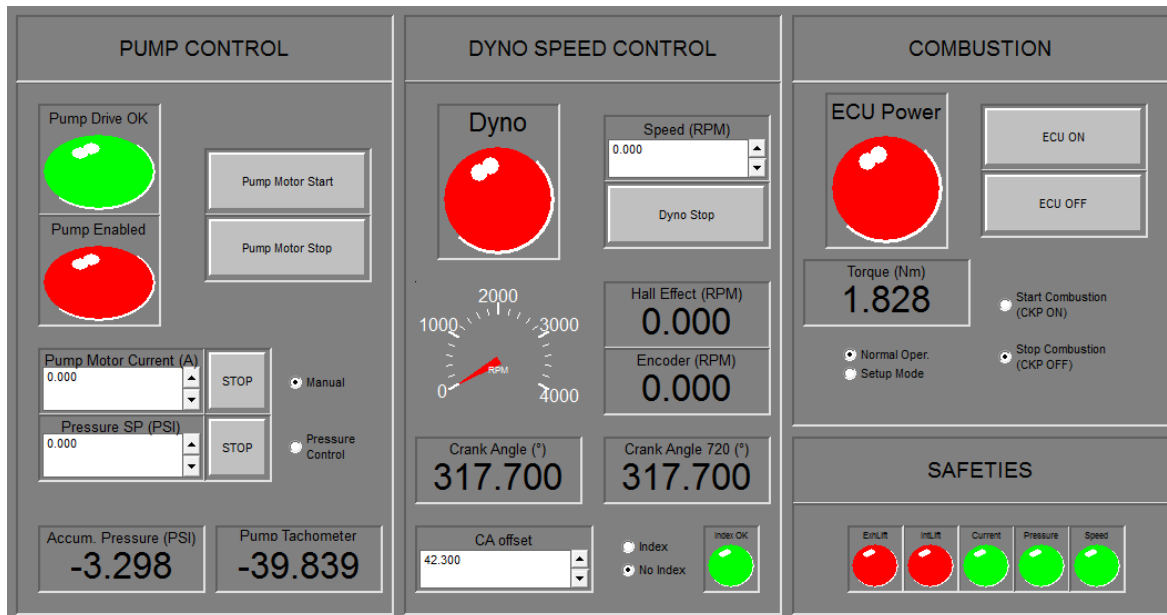


Figure 4.20: Combustion system safeties

5.1.1 ControlDesk GUI

The ControlDesk program made by dSpace was used to create the graphical user interface (GUI) between the operator and the Simulink program collecting data and controlling the setup. The operator can view sensor readings, change sensor calibrations, record data, and control the equipment through the ControlDesk interface.



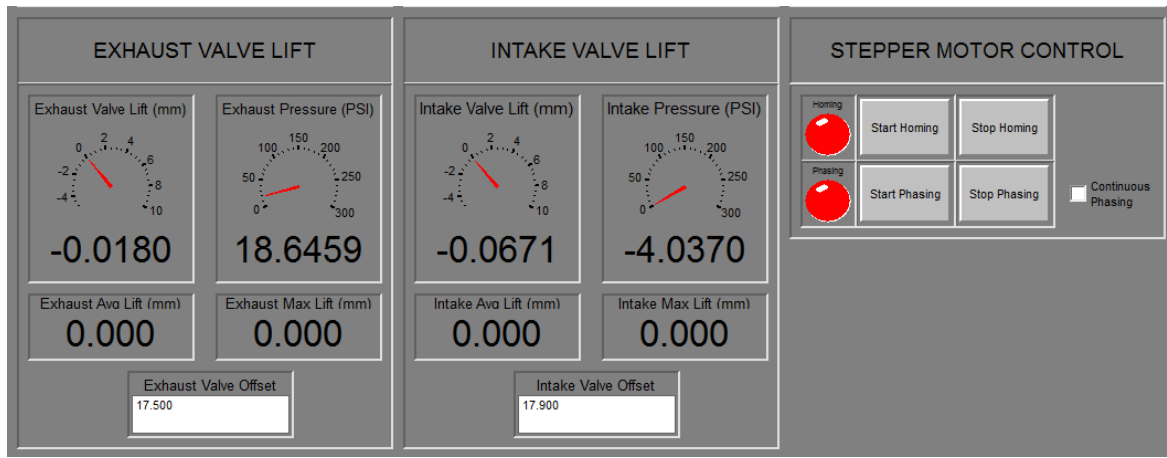


Figure 4.21: Main ControlDesk interface

Figure 4.21 shows the main interface for the HVVA system. Controls for the pump, dyno, and combustion can be seen at the top. The lower portion shows live sensor data for the engine valve lift heights and hydraulic cylinder pressures and buttons to start or stop linear actuator homing and positioning.

Valve timings can be set in the software and can be quickly switched between three set profiles (Figure 4.22).

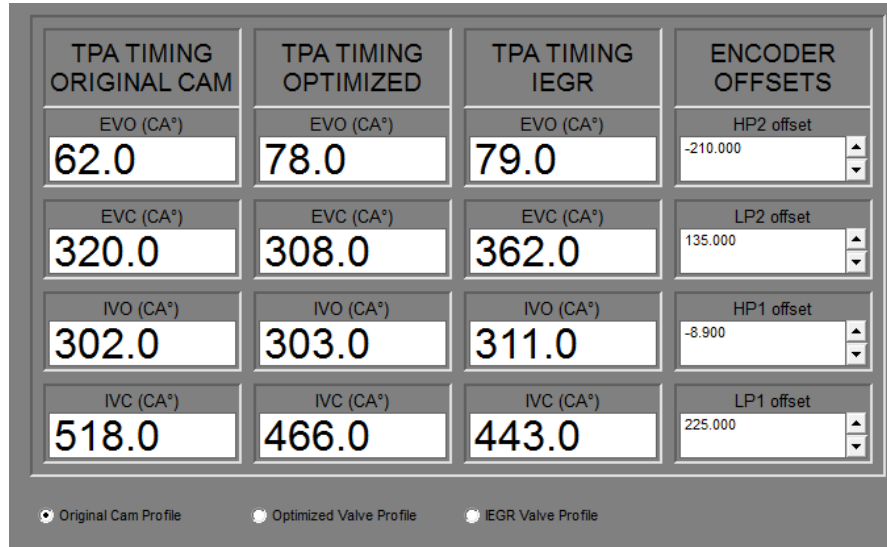


Figure 4.22: Valve timing settings

5.1.2 ECU Programming

An ECU was included as part of the EFI kit purchased to replace the engine carburetor. This ECU had pre-set maps for fuel injection, ignition timing, throttle position vs load, and more. The ECU manufacturer's EcoCAL software was used to manually adjust the amount of fuel being sent to the engine to achieve the desired air fuel ratio for different tests.

Chapter 6

System Validation & Experimental Results

6.1 Initial Testing

Before running the VVA valve timing strategies, the different components of the HVVA system were assembled and tested. Results of this initial testing are detailed below.

6.1.1 Linear Actuator Testing

After assembling the spool valves, gear train, and the phasing system, the linear actuators were tested. Before the system was connected to the crankshaft, the linear actuators were not strong enough to overcome the static friction in the system. After the belt from the crankshaft to the spool valves was connected, the linear actuators were tested again.

The linear actuators are strong enough to change the spool valve positions while the system is rotating. The actuators do not have enough force to continue phasing the spool valves at the maximum speed (the stepper motors stall out). However, even after adding a threshold to the actuator speed to prevent stalling, all expected changes to valve positions can be completed in under one second. The maximum phasing speed of the actuators without stalling was found to be 0.5 in/s (Figure 6.1). This is equivalent to 180°/s for the spool valve angle, 50% of the desired 360°/s.

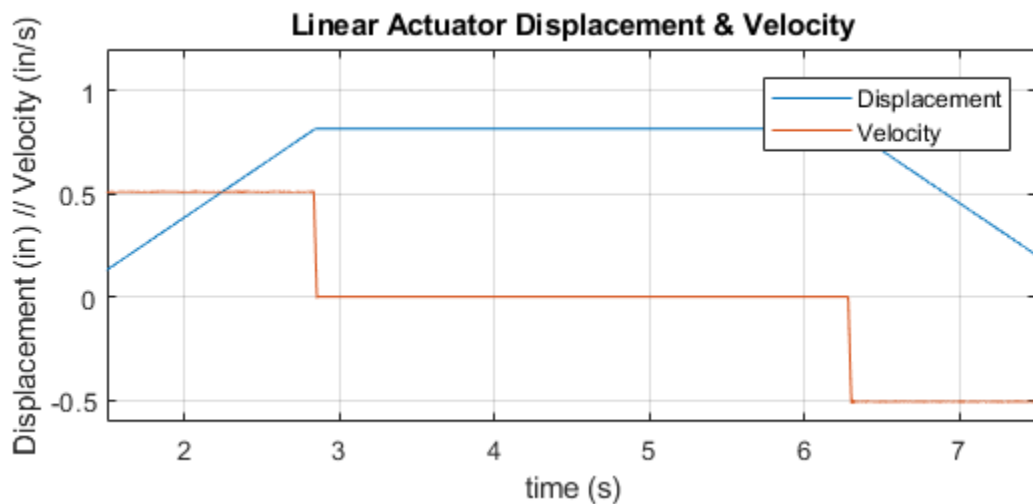


Figure 6.1: Linear actuator velocity test results

Periodically during testing, the intake high pressure spool valve will move out of position (the stepper motor drivers only supply 50% of max current for holding torque). To counteract this, the control loop permanently keeps each spool valve within $\pm 0.5^\circ$ of the setpoint.

6.1.2 Hydraulic Cylinder Testing

The hydraulic cylinders purchased from SMC have built in adjustable cushioning to reduce the speed of the cylinder when closing the engine valve. However, in the fully retracted position, even the lowest cushion setting reduced the closing speed of the engine valve too much (causing engine valve float). Hard stops were added to move the engine valve closed position further away from the fully retracted cylinder position. The current position only gives minimal cushioning but was acceptable for use on this test setup. This could be fine tuned by changing the size of the hard stops or using cylinders like those of the Fiat Multiair system (see Section 2.1.2).

Cylinder Positioning

The HVVA system controls the valve lift height by adjusting the system hydraulic pressure at the accumulator. A higher pressure will lead to a higher valve lift at any given engine speed. However, the purchased cylinders used on this system limit the range of adjustment for the engine valve lift heights.

The cylinders have consistent regions of normal operation separated by discontinuities in lift at certain stroke locations. Figure 6.2 shows the results of tests where increasing pressure was applied to the hydraulic cylinders. The normal operating range for the exhaust valve is limited from 3 to 5mm. The range for the intake valve is 3.8 to 5.5 mm.

The system uses only ~10% of the total stroke range of the purchased cylinders. They are being used outside of a typical use case and are not the ideal solution for a project requiring fine adjustment in position. The next design iteration should use custom cylinders (similar those of Fiat's Multiair system) with optimized diameter and stroke.

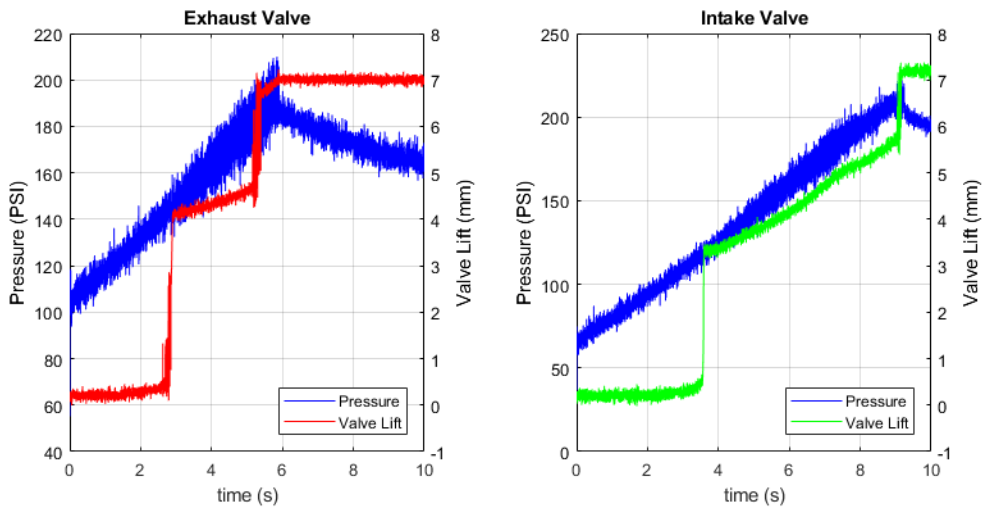


Figure 6.2: Exhaust and intake valve positions vs. applied pressure

6.1.3 Engine Valve Lift

In order to compare the VVT system to the stock cams on the engine, it is necessary to match the valve lift profiles produced by the stock cams. The new VVT system must be able to replicate the timing and valve lift height of the original profile and additional profiles generated through Yangtao Li's research [2].

Intake vs Exhaust Valve Lift Height

Initial experiments of the system showed a large discrepancy between the lift heights of the intake and exhaust valves (when running at constant engine and pump speeds, see Figure 6.3). This discrepancy was mainly due to the accumulator precharge pressure and different valve spring preloads as discussed below.

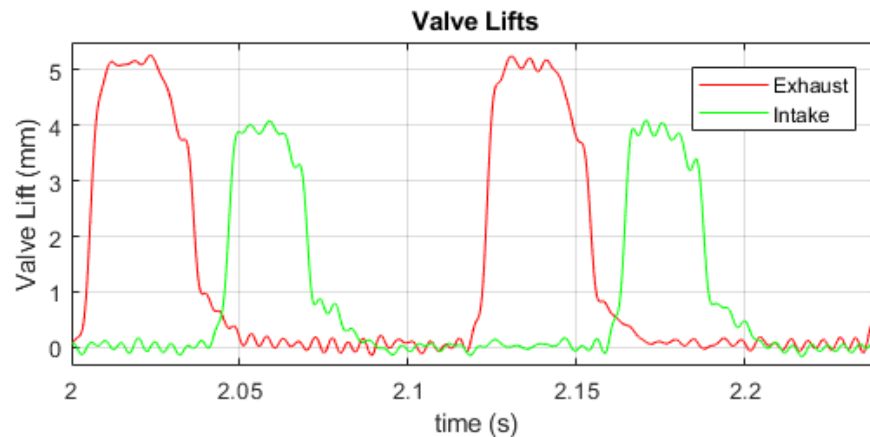


Figure 6.3: Intake and exhaust valve lifts before changes to valve springs & accumulator precharge

Accumulator Precharge Pressure

The precharge pressure of the hydraulic accumulator directly affects difference in lift height between the intake and exhaust valves. A higher precharge pressure will result in lower volumes of oil stored in the accumulator for a given operating pressure and a higher drop in supply pressure from the exhaust to the intake valve opening events (see Section 3.1.1).

Initial testing of the system used the same precharge pressure as Siddiqui's experiments. This testing revealed that the precharge pressure was much higher than the operating pressure of the system. Minimal fluid was being stored in the accumulator, so most of the stored fluid contributed to the exhaust valve lift and not the intake valve lift.

This pressure was adjusted to be 85 psi, less than the typical operating pressure of the system. Accumulator pressure was more stable between exhaust valve and intake valve strokes after adjusting the precharge pressure. This can be further optimized through simulations of the system.

Valve Spring Preload

The valve lift is sensitive to the initial preload of the engine springs. The higher the preload force of the springs, the higher the pressure required to open the valves.

The stock engine spring retainers had different preload distances for the intake and exhaust valves (Figure 6.4a). The stock intake valve retainer has approximately 2mm of extra preload vs the exhaust valve. Using springs with a stiffness of 25 kN/m, an extra 50N of force was needed to start to open the intake valve. Furthermore, the stock retainers were designed to be held in place by the camshaft. The HVVA system replaced the camshaft with hydraulic cylinders that did not keep the retainers in place. This resulted in dropping the exhaust valve into the cylinder during operation (Figure 6.4b). A different style of valve retainers was purchased. These retainers give even spring preloads between the two engine valves and hold the valves in place without requiring pressure from the camshaft.



(a) Intake Valve (left) & Exhaust Valve (right)



(b) Damaged engine valve

Figure 6.4: Engine valves

6.1.4 Valve Lift Height Drop (Pressure fluctuations)

After the accumulator precharge pressure was set to a lower pressure and the spring preloads were set equal, it was observed that both intake and exhaust valve lift height were unstable during testing. The engine valves lift heights (especially the exhaust valve) would fluctuate, sometimes dropping more than 2mm (Figure 6.5). The valve lift height measurement corresponded to fluctuations in the pressure measurements upstream of each hydraulic cylinder.

Similar results were produced through the Simulink simulation (Figure 6.6) only after the fluid inertia was accounted for in the tubing between the spool valves and hydraulic cylinders. These fluctuations decreased when the length of tubing used in the simulation was decreased.

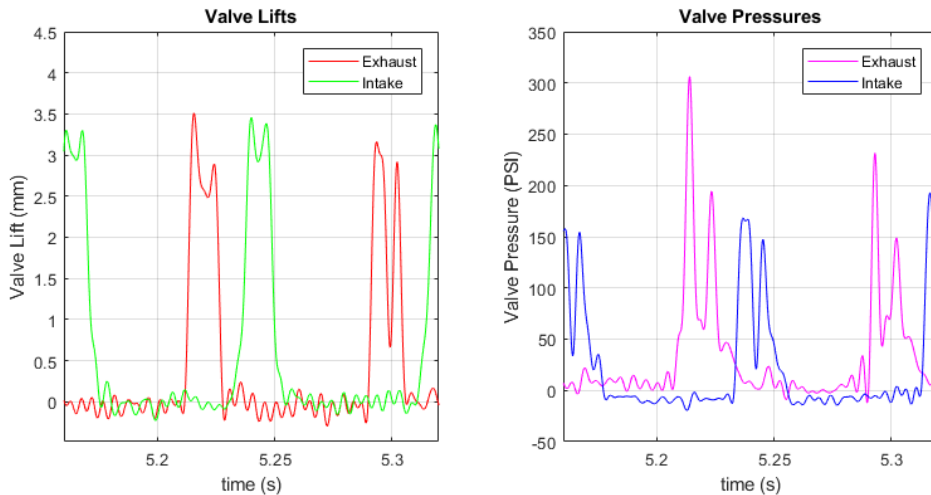


Figure 6.5: Valve lift height & pressure fluctuations

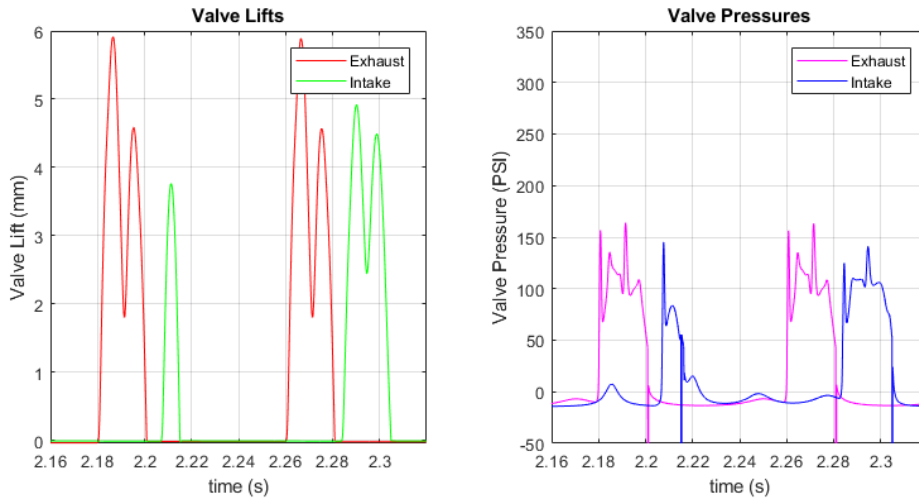


Figure 6.6: Simulation results after including fluid inertia

The simulation and experimental data indicate that the mass of the fluid in the relatively long tubing runs between the spool valves and the hydraulic cylinders is contributing to a ‘water hammer’ effect. The engine valve springs, accumulator, and oil compressibility all contribute to reducing the overall system stiffness allowing this effect to occur. This explains the periodic changes in pressure seen in the experimental data. The low pressure side of the fluctuations was enough to drop the valve height at some operating points.

Previous prototypes had check valves installed in between the HPSVs and the engine valve cylinders. These check valves were installed close to the cylinders and only the small section of fluid between the check valve and the cylinder could oscillate. The new HVVA system combined the LPSV and HPSV connections inside the spool valve block to minimize tubing. However, this layout does not incorporate the check valve used in the previous prototypes. An insert type check valve could be installed within the spool block itself, but the block would have to be mounted directly above the engine valves for this to be effective.

A normal check valve installed at the cylinders would prevent backflow to the LPSVs and the engine valves would not be able to close. Instead, one-way flow control valves were proposed as a solution. These valves have a needle valve to restrict the flow in one direction, but a check valve allows free flow in the opposite direction (Figure 6.7). The flow to open the valve would be restricted to reduce the amplitude of pressure fluctuations. Flow returning to the LPSVs would not be restricted.

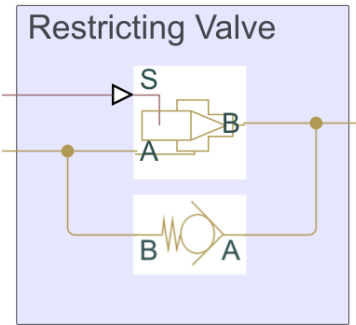


Figure 6.7: One-way flow control valve

One-way flow control valves were first added to the simulation to check if this was a valid solution. Results (Figure 6.8) showed a marked improvement in fluctuation of valve lift height (from 4mm to 0.5mm).

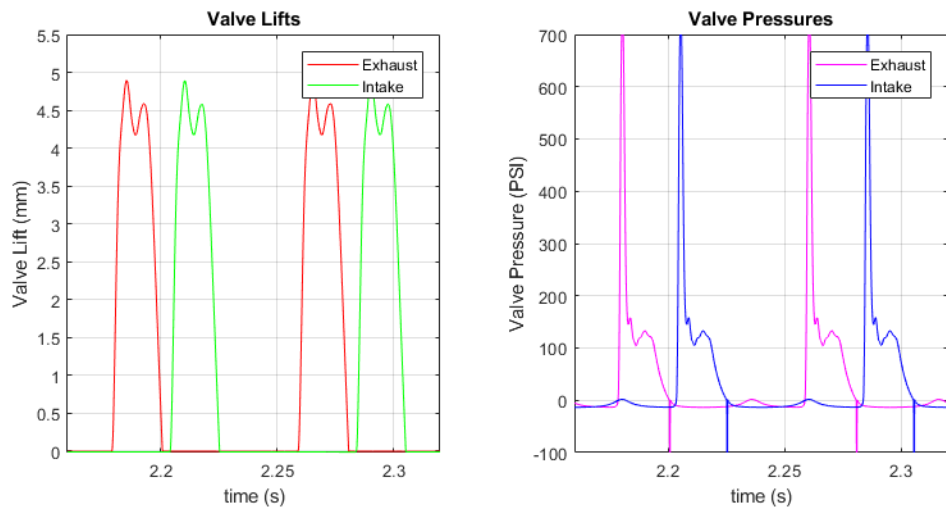


Figure 6.8: Simulation results after adding one-way restriction valves

After proving the effectiveness of the one-way valves in the simulation, they were purchased and installed in the actual system. After adjusting the flow control valves, similar improvements were seen in the physical system (Figure 6.9). Note that the pressure sensor is installed upstream of the flow control valve, so fluctuations in pressure are still visible (but will be damped before reaching hydraulic cylinders).

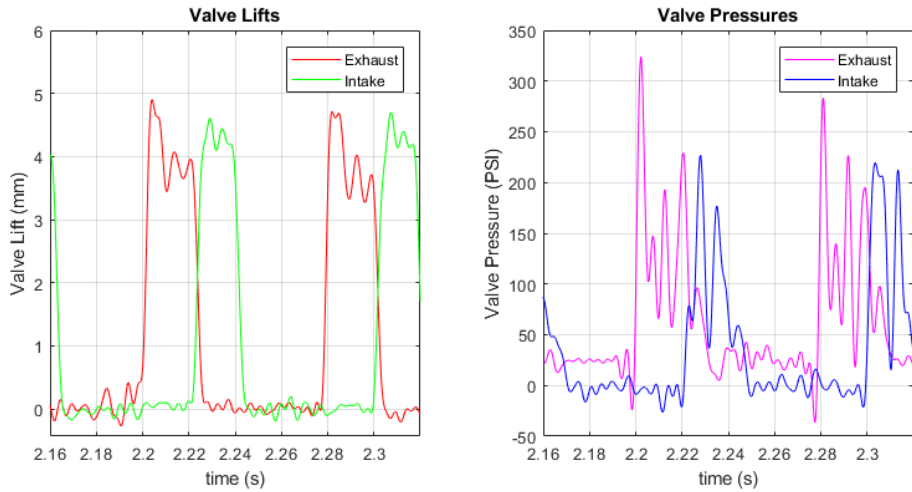


Figure 6.9: System results after one-way flow control valves added

6.1.5 Torque Fluctuations

After assembly, the new HVVA system was first tested without engine compression. This minimized the torque and vibration in the system for initial testing. A Lovejoy type coupler (Figure 6.10a) with a rubber spider (Figure 6.10b) was used to transfer the torque from the dyno to the engine. This rubber coupler was quickly destroyed (Figure 6.10c) when the spark plug was added to the engine and tests were run with engine compression.



(a) Lovejoy coupler (b) Rubber spider before testing (c) Rubber spider after testing

Figure 6.10: Rubber spider for Lovejoy coupler

A Hytrel plastic spider was strong enough when running compression tests but was damaged during initial combustion testing (Figure 6.11a). The Lovejoy coupling was replaced with a rigid coupling, and the key connecting the engine shaft to the coupler was sheared (Figure 6.11b).



(a) Hytrel spider after testing



(b) Sheared key

Figure 6.11: Hytrel spider & sheared key

A longer rigid coupler with tighter shaft fits was designed and machined to couple the engine and dyno. After this was installed, a resonance was observed in the torque readings (Figure 6.12). The data shows the torque vibrations lasting through the whole 720° engine cycle. As the torque is not damped out completely before the next cycle, the additional torque impulse (from combustion or compression) would add to the energy already there. This would cause a build up of energy in the system and is likely what caused damage to the couplers.

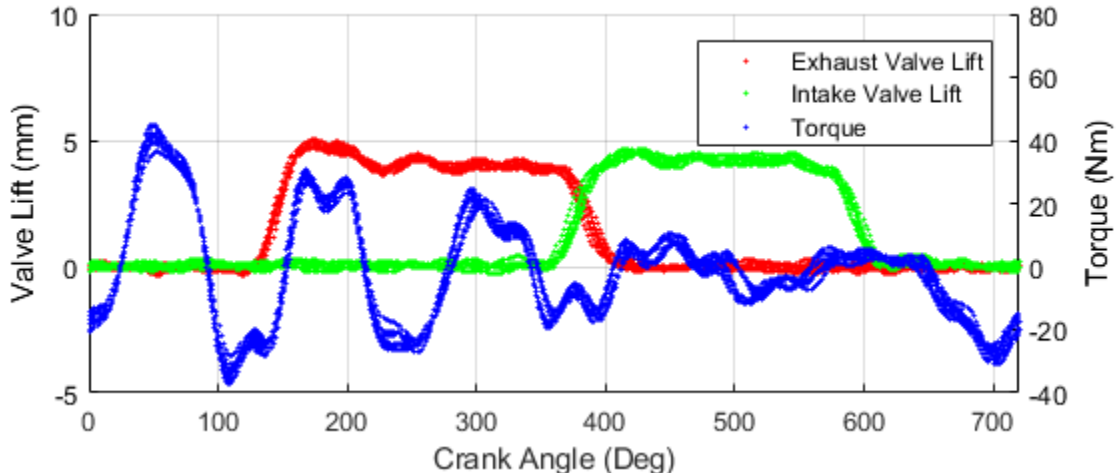


Figure 6.12: Torque fluctuations

The torque data was run through the MATLAB fast Fourier transform function. The dominant frequency was 60 Hz (Figure 6.13).

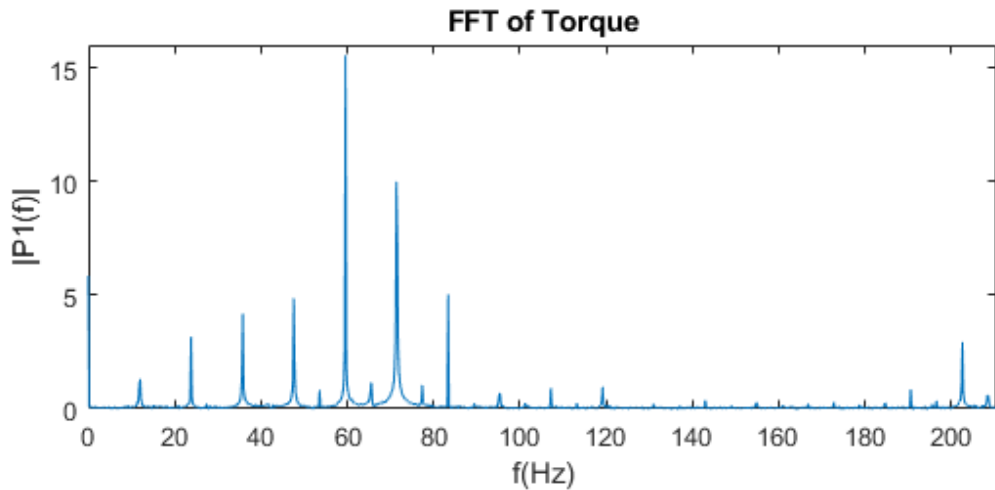


Figure 6.13: Fast Fourier transform of torque readings

By measuring the response to torque impulses at different locations along the axis of the shaft the resonance frequency of 60Hz was isolated to the flywheel of the test engine. The flywheel was removed from the engine and the resonance frequency increased. This was expected after reducing the rotational mass, I , and therefore increased the natural frequency, ω_n calculated as:

$$\omega_n = \sqrt{\frac{k_{tor}}{I}} \quad (6.1)$$

Subsequent tests (Figure 6.14) show any torque vibrations dampening out before the next cycle impulse.

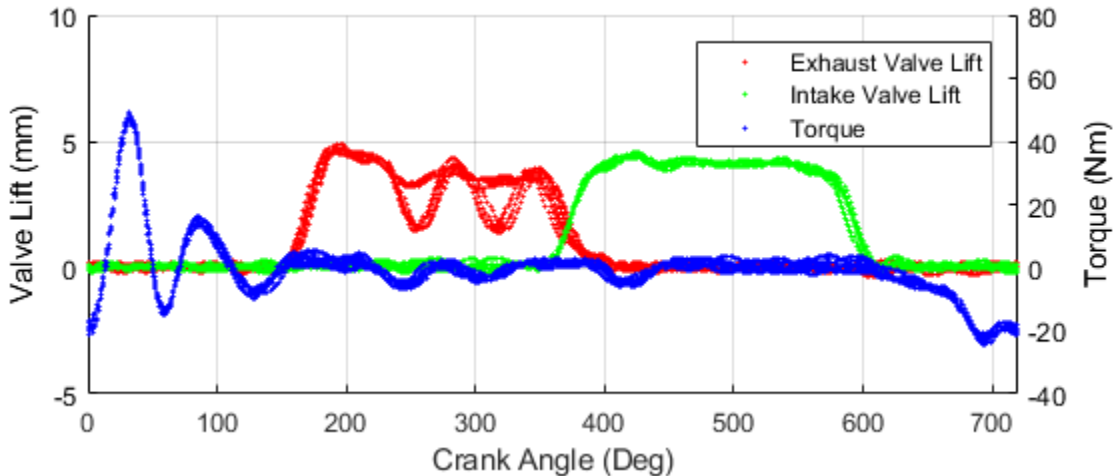


Figure 6.14: Torque test after engine flywheel removed.

6.1.6 System Power Consumption

The power consumption of the HVVA system was estimated in order to be compared with a conventional cam system valvetrain. The power consumption (Pwr_{HVVA}) was calculated using accumulator pressure (P_A) and pump flow (Q_A) data from a 1500 RPM engine speed test and the holding power of the linear actuators (Pwr_{LA}) as:

$$Pwr_{HVVA} = P_A Q_P + 4Pwr_{LA} \quad (6.2)$$

The results of this calculation are shown in Table 6.2.

Table 6.1: HVVA System Power Consumption

Description	Variable	Value
Accumulator Pressure	P_A	1.6 MPa
Pump Flow	Q_A	$7.17 \times 10^{-5} \text{ m}^3/\text{s}$
Linear Actuator Holding Power	Pwr_{LA}	7 W
HVVA Power Consumption	Pwr_{HVVA}	114 W

The calculated 114 W of power consumption is similar to the estimated 125W for a two valve cam based valve train (25% of the eight valve engine tested at 1500 RPM in [23]). However, the HVVA system power consumption calculated here does not include the frictional losses. Further testing would have to be done to fully compare this system to a cam based engine.

6.2 Valve Profile & Combustion Experiments

The main validation tests for the new HVVA system were derived from Li's experiments developed for the same test engine. Li's tests were run at 1000 RPM with the original engine camshaft timing (CAM), the full load optimized valve timing (OPT), and internal exhaust gas recovery timing (IEGR) for partial load throttleless operation. The different profiles are displayed in Figure 6.15. The same timings were used to run experiments at 1300, 1400, and 1500 RPM.

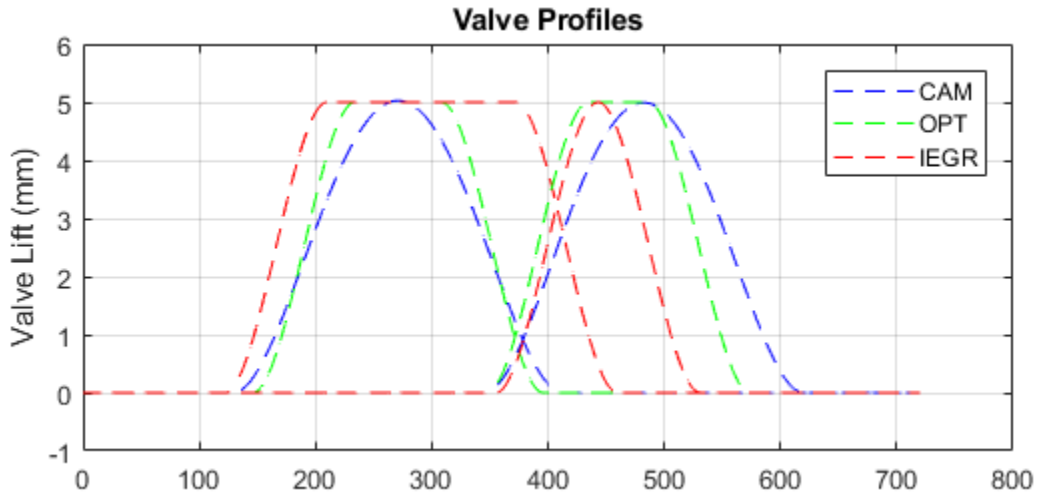


Figure 6.15: Valve profiles used in experiments

Li's thesis gives the tangent position TPA timings used for his 1000 RPM tests [33]. These were used as the initial positions for the new testing but had to be adjusted due to lag time when opening and closing valves at the higher test speeds. The lag present was very consistent and could easily be compensated for by adjusting timings. A further iteration of this project could minimize the lag time using a delay vs. engine speed lookup table. Final TPA timings were set to match the opening and closing points of each profile.

Table 6.2: Testing Details

Test	Profile	Engine Speeds (RPM)	Accumulator Pressure SP (PSI)	Adjusted TPA Timings (CA) [EVO/EVC/IVO/IVC]
CAM	Original Engine Camshaft Profile	1300	210	
		1400	220	62/320/302/518
		1500	230	
OPT	Optimized Valve Profile	1300	210	
		1400	220	78/308/303/466
		1500	230	
IEGR	Internal Exhaust Gas Recirculation Profile	1300	170	
		1400	190	79/362/311/443
		1500	210	

The original engine camshaft had a valve lift height of 5.5mm. Due to issues with cylinder positioning (see section 6.1.2), the valve lift was limited to ~4.5mm. The accumulator pressure setpoints required for 4.5mm of lift at the different engine speeds and valve profiles were determined through running experiments. The spark angle was set at 11° before TDC. Full test details can be found in Table 6.2 and results for the 1400 RPM engine speed testing are shown in the sections below. Results for the 1300 & 1500 RPM tests can be found in Appendix B.

Combustion was run for each profile at different air fuel ratios. The air fuel ratio was set manually by adjusting the total fuel output in the ECU. A constant spark angle and throttle position were used for all tests.

6.2.1 Original Camshaft Profile (CAM)

The CAM profile matches the valve lift profile of the stock camshaft originally installed on the Honda GX200 test engine. This profile is meant to optimize the power and efficiency of the engine in the normal operating range of 2000-3600 RPM. Results from this original profile can be used as a baseline measurement to compare to the optimized timing results.

A comparison of the camshaft profile and adjusted HVVA profile is shown in Figure 6.16. The opening and closing points of each valve are matched but the HVVA system has much faster opening and closing velocities.

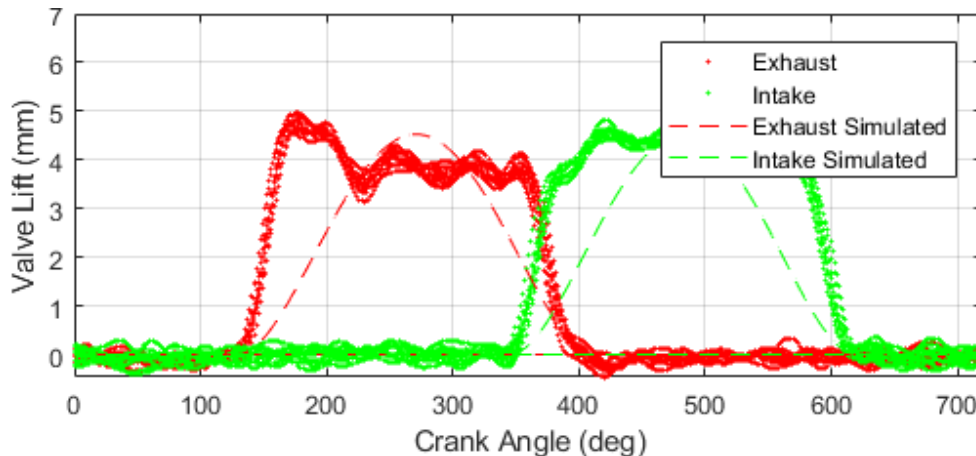


Figure 6.16: CAM simulated (original) profile and experimental results

Combustion testing using the CAM profile was run with an air fuel ratio (AFR) of 14.7 (stoichiometric) and a throttle position of 40%. This profile produced a mean torque of 4.16 Nm (Figure 6.17).

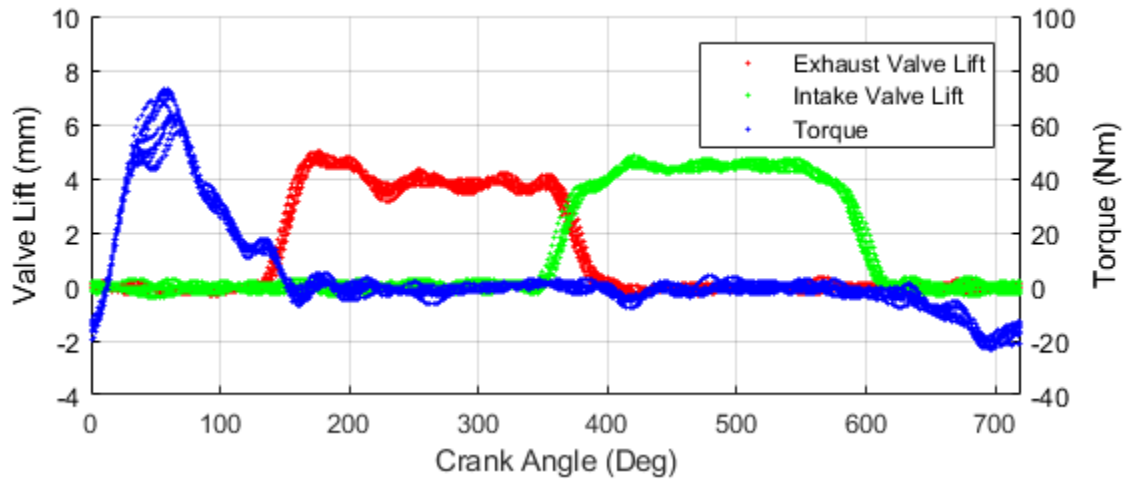


Figure 6.17: CAM profile torque results

6.2.2 Optimized Profile (OPT)

Li used his genetic algorithm optimization tool to determine the engine valve timings required to maximize the torque and efficiency for testing the Honda GX200 engine at 1000 RPM. These are the valve timings matched for the OPT profile experiments (Figure 6.18). This profile is expected to give higher torque and efficiency versus the CAM profile.

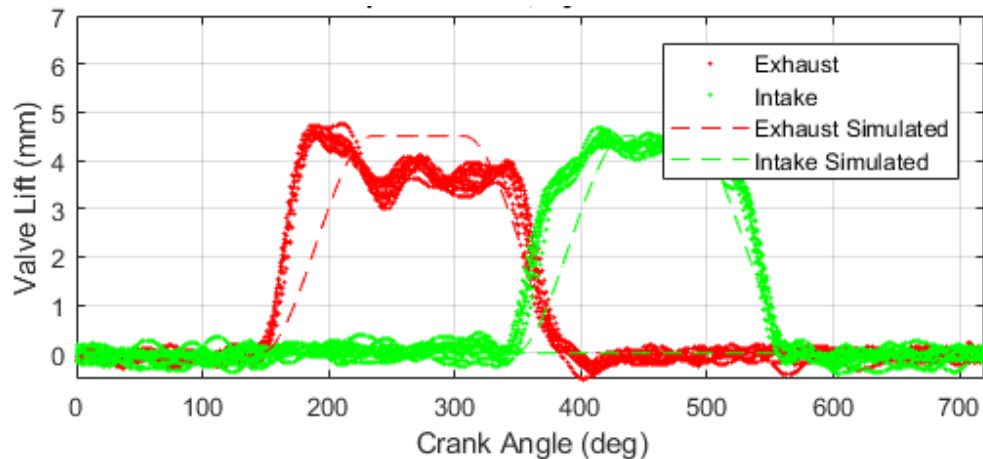


Figure 6.18: OPT simulated profile and experimental results

Combustion testing using the OPT profile was run with an AFR of 14.7 (stoichiometric) and a throttle position of 40%. This profile produced a mean torque of 4.77 Nm (Figure 6.19).

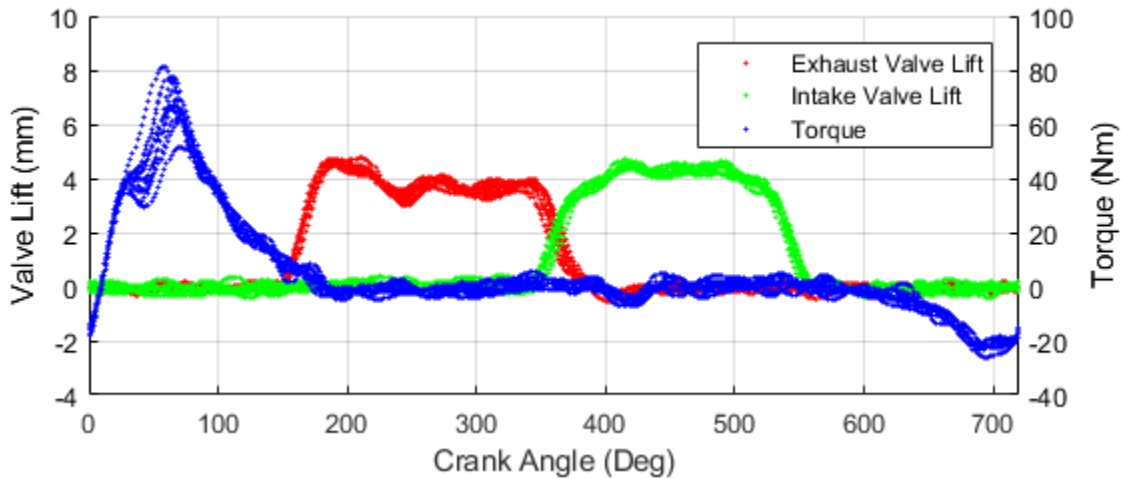


Figure 6.19: OPT profile torque results

6.2.3 IEGR Profile (IEGR)

As detailed in Section 2.1.1, internal exhaust gas recirculation can be used to throttle the engine without using the throttle valve. Closing the exhaust valve late gives positive valve overlap. There will be residual exhaust gases in the combustion chamber reducing the amount of fresh air charge (and reducing pumping loses). This is combined with early intake valve closure to increase the effective combustion ratio (ECR).

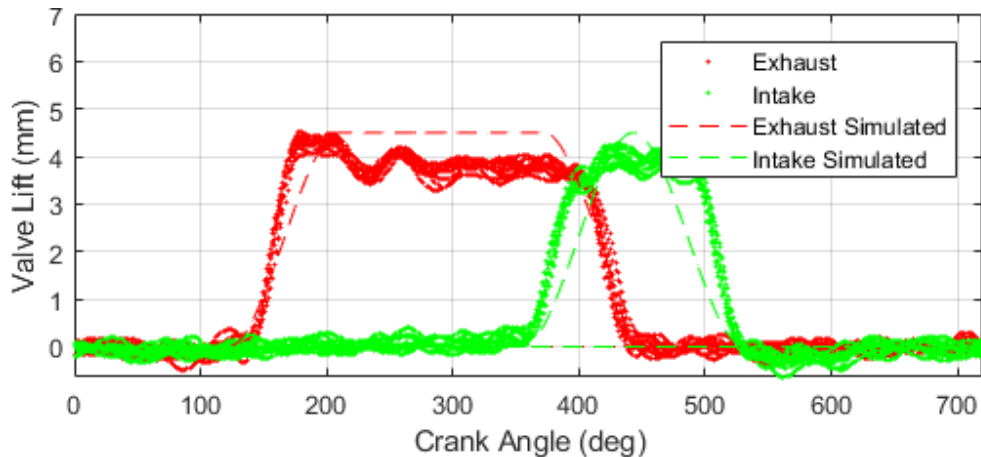


Figure 6.20: IEGR simulated profile and experimental results

Combustion testing using the IEGR profile was run with an AFR of 16.0 (lean: excess air) and a throttle position of 40%. The higher ECR of this profile allows for a leaner combustion mixture to be used. This profile produced a mean torque of 1.62 Nm (Figure 6.21).

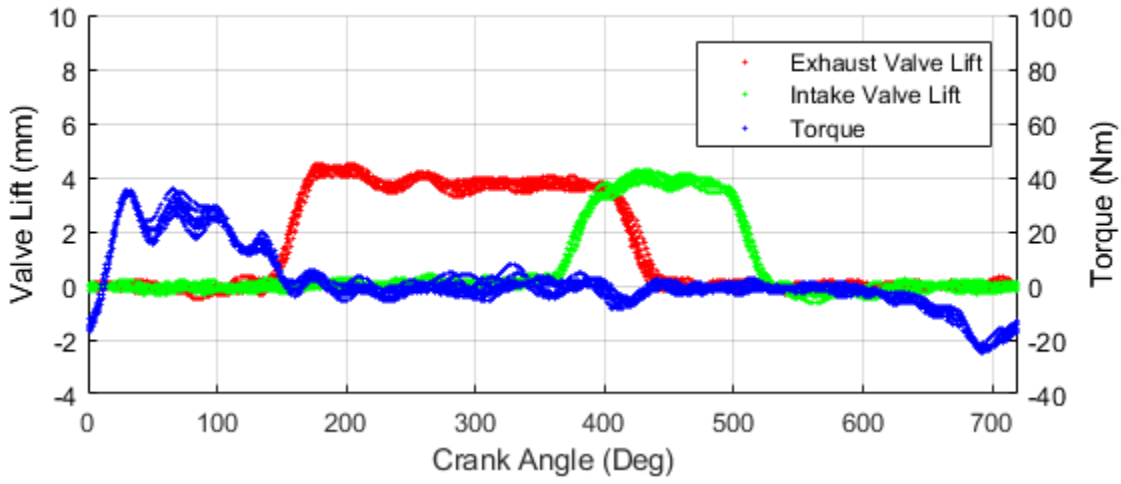


Figure 6.21: IEGR partial load profile torque results

6.2.4 Results

The results can be compared by looking at the total torque produced and how efficiently this torque was produced. The specific fuel consumption (b_e) is a measure of the total fuel consumed divided by the total power produced. It allows fuel economy to be accurately compared between tests with different load conditions.

The specific fuel consumption (b_e) is calculated by using the current fuel consumption (\dot{m}) and the specific power output (P_e) as [34]:

$$b_e = \frac{\dot{m}}{P_e} \quad (6.3)$$

The power output is calculated using the mean torque (T_m) and the rotational speed of the crankshaft (ω) as:

$$P_e = T_m \omega \quad (6.4)$$

Experimental results including the calculated specific fuel consumption are found in Table 6.3.

Table 6.3: Results of Combustion Testing

Valve Profile	Mean Torque	Air Fuel Ratio	Fuel Mass (per Cycle)	Estimated Air Volume (per Cycle)	Specific Fuel Consumption
CAM	4.16 Nm	14.7	15.9 mg	194.7 cc	0.303 mg/J
OPT	4.77 Nm	14.7	17.3 mg	212.2 cc	0.289 mg/J
IEGR	1.62 Nm	16.0	12.9 mg	171.4 cc	0.632 mg/J

The OPT profile produced more torque than the CAM profile with a lower specific fuel consumption. Thus, it was proved to be a more optimized profile for the engine at full load.

The IEGR profile reduced the engine load while maintaining the same throttle valve position. This reduction in torque was a combination of the IEGR reducing the fresh air charge into the cylinder and the increase in air fuel ratio.

Combined, these results show how the engine can be effectively tuned by adjusting the valve timings using the HVVA system.

6.3 Load Cycle Testing

A theoretical load cycle was created to test the response of the system to changing demands. The load cycle operates between low (33%), medium (66%), and high (100%) load points. The OPT profile was used for the high load and Li's GT Power Simulation was used to find IEGR profiles that result in 33% and 66% of the theoretical torque output of the OPT profile. The valve timings used are shown in Table 6.4.

The cycle spends ten seconds at each load point according to the pattern shown in Figure 6.22. Note that to avoid possible interference between the exhaust valve and the engine piston, the system was not stepped directly from high load to low load (if the higher system pressure from the high load position does not drop quickly, it will cause high valve lift at low load). This challenge could be corrected with a more detailed control system.

Open loop control was used to set the system pressure. Calibrated currents were sent to the pump drive to match the current operating profile and desired pressure. The pump settings were sent one second

before the valves were commanded to switch to the required profile to compensate for the delay in the hydraulic system.

Table 6.4: Load Cycle Testing Details

Profile	Test	Engine Speeds (RPM)	Accumulator Pressure SP (PSI)	Pump Drive Setpoint (Amps)	Adjusted TPA Timings (CA) [EVO/EVC/IVO/IVC]
IEGR	Low Load (33%)	1400	200	0.581	79/440/311/443
IEGR	Med. Load (66%)	1400	220	0.670	79/382/311/443
OPT	High Load (100%)	1400	220	0.735	78/308/303/466

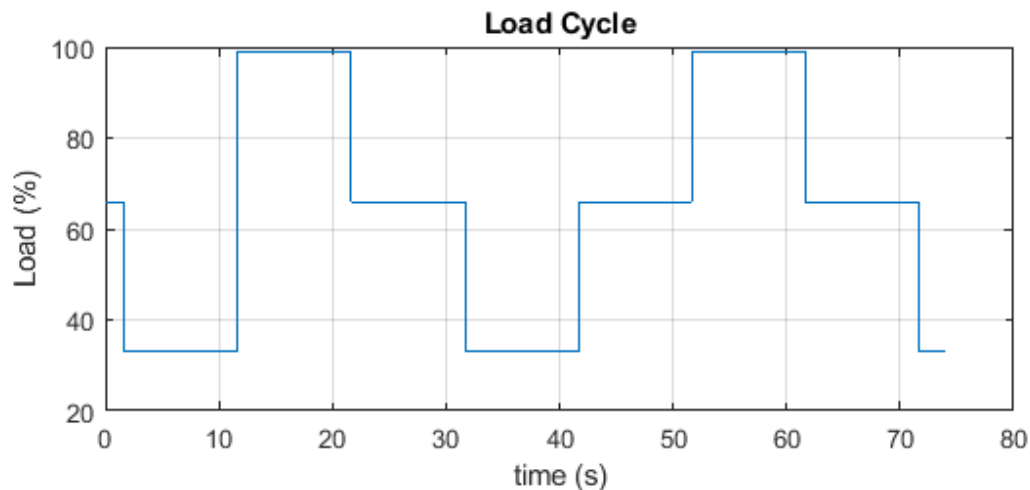


Figure 6.22: Simulated load cycle

6.3.1 Experimental Results

The experimental results for the load cycle are shown below. As the load was controlled using an IEGR strategy, the exhaust valve closing point was the valve timing that changed the most between cycles. The setpoint (SP) and present value (PV) positions of the LPSV used to close the exhaust valve are shown in

Figure 6.23. The largest change in position was from low load to full load (Figure 6.24). This change was completed in <1s.

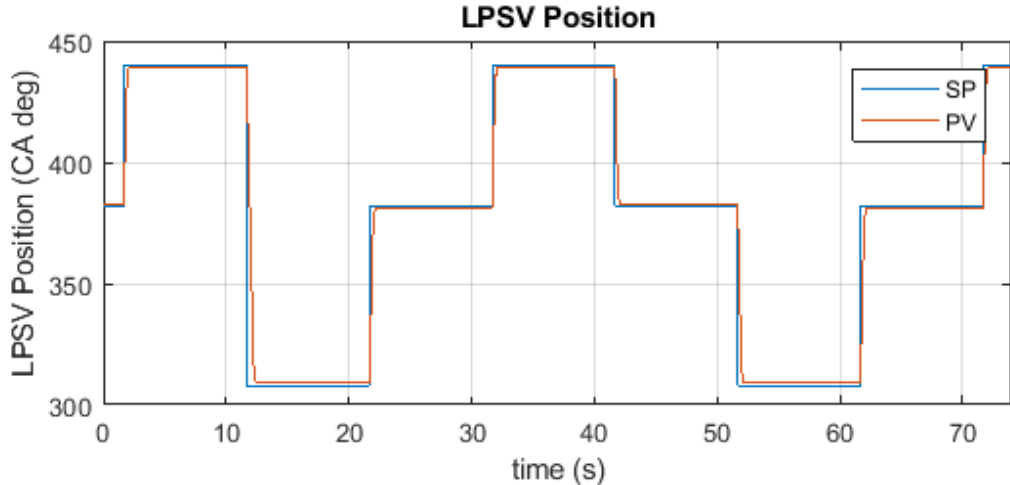


Figure 6.23: Spool valve position response

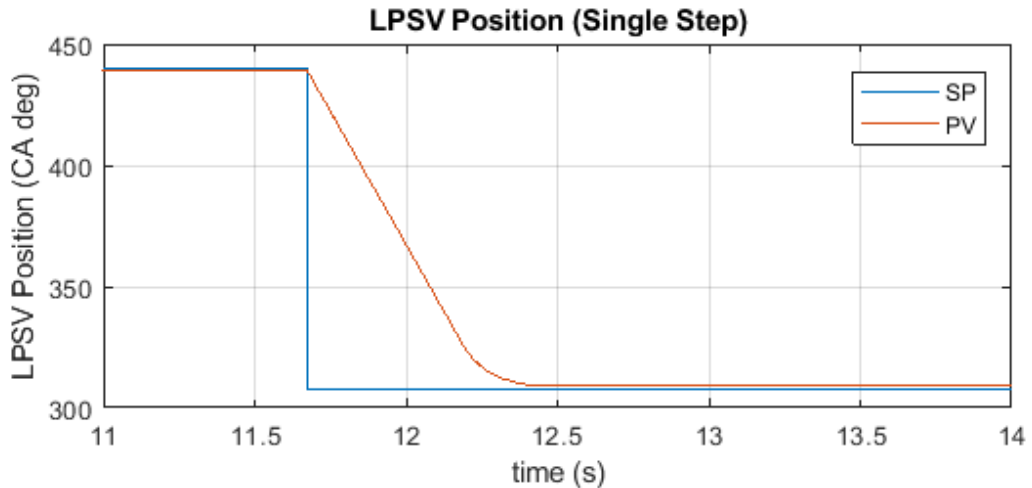


Figure 6.24: Single step spool valve position response

The system pressure response (Figure 6.25) was much slower than the spool valve response. The maximum settling time was ~6s when switching from high to medium or medium to low loads.

The average valve lift response (Figure 6.26) was faster than the pressure response but was seen to overshoot when switching between different load points. The valve lift is a function of both system pressure and spool valve position. Therefore, the valve lift would overshoot if the pressure changed

before the spool valve finished changing position when increasing the load, or if the spool valve changed position before the pressure changed when decreasing the load.

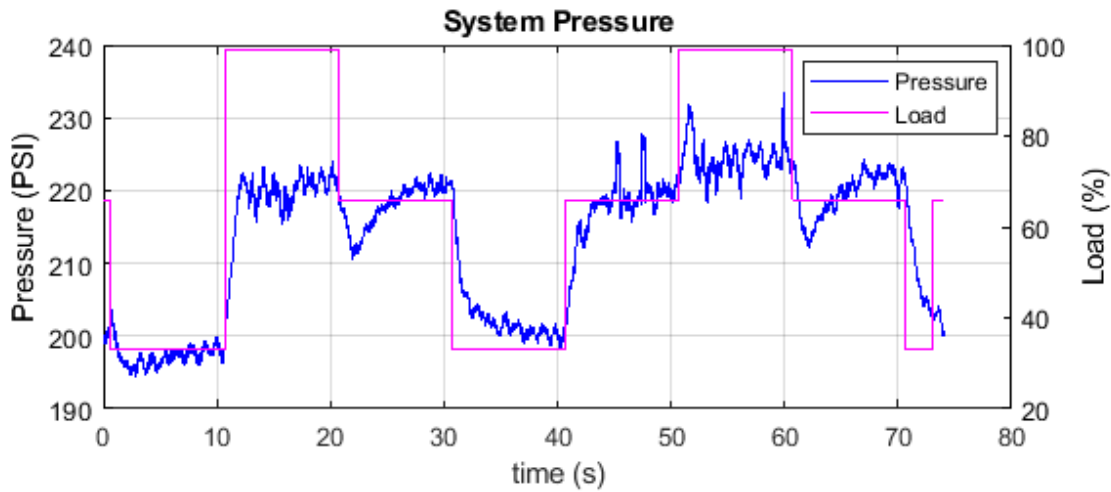


Figure 6.25: System pressure response

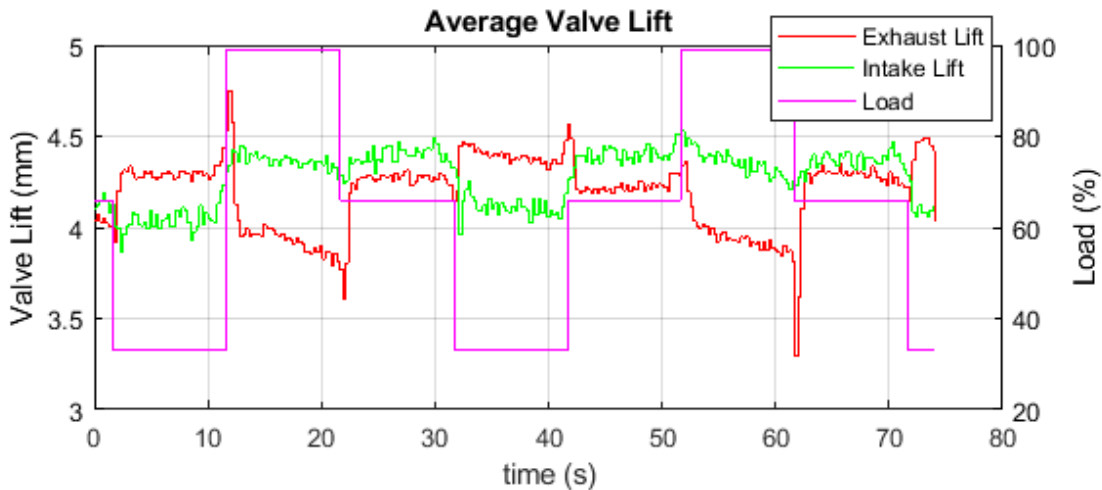


Figure 6.26: Average valve lift response

The load cycle testing demonstrates the ability of the HVVA system to adjust valve timings quickly and reliably while maintaining valve lift. However, the slow response of the hydraulic system results in unstable pressure and valve lift when changing between different load points.

6.4 Data Post Processing

The raw noisy sensor data was collected through the dSpace system and processed in MATLAB.

6.4.1 Noise & Sensor Accuracy

Connecting all the components and motor drives together in the control panel resulted in ~0.1V of electrical noise present in all sensor readings. The sensors and drives were not electrically isolated, and all shared a common ground.

The electrical noise had a significant impact on the linear displacement sensors, pressure transducers, and the torque sensor as these were only used in a relatively small part of their total range. For example, the pressure sensors had a 0-3000 PSI measuring range and a 0-10V output. For these pressure sensors, 0.1V equals 30 PSI. This is a significant portion of the typical operating range of 120-300 PSI. For each of these sensors, the noise level is significantly higher than the sensor accuracy (Table 6.5).

Table 6.5: Sensor Accuracies & Relative Noise Levels

Sensor	Accuracy	Full-Scale Range	Output	Operating Range	Relative Noise Level
Linear Displacement Sensor	0.05%	0-50 mm	0-10 VDC	0-10 mm	5%
Pressure Transducer	0.5%	0-3000 PSI	0-10 VDC	0-300 PSI	10%
Torque Transducer	0.05%	0-500 Nm	0-10 VDC	0-150 Nm	3.3%

The ECU O2 sensor could not be used due to the short duration of combustion tests. An O2 sensor external to the ECU was used to measure the AFR for each combustion test. The installation location of this O2 sensor allowed for potential air leakage. The AFRs in Table 6.3 may be more lean than what is shown as a result, but the same O2 sensor was used for all readings (all tests are comparable relative to each other).

All these sensors were adequate for the required validation of the system. Their readings proved the system main functions and relative readings demonstrated the improvements possible when using VVA strategies. Any further testing and theoretical model calibration may require reducing system noise or buying sensors with smaller full-scale ranges to get more accurate readings.

6.4.2 Filtering

The noisy data is filtered using a low pass finite impulse response (FIR) filter with a passband frequency of 200 Hz.

A moving average filter works well in the time domain (provide good smoothing) but not as well in the frequency domain (it loses sharp transitions in data) [35]. The FIR filter is applied forwards & backwards to eliminate the filter phase delay [36].

Chapter 7

Conclusions & Future Work

7.1 Observations

Mechanical System

The mechanical system ran smoothly through many tests, both with and without combustion. The whole assembly showed greatly reduced vibrations compared to the previous prototype (current prototype did not have any damaged sensors due to vibration). The only mechanical vibration issue found during testing was due to the flywheel of the test engine, not the HVVA assembly or installation.

The redesigned phasing system worked very well to set the valve opening and closing times. However, the linear actuators are running much slower than their maximum speed. There was unexpectedly high rotary seal friction and some assembly misalignment between the lead screws and nuts. These factors reduced the available maximum phasing speed to 180°/s.

The previous prototype required an envelope of 0.16 m³ to contain all the spool valves and phasing assemblies. The new spool valve and phasing assembly only requires 0.011 m³, less than 10% of the previous system.

Hydraulic System

Pressure readings for this system revealed fluctuating characteristics of the hydraulic system due to the high-speed dynamics present. When running at high speeds, the sudden opening of the HPSVs creates a pressure wave in the tubing between the spool valve and the hydraulic cylinder. If there is a long run of fluid in this section of tubing, the inertia of the fluid combined with the stiffness of the valve spring, steel tubing, and fluid compressibility combine to create pressure waves. These fluctuations were likely present but not measured in experiments with previous designs. These pressure waves must be considered in future designs, especially as the speed of the system increases.

The purchased hydraulic cylinders did not operate as expected. Instead of smoothly operating between 0-6mm of lift, they jumped between valve lifts and only had small windows of linear operation. They were being used outside their typical use (high cyclic loading, low lift) and were not ideal for this project.

The hydraulic system showed minimal leakage. There was no leakage through the rotary seals on the spool valve shafts (despite using simpler & less expensive seals), from the spool valve block, or from the hydraulic cylinders. This was a major benefit of reducing the amount of hydraulic tubing and fittings.

7.2 Conclusions

The main objective of this project was to design and build a reliable functioning update of the HVVA system that was more compact than the previous prototype. It required an adjustable combustion system to fully validate Li's results for various engine valve timing strategies and a design that could be rigidly assembled to the test table to minimize vibrations.

The system was successfully built and ran reliably through many different tests including testing the engine with combustion. The newly designed phasing system was proven to work and phase between normal profile changes in <1s. Each of the individual valve timings could be adjusted from 0 to 720°CA, making the system fully flexible.

It was much more compact than the previous assembly: the total volume of all four spool valves and phasing assemblies was <10% of the volume of the previous prototype. This brings the system much closer to a setup that could be installed directly on an existing engine block.

The vibration of the experimental setup is minimal compared to the previous system and there were no sensor failures despite extensive testing of the setup.

The addition of electronic fuel injection to the combustion system was successfully used to validate Li's research and makes the HVVA system a better platform for further research in variable valve actuation strategies.

The new HVVA system continues to prove the validity of the MVSL's HVVA concept. It can be used to run tests and experiments to continuously improve this concept and bring it to the next stage of development.

7.3 Recommendations/Future Work

The testing already completed with the new system has given a greater understanding of the HVVA concept. Possible ideas for updating and improving the design have been generated through this testing and are given below.

7.3.1 Mechanical

Multi-Cylinder Test Engine

The spool valve assembly can be expanded for use on a larger engine. The same HVVA assembly could be used for a two-cylinder engine by adding ports to the bottom of the spool valve block. These ports would open or close the second cylinder engine valve 360° (crank angle) after the first cylinder engine valve event. The two ports can be copied along the length of spool block for every two additional engine cylinders. To open or close the engine valves through these extra ports, additional ports would also be added along the length of the spool. For a four-cylinder engine, a second port is added to the spool that radially trails the first port by 90° (Figure 7.1).

Figure 7.1).

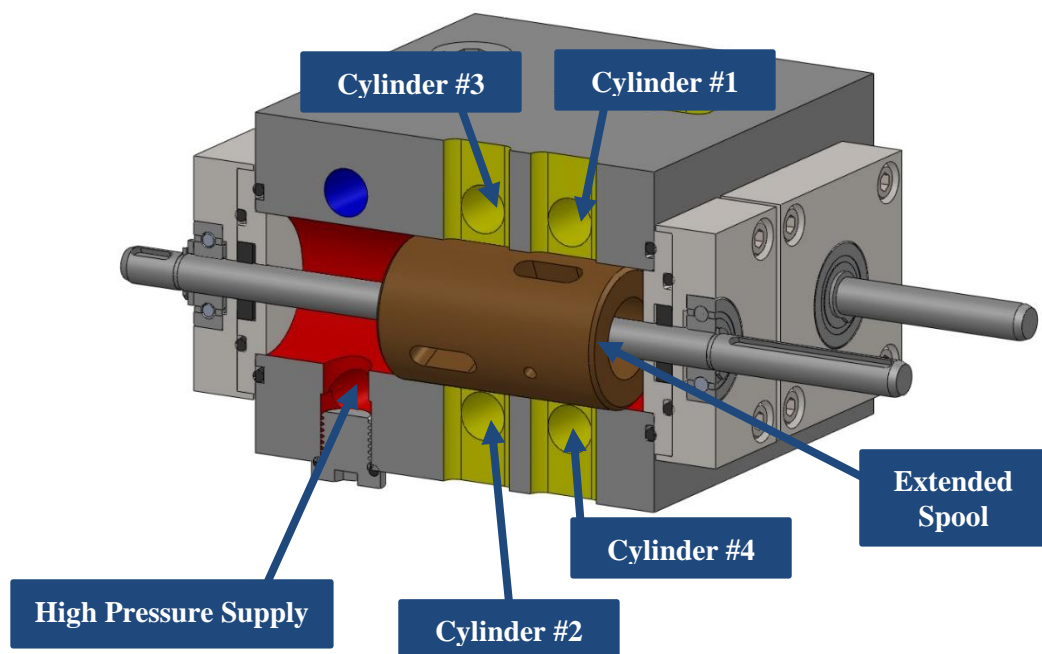


Figure 7.1: HPSV cross section for four-cylinder engine with firing order 1-3-4-2

Phasing System

This project proved the concept of the new phasing system, but it can be further improved and optimized.

This system uses 1.25" long lead screws with a 1" lead, providing $>360^\circ$ of spool valve phasing. The length of the lead screws should be shortened to the exact length needed for the adjustment range of each

spool valve. This would reduce the total assembly length, spool valve shaft length, and the required linear actuator range.

Linear Actuators

The linear actuators could be hydraulically powered instead of using electric actuators. Hydraulic directional valves controlled by solenoid valves would change the direction of actuator motion or hydraulically lock it in place. The current system requires a constant holding torque applied to the linear actuators to hold the phasing positions, requiring constant power (7W for each actuator).

7.3.2 Hydraulic

Tubing

The pressure fluctuations seen during testing highlight the importance of reducing the total volume of fluid between the high pressure spool valves and hydraulic cylinders. This volume should be minimized for the next design. This could be done by mounting an HVVA system directly on top of an engine block.

Check Valves

Check valves should be installed between the HPSVs and the hydraulic cylinders. A check valve installed as close to the cylinder as possible will effectively reduce the volume between the spool valve and cylinder. Press-in check valves could be installed directly in the spool valve block (Figure 7.2).

Air Bleed

The hydraulic system should be updated to include easy to use air bleed ports on top of the spool valve block. The current design requires 24 screws to be removed before the block can be purged of air. This could be reduced to one bleed screw per spool valve.

Accumulator

To achieve more uniform lift between the intake and exhaust valves, each HPSV should have its own accumulator. A smaller spring-loaded accumulator with a check valve preventing flow out of the spool valve would be installed in the same bore as the high pressure spool (Figure 7.2). In this setup, both the intake and exhaust valves would see the same pressure during opening events. If adjustable pressure bleed valves were installed downstream of each check valve, the lift heights of intake and exhaust valves could also be controlled separately.

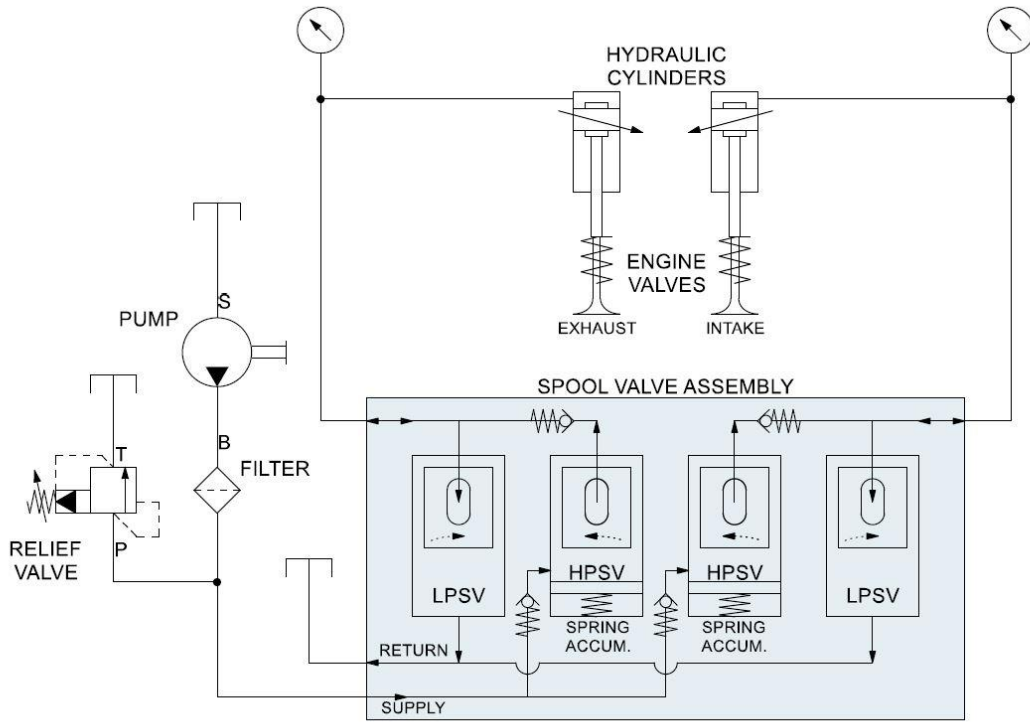


Figure 7.2: Updated hydraulic schematic

Hydraulic Cylinders

The purchased hydraulic cylinders limited the ability of the system to adjust valve lift height and valve cushioning. Hydraulic cylinders like those on the Fiat Multiair system should be used instead. These cylinders would be threaded directly into the spool valve block, have the total stroke limited to the desired valve lift height, and have a permanent orifice for cushioning the closing of the valves.

7.3.3 Software/Control

Lift Control

The current setup controls the accumulator pressure by adjusting the current sent to the hydraulic pump drive. Lift control was not possible with the hydraulic cylinders currently in use. After installing cylinders that can operate over the whole range of lift of the engine valves, a valve lift height controller should be employed.

Timing

The timing positions of the current setup were manually tuned to match the required valve profiles. A future version of this project should use offline mapping of valve timings for desired IVO/IVC/EVO/EVC at different engine speeds. This mapping can then be used to automatically adjust the spool valve positions to achieve desired valve timings.

Fuel Injection

To make the system as flexible as possible, the ECU should be removed from the system. The fuel injection, spark timing, and air fuel ratio could all then be controlled directly by the dSpace system. This would require that the fuel injector, fuel pump, CDI, and O2 sensor be connected to and controlled by dSpace.

References

- [1] E. Sher and T. Bar-Kohany, "Optimization of variable valve timing for maximizing performance of an unthrottled SI engine—a theoretical study," *Energy*, vol. 27, (8), pp. 757-775, 2002. Available: <https://www.sciencedirect.com/science/article/pii/S0360544202000221>. DOI: 10.1016/S0360-5442(02)00022-1.
- [2] Y. Li *et al*, "Power and fuel economy optimizations of gasoline engines using hydraulic variable valve actuation system," *Applied Energy*, vol. 206, pp. 577-593, 2017. Available: <http://www.sciencedirect.com/science/article/pii/S0306261917312412>. DOI: //doi.org/10.1016/j.apenergy.2017.08.208.
- [3] M. Pournazeri, "Development of a New Fully Flexible Hydraulic Variable Valve Actuation System," University of Waterloo, 2012.
- [4] M. Chermesnok, "Hydraulic Variable Valve Timing Testing and Validation," University of Waterloo, 2016.
- [5] M. S. Siddiqui, "Hydraulic Variable Valve Actuation on a Single Cylinder Engine," University of Waterloo, 2017.
- [6] Mechadyne Int. "The Impact of Valve Events Upon Engine Performance and Emissions," *Mechadyne Int.*, 2006. [Online]. Available: <https://www.mechadyne-int.com/app/uploads/2015/05/the-impact-of-variable-valve-actuation-on-engine-performance-and-emissions.pdf>. [Accessed: September, 2018].
- [7] A. Muir. "The engine - how the valves open and close," *How a Car Works*, 2016. [Online]. Available: <https://www.howacarworks.com/basics/the-engine-how-the-valves-open-and-close>. [Accessed: May 9, 2019].
- [8] C. M. Hall *et al*, "Control-oriented modelling of combustion phasing for a fuel-flexible spark-ignited engine with variable valve timing," *International Journal of Engine Research*, vol. 13, (5), pp. 448-463, 2012. Available: <http://journals.sagepub.com/doi/full/10.1177/1468087412439019>. DOI: 10.1177/1468087412439019.
- [9] A. Cairns *et al*, "Combining Unthrottled Operation with Internal EGR under Port and Central Direct Fuel Injection Conditions in a Single Cylinder SI Engine," *SAE Technical Paper 2009-01-1835*, 2009. Available: <https://doi.org/10.4271/2009-01-1835>. DOI: //doi.org/10.4271/2009-01-1835.
- [10] G. B. Parvate-Patil, H. Hong and B. Gordon, "An Assessment of Intake and Exhaust Philosophies for Variable Valve Timing," *SAE Technical Paper 2003-32-0078*, 2003. Available: <https://doi.org/10.4271/2003-32-0078>. DOI: //doi.org/10.4271/2003-32-0078.
- [11] K. C. Colwell. "Timing Changes: How Honda's VTEC Variable-Timing System Works," *Car and Driver*, 2015. [Online]. Available: <https://blog.caranddriver.com/timing-changes-how-hondas-vtec-variable-timing-system-works/>. [Accessed: Feb 8, 2018].

- [12] Audi Automotive Group. "Audi valvelift system," *Audi Technology Portal*, 2011. [Online]. Available: https://www.audi-technology-portal.de/en/drivetrain/fsi-tsi-engines/audi-valvelift-system_en. [Accessed: Feb 7, 2018].
- [13] S. Manna, "BMW Valvetronic systems: How they function and how to fix them," *Motor Age*, vol. 136, pp. 76, September 1, 2017.
- [14] D. Sherman. "Fiat's Multiair Engine," *Automobile Magazine*, 2010. [Online]. Available: <https://www.automobilemag.com/news/fiats-multiair-engine/>. [Accessed: May 11, 2019].
- [15] F. Chen *et al*, "Simulation and experimental research of hydraulic pressure and intake valve lift on a fully hydraulic variable valve system for a spark-ignition engine," *Advances in Mechanical Engineering*, vol. 10, (5), 2018. Available: <https://doi.org/10.1177/1687814018773156>. DOI: 10.1177/1687814018773156.
- [16] Z. D. Lou *et al*, "Camless Variable Valve Actuator with Two Discrete Lifts," *SAE Technical Paper*, (2015-01-0324), 2015. Available: <https://doi.org/10.4271/2015-01-0324>. DOI: //doi.org/10.4271/2015-01-0324.
- [17] Y. Shiao, M. B. Kantipudi and J. Jiang, "Novel Spring-Buffered Variable Valve Train for an Engine Using Magneto-Rheological Fluid Technology," *Frontiers in Materials*, vol. 6, (95), 2019.
- [18] Freevalve. "Freevalve Technology," *Freevalve*, 2018. [Online]. Available: <http://www.freevalve.com/technology/freevalve-technology/>. [Accessed: May 11, 2019].
- [19] R. Stone *et al*, "Intelligent Valve Actuation – a Radical New Electro-Magnetic Poppet Valve Arrangement," 2017.
- [20] O. Rajput, Y. Ra and K. Ha, "Numerical parametric study of a six-stroke gasoline compression ignition (GCI) engine combustion," in *ASME 2018 Internal Combustion Engine Division Fall Technical Conference*, November 2018, .
- [21] D. Leggett. "Hyundai Motor Group unveils 'CVVD' engine tech," *Just Auto*, 2019. [Online]. Available: https://www.just-auto.com/news/hyundai-motor-group-unveils-cvvd-engine-tech_id189492.aspx. [Accessed: Jul 22, 2019].
- [22] H. Li *et al*, "Adaptive LQT Valve Timing Control for an Electro-Hydraulic Variable Valve Actuator," *IEEE Transactions on Control Systems Technology*, pp. 1-13, 2018. . DOI: 10.1109/TCST.2018.2861865.
- [23] Christopher W. Turner *et al*, "Design and Control of a Two-stage Electro-hydraulic Valve Actuation System," *SAE Transactions*, vol. 113, pp. 833-846, 2004. Available: <https://www.jstor.org/stable/44723556>.
- [24] Mohammad Pournazeri and Amir Khajepour, "Systems and methods for variable valve actuation," United States Patent 9194264, 2015.

- [25] B. Bailey. "Sizing Tube to Maximize Hydraulic System Efficiency," *Parker*, 2013. [Online]. Available: <http://blog.parker.com/sizing-tube-to-maximize-hydraulic-system-efficiency>. [Accessed: Jun 7, 2019].
- [26] Engineering ToolBox. "Flow Coefficients - Cv - and Formulas for Liquids, Steam and Gases - Online Calculators," *The Engineering ToolBox*, 2003. [Online]. Available: https://www.engineeringtoolbox.com/flow-coefficients-d_277.html. [Accessed: Jun 12, 2019].
- [27] HYDAC. "Sizing Accumulators," *HYDAC*, 2013. [Online]. Available: <http://www.hydac-na.com/sites/hydac-na/SiteCollectionDocuments/AOSS-%20accumulators.pdf>. [Accessed: Jun 12, 2019].
- [28] PBC Linear. "What is Lead Screw Efficiency?" *PBC Linear*, 2018. [Online]. Available: <https://www.pbclinear.com/Blog/2018/February/What-is-Lead-Screw-Efficiency-in-Linear-Motion>. [Accessed: Jun 18, 2019].
- [29] Haydon Kerk Pittman. "Overview of Leadscrew Assemblies," *Haydon Kerk Pittman*, 2015. [Online]. Available: https://www.haydonkerkpittman.com-/media/ametekhaydonkerk/downloads/technical%20documents/haydon_kerk_lead_screw_technology_engineering_data.pdf?la=en. [Accessed: Jun 18, 2019].
- [30] D. McCloy, *Control of Fluid Power : Analysis and Design*. (2d ed. - ed.) Chichester Eng.] : New York: E. Horwood ; Halsted Press, 1980.
- [31] N. Manring, *Hydraulic Control Systems*. Hoboken, N.J.: John Wiley & Sons, 2005.
- [32] V. Vandoren. "Fundamentals of lambda tuning," *Control Engineering*, 2013. [Online]. Available: <https://www.controleng.com/articles/fundamentals-of-lambda-tuning/>. [Accessed: Jul 2, 2019].
- [33] Y. Li author., "Power and Fuel Economy Optimization of Unthrottled Spark-Ignition Engines using Highly Flexible Hydraulic Variable Valve Actuation System," University of Waterloo, Waterloo, Ontario, Canada, 2018.
- [34] R. Van Basshuysen 1932- and F. Schäfer 1948-, Eds., *Internal Combustion Engine Handbook : Basics, Components, Systems, and Perspectives*. Warrendale, PA: SAE International, 2004.
- [35] Mathworks. "How Is a Moving Average Filter Different from an FIR Filter?" *Mathworks Help*, [Online]. Available: <https://www.mathworks.com/help/dsp/ug/how-is-moving-average-filter-different-from-an-fir-filter.html>. [Accessed: July 09, 2019].
- [36] J. O. Smith III, "Forward-backward filtering," in *Introduction to Digital Filters with Audio Applications*, 1st ed., J. Strawn, Ed. 2007, [Online]. Available: https://ccrma.stanford.edu/~jos/fp/Forward_Backward_Filtering.html.

Appendix A

Parts Lists

A.1 Mechanical Parts lists

Part Description	Manufacturer	Part Number
Rotary Seal	KC Seals	RO05 (9mm shaft)
Lead Screw	Haydon Kerk	LSSSKR-075-1000-FY10 (RH & LH)
Lead Screw Nut	Haydon Kerk	BFWFNR-075-1000-BZ00
Timing Belt Pulley (Crankshaft)	Misumi	ATP25XL037_B_N19
Timing Belt Pulley (Spool Valves)	Misumi	ATP50XL037-A-V22-Z45-J10.0
Timing Belt	Misumi	TBN210XL037
Belt Tensioner	Misumi	TNSR10-Y25-F8
Spur Gear	Misumi	GEAHB2.0-30-20-B-28-DHL-Z45-J16

A.2 Hydraulic Parts List

Part Description	Manufacturer	Part Number
Hydraulic Pump	McMaster-Carr	9296K130
Accumulator	McMaster-Carr	6716K420
Flow Control Valve	McMaster-Carr	1042K160
Filter	Arrow Pneumatics	9153V-10
Check Valve	Anderson Brass Co.	3/8" NPT
Pressure Relief Valve	Eaton-Vickers	MCSCJ012DG000010
Hydraulic Cylinder	SMC	CHNF20-50

A.3 Electrical Parts List

Part Description	Manufacturer	Part Number
Pressure Transducer	Transducers Direct	TD1000DDG300003Q001M
Linear Actuator	Haydon Kerk	43H4B-12-1.25-12-PTFE-ENC-M3
Rotary Encoder (Linear Actuator)	US Digital	E5-1024-315-1E-D-H-D-B
Rotary Encoder (Crankshaft)	Encoder Products Co.	25T-25SE-1200NV1RPP-SMH
Hall Effect Sensor (Engine Speed)	Digi-key	55505-00-02-A-ND
Linear Displacement Sensor	SICK	MPS-050CLTU0
Torque Transducer	HBM	T40B 500Q

A.4 Combustion Parts List

Part Description	Manufacturer	Part Number
ECU (4T2C)	Ecotrons	EC2T1CDTCDA2I
O2 Sensor (Narrow Band)	Ecotrons	ENOW18
O2 Sensor (Wide Band)	Innovate Motorsports	LM-2
Fuel Injector (190g/min)	Ecotrons	EFIJ-4-190
Fuel Pump (small)	Ecotrons	EFP-25D
Ignition Coil	Qazaky	100201

Appendix B

Full Combustion Results

B.1 Testing at 1300 RPM Engine Speed

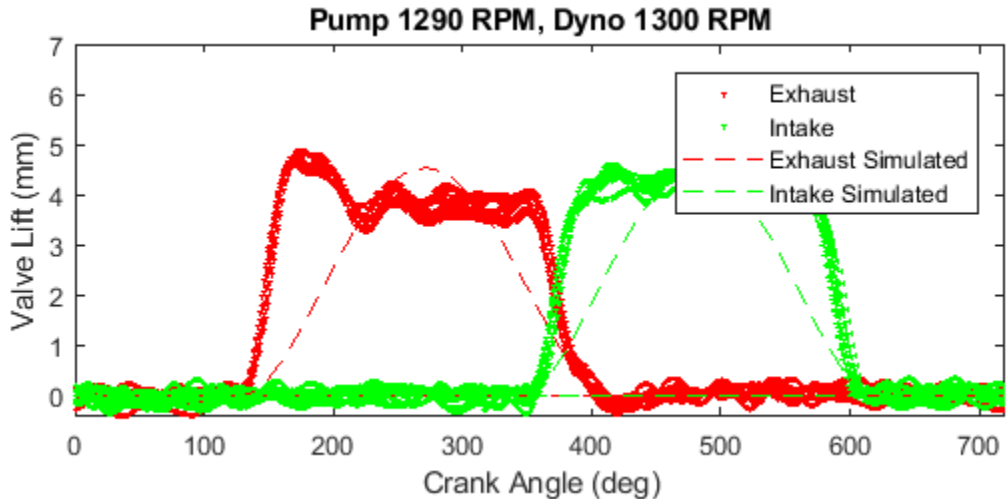


Figure B.1: CAM simulated (original) profile and experimental results

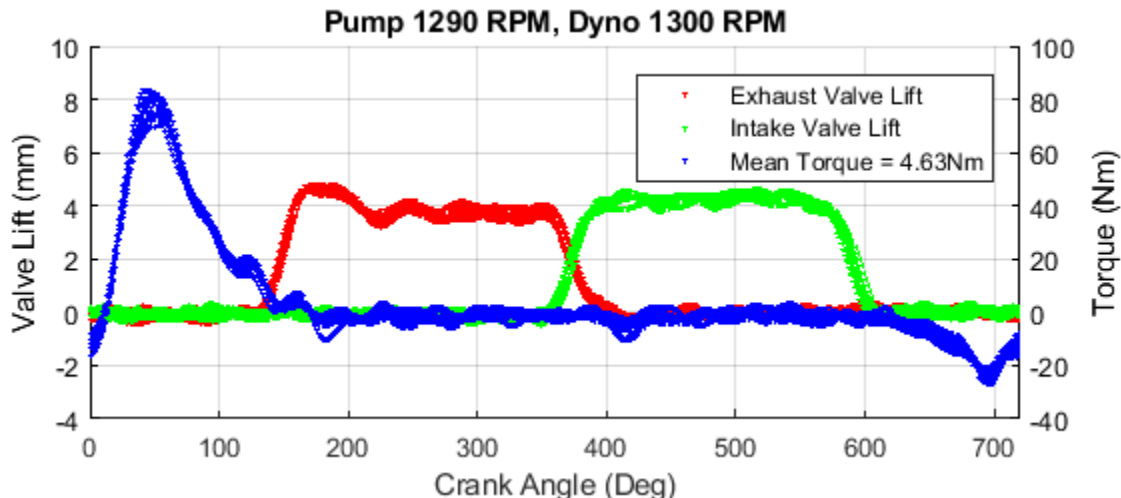


Figure B.2: CAM profile torque results

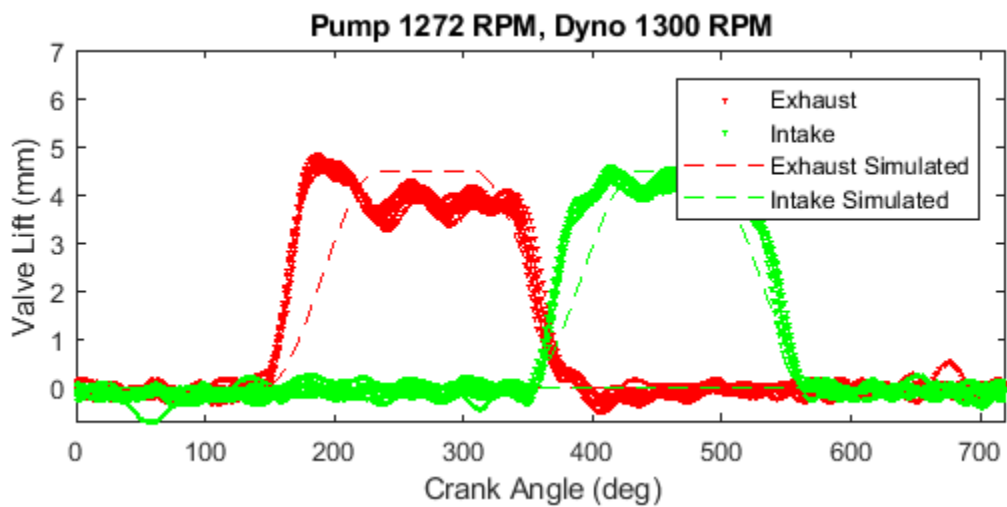


Figure B.3: OPT simulated profile and experimental results

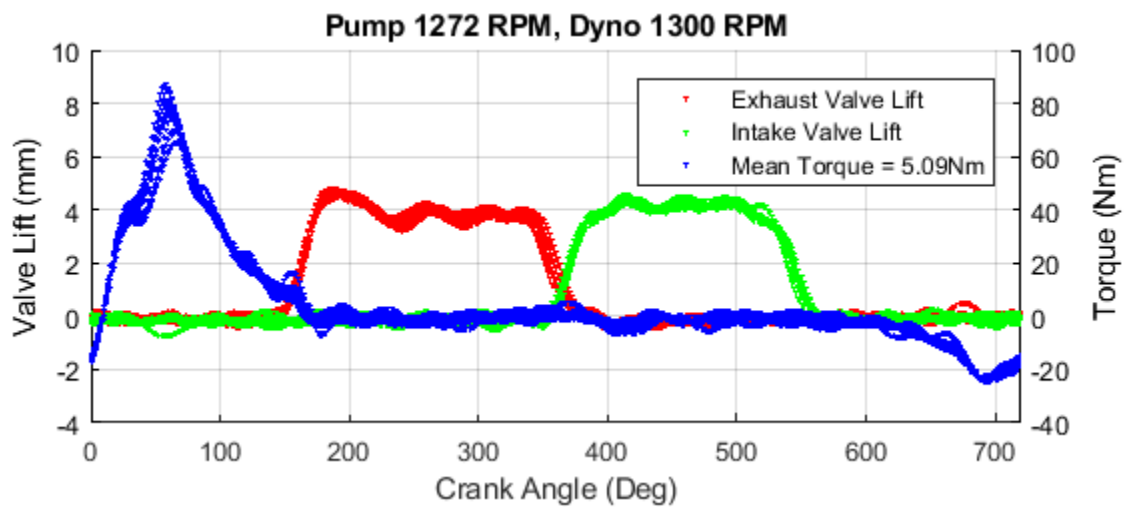


Figure B.4: OPT profile torque results

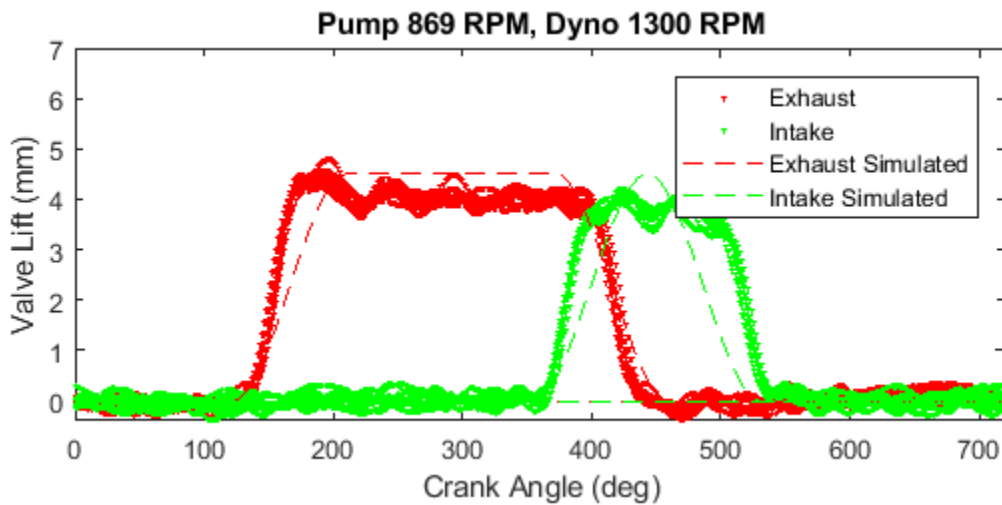


Figure B.5: IEGR simulated profile and experimental results

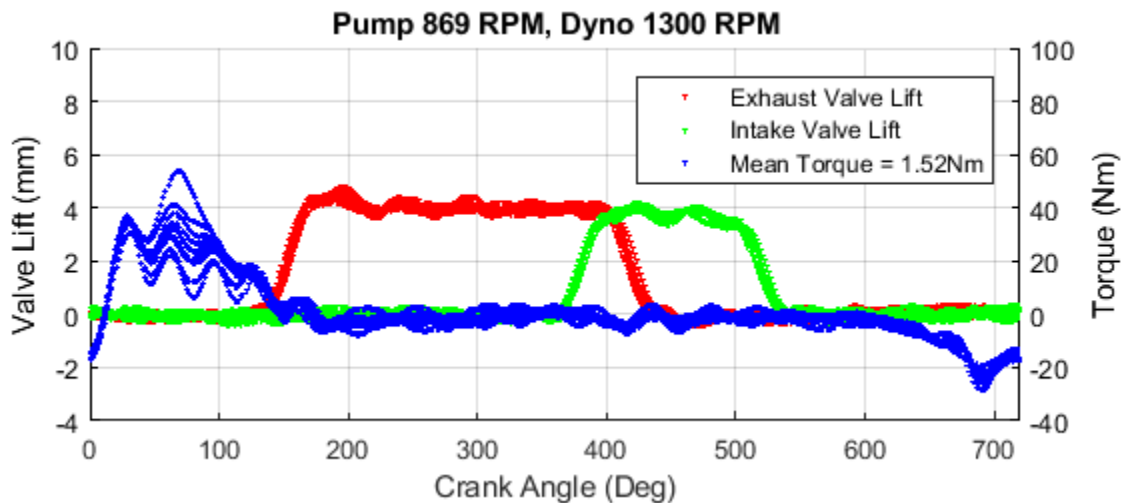


Figure B.6: IEGR partial load profile torque results

Table B.1: Results of Combustion Testing at 1300 RPM Engine Speed

Valve Profile	Mean Torque	Air Fuel Ratio	Fuel Mass (per Cycle)	Estimated Air Volume (per Cycle)	Specific Fuel Consumption
CAM	4.63 Nm	14.7	16.5 mg	201.7 cc	0.283 mg/J
OPT	5.09 Nm	14.7	17.7 mg	217.0 cc	0.277 mg/J
IEGR	1.52 Nm	16.0	12.9 mg	171.4 cc	0.673 mg/J

B.2 Testing at 1500 RPM Engine Speed

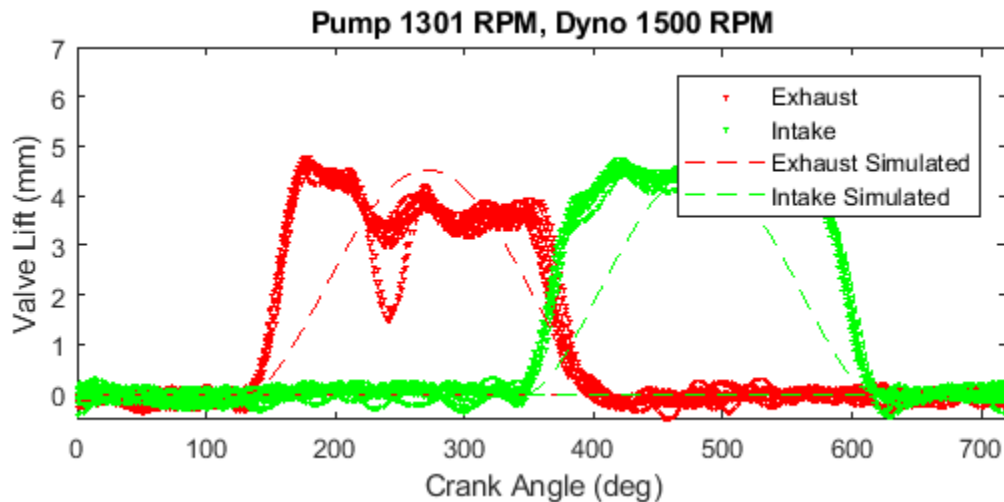


Figure B.7: CAM simulated (original) profile and experimental results

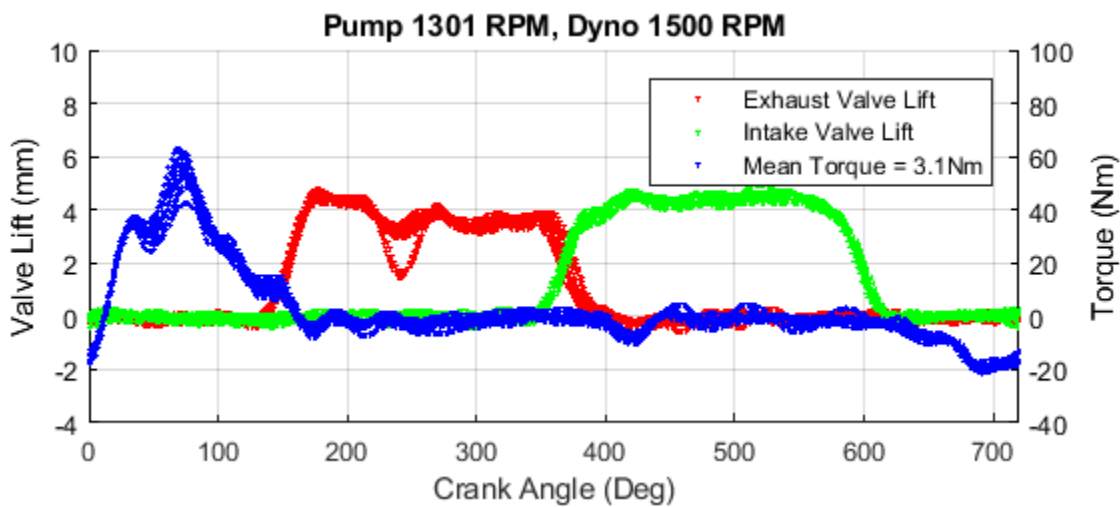


Figure B.8: CAM profile torque results

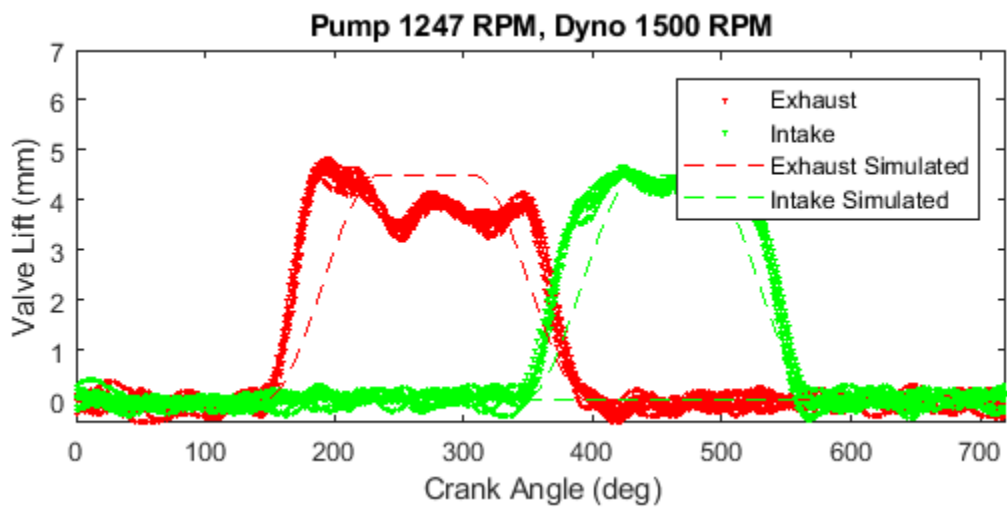


Figure B.9: OPT simulated profile and experimental results

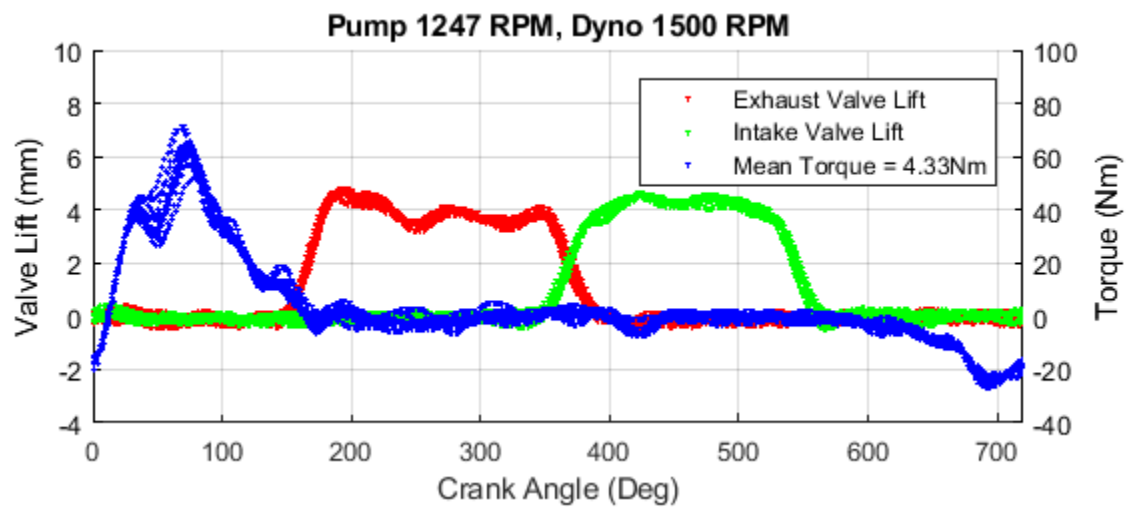


Figure B.10: OPT profile torque results

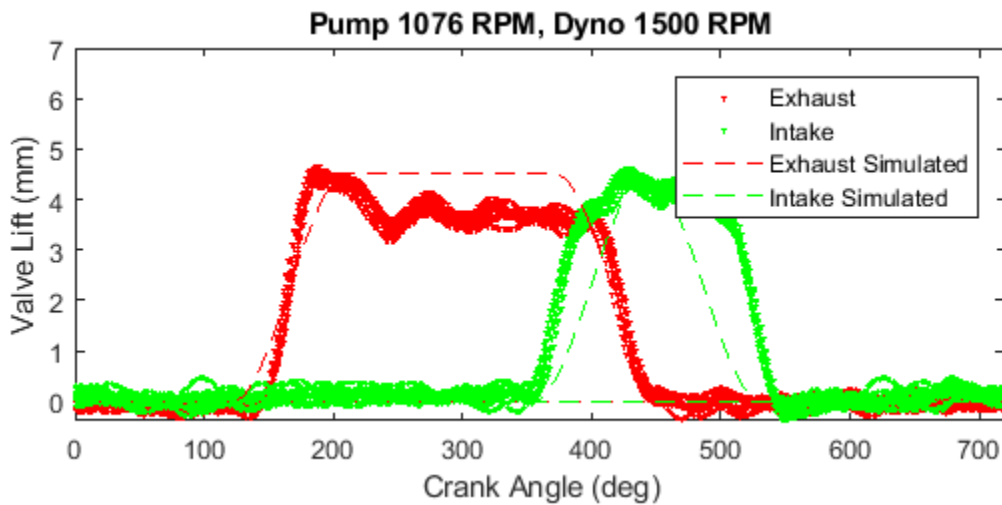


Figure B.11: IEGR simulated profile and experimental results

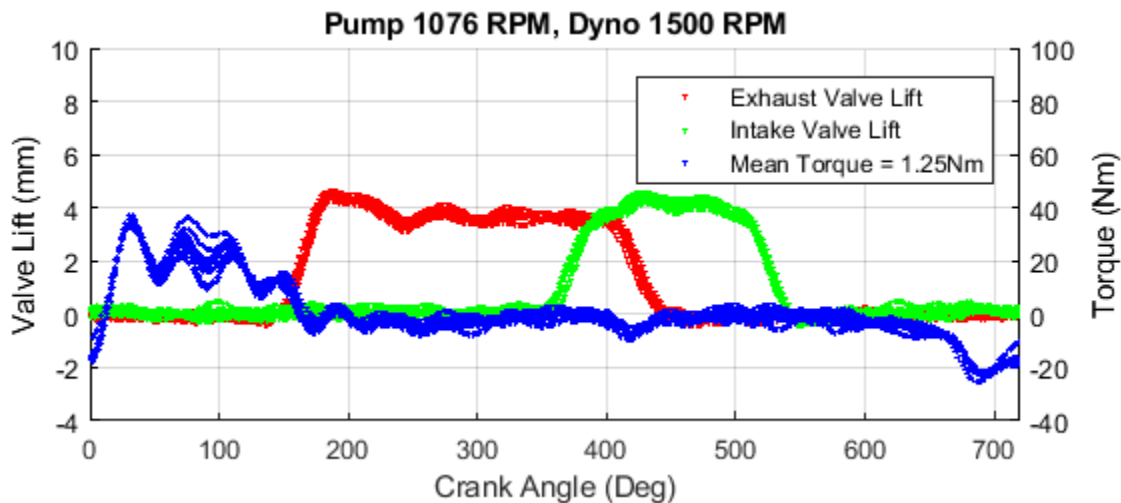


Figure B.12: IEGR partial load profile torque results

Table B.2: Results of Combustion Testing at 1500 RPM Engine Speed

Valve Profile	Mean Torque	Air Fuel Ratio	Fuel Mass (per Cycle)	Estimated Air Volume (per Cycle)	Specific Fuel Consumption
CAM	3.10 Nm	14.7	15.8 mg	194.0 cc	0.406 mg/J
OPT	4.33 Nm	14.7	17.1 mg	209.1 cc	0.314 mg/J
IEGR	1.25 Nm	16.0	13.5 mg	180.3 cc	0.861 mg/J